



**University of Venda**

**School of Environmental Sciences  
Department of Ecology and Resource Management**

**SEQUESTRATION OF HAZARDOUS DYE FROM AQUEOUS  
SOLUTION USING RAW AND MODIFIED AGRICULTURAL WASTE  
MATERIALS**

**BY**

**JEGEDE MOBOLAJI MOJISOLA**

**Student No: 18022757**

**A master's dissertation submitted to the Department of Ecology and  
Resource Management in fulfilment of the requirements for Master of  
Environmental Sciences**

**Supervisor  
Dr. J.N. Edokpayi**

**Co-supervisor  
Dr O.S. Durowoju**

**June, 2021**

## DECLARATION

I, Mobolaji Mojisola Jegede, hereby declare that this dissertation for the master's in environmental sciences degree at the University of Venda, hereby submitted by me, has not been previously submitted for a degree at this or any other institution. This is my work in design and execution, and all reference materials contained herein have been duly acknowledged.



Signature

20 April 2021

Date

## DEDICATION

My sweetheart- **Professor A. O. Jegede**

Thank you for making me to trust and believe that under the heaven of this great God, all things are possible!

## ACKNOWLEDGEMENTS

Unto JESUS, my ever-present help in this journey, I thank you. Indeed, you have done all things well!

I have seen further in this master's journey because I have stood on the shoulders of giants. Therefore, my special appreciation goes to my supervisor- Dr. J.N. Edokpayi. Of no less importance to me is my co-supervisor- Dr. O.S. Durowaju. Thanking you both for your committed mentorship, direction and guidance from the commencement of this programme to the end.

I am indeed thankful to people who did not leave me alone to my struggles. A big thanks to colleagues like Stanley Ndlovu, Tobi Owojori, Mukethwa Mannzhi for being so helpful. I am touched and grateful to Mrs. Kemi Adebayo, who opened the door of her house to me when I needed to be close to campus in order to hasten my laboratory analyses, even at the challenging times of COVID 19. I am also grateful to Mr. Adeyemi Adeeyo for his assistance at the early stage of sample collection, Mrs. Rene Pearce, Mr. George Akintola and Dr. Toyin Marshal who all created time out of their busy schedule to dot my 'I's and cross my 'T's. I enjoyed so much encouragement from you all and other people who I cannot mention their names here for the sake of time and space. I appreciate you all.

I extend my deepest gratitude to my children- Toluwani, Oluwatoni, Temiloluwa and Oluwataayo for their understanding; my sisters- Adebimpe and Titilope, my parents- Mr & Mrs Babatunde for their spiritual and moral encouragement. Lastly and most importantly, to my own DJ- Professor A.O. Jegede for always being there for me and for being a worthy role model to me and our children. Yes! Your saying is true my DJ, 'somehow for the better, we all remain focused and committed to the faithful one who has promised, the climate will change'!

## ABSTRACT

World Bank reported in 2015 that dye effluent is responsible for 20% of water pollution problem globally. Dye consuming industries generate large volume of wastewater which is discharged into various environmental media (land and water body). This effluent is hazardous to both aquatic and human life. Human exposure to dye contaminated water has been attributed to risk of cancer development, skin irritation, eye inflammation, severe damage to brain, kidney, liver, reproductive system and central nervous system. Physical, chemical and biological methods of dye sequestration from wastewater have been employed. However, some of these methods are expensive, ineffective and are not applicable to real effluent. Adsorption process using commercial activated carbon as adsorbent has been widely used for effluent treatment. However, despite its efficient use, activated carbon remains a challenge. This has led to search for available and abundant agricultural waste materials as alternatives for expensive activated carbons. *Litchi chinensis* peel powder and *Dicerocaryum eriocarpum* seed powder in their raw (RL and RDE) and modified (CL and CDE) forms were used as potential adsorbents for adsorptive sequestration of congo red dye from simulated dye effluent. Biosorbents were characterised before and after adsorption of congo red dye by Fourier transform infrared spectroscopy (FTIR), Scanning electron microscopy (SEM), Energy dispersive X-ray spectroscopy (EDS), Brunauer, Emmett and Teller (BET) surface area analysis and, X-ray diffraction (XRD). Determination of the point of zero charge (PZC) suggested congo red dye sorption from aqueous solution would be best in acidic pH. Operating parameters such as contact time, temperature, adsorbent dosage and dye concentration, adsorbate pH, adsorbent size, matrix effect, were all investigated for the best conditions for optimum congo red dye removal from aqueous solution using batch adsorption technique. Experimental parameters for optimum removal of congo red dye using raw biosorbents (RL and RDE) were 0.15 g mass of adsorbent, 90 min equilibrium time, 200 rpm agitation speed, temperature at 30 °C, pH of 2 and particle size of <125 µm. Also, experimental parameters for optimum removal of congo red dye using modified biosorbents (CL and CDE) were 0.05 g, equilibrium time of 15 min for CL, 90 min for CDE, 200 rpm agitation speed, temperature at 80 °C, pH of 2 and particle size of <125 µm. Optimisation of all these parameters achieved adsorption efficiency close to 100 % for raw and modified biosorbents. The kinetic of the adsorption processes for the biosorbents were ascertained by employing the pseudo first order, pseudo second order and intra-particle diffusion kinetic models. The pseudo-second order kinetic model best described the adsorption process. Equilibrium adsorption data was also evaluated using Langmuir, Freundlich and Temkin isotherm models and Langmuir model best described the adsorption process. Maximum adsorption capacities

for biosorbents were RL- 55.56 mg/g, CL- 58.48 mg/g, RDE- 51.02 mg/g and CDE- 53.19 mg/g. Thermodynamic study revealed that the adsorption process was feasible and spontaneous. Adsorption of congo red dye from aqueous solution using raw biosorbents was exothermic while that of modified biosorbents was endothermic adsorption process. Desorption study found NaOH solution as the most suitable desorbing solvent. The five cycled regeneration/adsorption experiments showed that the regenerated biosorbents efficiently removed congo red dye from aqueous solution close to their virgin samples for the first three cycles. This research therefore establishes raw and modified *Litchi chinensis* peels and *Dicerocaryum eriocarpum* seeds as potential eco-friendly, affordable, abundant, and effective biosorbents for sequestration of hazardous dye from wastewater.

Keywords: Adsorption, Congo red, *Dicerocaryum eriocarpum*, dyes, *Litchi chinensis*, isotherm, kinetic, thermodynamics.

## TABLE OF CONTENTS

<b>DECLARATION</b>	<b>ii</b>
<b>DEDICATION</b>	<b>iii</b>
<b>ACKNOWLEDGEMENTS</b>	<b>iv</b>
<b>ABSTRACT</b>	<b>v</b>
<b>TABLE OF CONTENTS</b>	<b>vii</b>
<b>LIST OF TABLES</b>	<b>xi</b>
<b>LIST OF FIGURES</b>	<b>xii</b>
<b>LIST OF ABBREVIATIONS AND ACRONYMS</b>	<b>xiv</b>
<b>LIST OF UNITS AND SYMBOLS</b>	<b>xv</b>
<b>CHAPTER ONE: INTRODUCTION</b>	<b>1</b>
<b>1.1 Background</b>	<b>1</b>
<b>1.2 Statement of the problem</b>	<b>3</b>
<b>1.3 Motivation</b>	<b>5</b>
<b>1.4 Objectives</b>	<b>5</b>
1.4.1 Main Objective	5
1.4.2 Specific objectives	5
<b>1.5 Research questions</b>	<b>6</b>
<b>1.6 Description of plant materials</b>	<b>6</b>
<b>1.6.1 <i>Dicerocaryum eriocarpum</i> (DE)</b>	<b>6</b>
<b>1.6.2 <i>Litchi chinensis</i> (LC)</b>	<b>7</b>
<b>CHAPTER TWO: LITERATURE REVIEW</b>	<b>9</b>
<b>2.1 Dyes: sources and properties</b>	<b>9</b>
<b>2.2 Emergence of synthetic dyes</b>	<b>9</b>
<b>2.3 Classification of synthetic dyes</b>	<b>10</b>
<b>2.4 Environmental impact of dye effluent</b>	<b>13</b>
<b>2.5 Review of dye sequestration methods</b>	<b>14</b>
2.5.1 Chemical Methods	17
2.5.2 Biological Methods	18
2.5.3 Physical methods	19
<b>2.6 Adsorption</b>	<b>20</b>

2.6.1 Review of adsorption process	21
2.6.2 Modification of adsorbent	24
<b>2.7 Experimental parameters affecting adsorption of dye</b>	<b>25</b>
2.7.1 Effect of contact time	25
2.7.2 Effect of pH	26
2.7.3 Effect of adsorbent dosage	26
2.7.4 Effect of temperature	27
2.7.5 Effect of dye concentration	27
<b>2.8 Characterisation methods of plant materials</b>	<b>27</b>
2.8.1 Fourier Transform Infrared Spectroscopy (FTIR)	28
2.8.2 Scanning Electron Microscopy - Energy Dispersive X-ray Spectroscopy (SEM-EDS)	28
2.8.4 X-Ray Diffraction (XRD)	29
2.8.5 Thermo Gravimetric Analysis (TGA)	29
<b>2.9 Adsorption Kinetics</b>	<b>29</b>
2.9.1 Pseudo-first order	29
2.9.2 Pseudo-second order	30
2.9.3 Intra-particle diffusion	30
<b>2.10 Adsorption Isotherms</b>	<b>31</b>
2.10.1 Langmuir Isotherm	31
2.10.2 Freundlich Isotherm	31
2.10.3 Temkin Isotherm	32
2.10.4 Dubinin-Radushkevich Isotherm	32
<b>2.11 Adsorption thermodynamics</b>	<b>33</b>
<b>CHAPTER THREE: RESEARCH METHODOLOGY</b>	<b>34</b>
<b>3.1 Research design</b>	<b>34</b>
<b>3.2 Preparation of adsorbent</b>	<b>34</b>
<b>3.3 Modification of adsorbent</b>	<b>35</b>
<b>3.4 Characterization of the adsorbent</b>	<b>36</b>
3.4.1 Fourier Transform Infra-Red (FTIR)	36
3.4.2 Scanning Electron Microscopy and Energy Dispersive X-Ray Spectroscopy (SEM-EDS)	36
3.4.3 Brunauer, Emmet and Teller (BET) Technique	37
3.4.4 X-Ray Diffraction	37
<b>3.5 Determination of point of zero charge</b>	<b>37</b>
<b>3.6 Preparation and calibration of dye solution</b>	<b>38</b>



<b>3.7 Biosorption study</b>	<b>39</b>
3.7.1 Agitation time	40
3.7.2 Temperature	40
3.7.3 Adsorbent dosage and adsorbate concentration	41
3.7.4 pH	41
3.7.5 Particle size of adsorbents	41
3.7.6 Effect of matrix	41
3.7.7 Removal efficiency of adsorbents on other dyes	41
<b>3.8 Adsorption kinetics</b>	<b>42</b>
<b>3.9 Adsorption isotherms</b>	<b>43</b>
<b>3.10 Adsorption thermodynamics</b>	<b>45</b>
<b>3.11 Desorption Study/Regeneration</b>	<b>46</b>
<b>3.12 Data interpretation</b>	<b>46</b>
<b>3.13 Quality assurance</b>	<b>46</b>
<b>CHAPTER FOUR: RESULTS AND DISCUSSION</b>	<b>48</b>
<b>4.1 Preamble</b>	<b>48</b>
<b>4.2 Characterisation of adsorbents</b>	<b>48</b>
4.2.1 Fourier Transform Infrared Spectroscopy (FTIR)	48
4.2.2 Scanning electron micrograph (SEM)	51
4.2.3 Energy dispersive X-ray spectroscopy (EDS)	54
4.2.4 Brunauer, Emmett, and Teller Technique (BET)	57
4.2.5 X-Ray Diffraction	58
<b>4.3 Point of zero charge (PZC)</b>	<b>60</b>
<b>4.4 Effect of experimental parameters on adsorption of Congo red from aqueous solution</b>	<b>61</b>
4.4.1 Effect of contact time	61
4.4.2 Effect of temperature	63
4.4.3 Effect of dosage and concentration	64
4.4.4 Effect of pH	65
4.4.5 Effect of particle size of adsorbent	66
4.4.6 Effect of matrix	67
4.4.7 Removal efficiency of adsorbents on selective dyes	69
<b>4.5 Adsorption kinetics</b>	<b>70</b>
<b>4.6 Adsorption isotherms</b>	<b>75</b>
<b>4.7 Adsorption thermodynamics</b>	<b>81</b>
<b>4.8 Desorption study/Regeneration</b>	<b>83</b>

<b>CHAPTER FIVE: CONCLUSION AND RECOMMENDATION</b>	<b>86</b>
<b>5.1 Preamble</b>	<b>86</b>
<b>5.2 Conclusion</b>	<b>86</b>
<b>5.3 Recommendation</b>	<b>87</b>
<b>REFERENCES</b>	<b>88</b>
<b>APPENDIX</b>	<b>106</b>

## LIST OF TABLES

Table 2.1: Commonly used dyes and their hazardous effects	16
Table 2.2: Summary of dyes sequestration methods	24
Table 3.1: Physicochemical properties of Congo red dye	38
Table 4.1: BET structure parameters of biosorbents	58
Table 4.2: Characteristics of surface water from Mutale river	68
Table 4.3: Kinetic model parameters for RL and CL	71
Table 4.4: Kinetic model parameters for RDE and CDE	71
Table 4.5: Isotherm model parameters adsorption of CR dye onto RL and CL	76
Table 4.6: Isotherm model parameters adsorption of CR dye onto RDE and CDE	77
Table 4.7: Maximum adsorption capacity of CR dye onto various biosorbents in literature	81
Table 4.8: Thermodynamic parameters for CR dye adsorption onto RL and CL	82
Table 4.9: Thermodynamic parameters for CR dye adsorption onto RDE and CDE	82

## LIST OF FIGURES

Figure 1.1: Jian River in Northern China	4
Figure 1.2: <i>Dicerocaryum eriocarpum</i> plant	7
Figure 1.3: <i>Litchi chinensis</i> fruit tree	8
Figure 2.1: Examples of dye classes and their chemical structures	12
Figure 3.1: Methodology design	34
Figure 3.2: Images of novel plant materials	35
Figure 3.3: Chemical structure of citric acid	36
Figure 3.4: Chemical structure of Congo red	38
Figure 3.5: Calibration curve for aqueous solution of congo red	39
Figure 3.6: Experimental set ups for Biosorption study	40
Figure 4.1: FTIR spectra of (A) RL and CL, (B) RDE and CDE	49
Figure 4.2: FTIR spectra of (A) RL and SRL, (B) CL and SCL	50
Figure 4.3: FTIR spectra of (A) RDE and SRDE, (B) CDE and SCDE	51
Figure 4.4: SEM of RL and CL before CR dye adsorption	52
Figure 4.5: SEM of SRL and SCL after CR dye adsorption	53
Figure 4.6: SEM of RDE and CDE before CR dye adsorption	53
Figure 4.7: SEM of SRDE and SCDE after CR dye adsorption	54
Figure 4.8: EDX spectra of RL and CL	55
Figure 4.9: EDX spectra of SRL and SCL	56
Figure 4.10: EDX spectra of RDE and CDE	56
Figure 4.11: EDX spectra of SRDE and SCDE	57
Figure 4.12: XRD of (A)- RL and SRL, (B)- CL and SCL	59
Figure 4.13: XRD of (A)- RDE and SRDE, (B)- CDE and SCDE	60
Figure 4.14: Point of zero charge for RL and CL	61
Figure 4.15: Point of zero charge for RDE and CDE	61
Figure 4.16: Effect of time on adsorption of CR dye onto RL and CL	62
Figure 4.17: Effect of time on adsorption of CR dye onto RDE and CDE	62
Figure 4.18: Effect of temperature on adsorption of CR dye onto RL and CL	63
Figure 4.19: Effect of temperature on adsorption of CR dye onto RDE and CDE	63
Figure 4.20: Effect of dosage and concentration on adsorption of CR dye onto RL and CL	64
Figure 4.21: Effect of dosage and concentration on adsorption of CR dye onto RDE and CDE	65
Figure 4.22: Effect of pH on the uptake of CR dye by RL and CL	66

Figure 4.23: Effect of pH on the uptake of CR dye by RDE and CDE	66
Figure 4.24: Effect of particle sizes of RL and CL on adsorption of CR dye	67
Figure 4.25: Effect of particle sizes of RDE and CDE on adsorption of CR dye	67
Figure 4.26: Effect of matrix on adsorption of CR dye onto RL and CL	68
Figure 4.27: Effect of matrix on adsorption of CR dye onto RDE and CDE	68
Figure 4.28: Removal efficiency of RL and CL on selective dyes	69
Figure 4.29: Removal efficiency of RDE and CDE on selective dyes	69
Figure 4.30: Kinetic model plots of RL	72
Figure 4.31: Kinetic model plots of CL	73
Figure 4.32: Kinetic model plots of RDE	74
Figure 4.33: Kinetic model plots of CDE	75
Figure 4.34: Isotherm model plots of RL	77
Figure 4.35: Isotherm model plots of CL	78
Figure 4.36: Isotherm model plots of RDE	79
Figure 4.37: Isotherm model plots of CDE	80
Figure 4.38: Van't Hoff plots of RL and CL	83
Figure 4.39: Van't Hoff plots of RDE and CDE	83
Figure 4.40: Desorption of SRL and SCL	84
Figure 4.41: Desorption of SRDE and SCDE	84
Figure 4.42: Regeneration and reuse cycles of SRL and SCL	85
Figure 4.43: Regeneration and reuse cycles of SRDE and SCDE	85

## LIST OF ABBREVIATIONS AND ACRONYMS

BET	Brunauer, Emmett and Teller
CDE	Citric acid modified <i>Dicerocaryum eriocarpum</i>
CL	Citric acid modified <i>Litchi chinensis</i>
Cl <sup>-</sup>	Chloride ion
CO	Carbon monoxide
CO <sub>2</sub>	Carbon (iv) Oxide
CR	Congo red
DE	<i>Dicerocaryum Eriocarpum</i>
EDS	Energy dispersive x-ray spectroscopy
Fe	Iron
Fe <sup>2+</sup>	Iron (II) ion
Fe <sup>3+</sup>	Iron (III) ion
FTIR	Fourier Transform Infra-Red
H <sub>2</sub> O	Water
H <sub>2</sub> O <sub>2</sub>	Hydrogen peroxide
HCl	Hydrochloric acid
LC	<i>Litchi chinensis</i>
NaOH	Sodium hydroxide
No	Number
OH <sup>-</sup>	Hydroxyl ion
O <sub>3</sub>	Ozone
PZC	Point of zero charge
RDE	Raw <i>Dicerocaryum eriocarpum</i>
RL	Raw <i>Litchi chinensis</i>
SEM	Scanning Electron Microscope
SRDE	Spent raw <i>Dicerocaryum eriocarpum</i>
SCDE	Spent citric acid modified <i>Dicerocaryum eriocarpum</i>
SRL	Spent raw <i>Litchi chinensis</i>
SCL	Spent citric acid modified <i>Litchi chinensis</i>
SO <sub>4</sub> <sup>2-</sup>	Sulphate (VI) ion
U.S	United States
UV	Ultra-violet
WHO	World Health Organisation
XRD	X-Ray Diffraction

## LIST OF UNITS AND SYMBOLS

>	Greater than
<	Less than
%	Percentage
$C_e$	Equilibrium concentration of CR dye (mg/L)
$C_f$	Final concentration of CR dye (mg/L)
$C_o$	Initial CR dye concentration (mg/L)
cm	centimetre
$E_a$	Energy of activation
$K_1$	Pseudo first order rate constant (1/minute)
$K_2$	Pseudo second order rate constant (g/mg min)
$K_f$	Freundlich adsorption constant (mg/g (L/mg) <sup>1/n</sup> )
$K_l$	Langmuir isotherm constant (L/mg)
$K_p$	Intra-particle diffusion rate constant (mg/g min)
$K_o$	equilibrium constant
$q_e$	Amount of adsorbate per gram of the adsorbent at equilibrium (mg/g)
$q_o$	Maximum adsorption capacity (mg/g)
$q_t$	Amount of adsorbate adsorbed at time t (mg/g)
$Q_{max}$	Maximum amount of CR dye adsorbed
:	Ratio
$\mu$	Micro
$\mu\text{m}$	Micrometer
$\text{\AA}$	Armstrong
$\text{cm}^{-1}$	Per centimetre
deg/min	degree per minute
g	Gramms
Kg	Kilograms
kV	Kilovolt
L/mg	Litre per milligram
m	Meters
M	Molar
mA	milli Ampere
Meq	Milli equivalent
mg	Milligram
mg/g	Milligram per gram

mg/L	Milligram per Litre
min	Minute
mL	Millilitre
mm	Millimetre
mmol	Millimoles
nm	Nano meter
°C	Degree Celsius
pH <sub>e</sub>	Equilibrium pH
pH <sub>o</sub>	Initial pH
pH <sub>f</sub>	Final pH
R	Universal gas constant
rpm	Revolutions per minute
T	Temperature
ΔG	Change in free energy
ΔH	Change in Enthalpy
ΔpH	Change in pH
θ	theta
λ	Lambda
m	Mass of adsorbent used (g)
n	Adsorption intensity
t	Time (minute)
v	Volume of solution (L)



## CHAPTER ONE: INTRODUCTION

### 1.1 Background

Water pollution is one of the environmental challenges of the 21st century facing mankind. Portable water is generally hard to come by in most communities of the developing countries due to daily domestic and industrial human activities which tend to pollute water bodies thereby reducing its quality (Edokpayi et al., 2017). Pollution of water bodies are majorly from domestic effluents and sewage, industrial effluents, agricultural effluents, radioactive wastes, thermal, and oil pollution (Kumar et al., 2010). Industrial effluent which is one of the major sources of water pollution consists of both organic and inorganic substances. Notable organic and inorganic substances that can be found in industrial wastewater are dyestuff, pesticide residues, solvents and cleaning fluids, dissolved residue from fruit and vegetables, lignin from pulp and paper, brine and metals to name a few (Malik et al., 2007; Wanyonyi et al., 2014).

Synthetic dyes contamination of surface water which is the focus of this study is mainly from manufacturing industries such as textile, pulp and paper, leather, tannery, paints, food, pharmaceutical and electroplating industries (Aksu and Karabayir, 2008; Farias et al., 2018). Despite hazardous impact on the environment, synthetic dyes are ever in increasing demand due to their low cost, pigment property, stable and sunfast nature (Rosa et al., 2018). At present, there are about 10,000 different commercial dyes and pigments in existence (Owamah et al., 2013; Vital et al., 2016) and world production of synthetic dye is estimated at about 800,000 tons annually (Hassaan and El Nemr 2017). Textile industries are the major users of world production of synthetic dyes. Production of textile is a fresh water consuming process. It takes about 0.08-0.15 m<sup>3</sup> of water to produce 1 kg of fabrics. During dyeing process, about 20-30 % of synthetic dye does not bind to the fabrics and are included in large volume of wastewater generated which are eventually discharged as effluent to the environment (Wang et al., 2002; Vital et al, 2016). An estimated value of about 1,000 – 3,000 m<sup>3</sup> of wastewater is discharged after processing about 12 – 20 tons of textiles per day (Al-Kdasi et al., 2004; Hassaan and El Nemr, 2017). This leads to discharge of more than 1.5 x 10<sup>8</sup> m<sup>3</sup> coloured effluents annually (Feng *et al.*, 2011).

The discharge of untreated dye effluent into the environment poses a lot of serious problem to human health as synthetic dye may be degraded to highly poisonous, mutagenic, and carcinogenic products (Mathur and Bhartnager, 2007; Saleh et al., 2011). Human exposure to such water has led to increase in potential cancer risk, skin irritation, eye inflammation (Suteu et al., 2007), severe damage to brain, kidney, liver, reproductive system and central nervous system (Hai et al., 2007). Surface water colouration, which is a resultant effect of dye effluent, reduces aesthetic value of water thus, making it unsuitable for recreation, irrigation and domestic use.

Furthermore, light penetration is significantly reduced in coloured water body thereby hindering photosynthetic activity. This eventually affects growth or brings about death of aquatic lives (Maurya et al., 2008; Salleh et al., 2011; Berradi et al., 2019). Therefore, it is important to devise methods to successfully remove hazardous dyes from wastewater before being reused or discharged into water bodies.

It is worthy to note that scientists have devised several methods for treatment of dye effluent, notable is the adsorption process. Adsorption process is considered as very effective method compared to other available methods of wastewater treatment because it is cost effective, flexible design, easily operated and sensitive to targeted contaminant (Ahmad and Kumar, 2010; Feng et al., 2011; Farias et al., 2018). Adsorption process using commercial activated carbon has been widely used for effluent treatment. However, despite its generous use in wastewater treatment, commercial activated carbon remains an expensive material (Akar et al., 2009; Sharma et al., 2011; Farias et al., 2018). This has led to the search for low-cost agricultural waste/plant material with similar potential properties to replace commercial activated carbons. Recent research interests are focusing on the use of various agricultural biomass as adsorbent for removal of hazardous dye from industrial effluent. These solid wastes/materials are biodegradable and readily obtainable in large amount with little or no value and often cause a disposal problem (Salleh et al., 2011; Tushar and Dawood, 2014). Some of the agricultural wastes that have been used as bio-sorbent for removal of synthetic dye from industrial effluent to mention just a few are: rice husk (Firas, 2013), corn husk (Malik et al., 2016), coffee waste (Lafi et al., 2019), banana peel (Oyekanmi et al., 2019), marula seed husk (Edokpayi et al., 2019) walnut (Uddin and Nasar, 2020), macadamia seed husk (Felista et al., 2020) and litchi seed (Edokpayi and Makete, 2021).

The present study is principally focusing on adsorptive sequestration of Congo red (CR) from aqueous solution using *Litchi chinensis* (LC) peel and *Dicerocaryum eriocarpum* (DE) seed. Congo red dye is cancerous to human, poisonous to plants and animals. It is widely used in textile, tannery, printing, paper, rubber and plastics industries, and abundantly present in their effluents (Purkait et al., 2007; Mittal et al., 2009; Ahmad and Kumar, 2010; Wang et al., 2011; Farias et al., 2018). Thus, knowledge of the performance of Litchi peel and DE seed on CR removal will contribute to the development of more low-cost and efficient adsorbents for treatment of dye effluents containing congo red and other azo dyes. Litchi peels are usually discarded as industrial or domestic food waste. Also, *Dicerocaryum eriocarpum* seeds are considered nuisance to the environment because of their thorny nature. These two materials are advantageous in the sense that they are readily available, can be easily prepared and converted to useful products.

## 1.2 Statement of the problem

Water shortage and water pollution are major global problems; especially in under-developed and developing nations of the world due to pollution of about 3 % available fresh water through day to day human activities (Guppy and Anderson, 2017). For instance, a nation like South Africa; a semi-arid country with low precipitation is under serious threat of water shortage. According to a document for water growth and development by the Department of Water Affairs and Forestry (DWAF), it has been predicted that South Africa may experience extreme water shortage by 2025 if her water resources are not well managed. A development that may have adverse effect, in particular, on rural dwellers (Jegede and Shikwambane, 2021). This therefore calls for urgent intervention to conserve and protect the limited water resources available from continuous pollution to meet up with water demand both now and in future (Cillie and Odendaal, 2010).

There is clamour globally for industrialisation and diversification of economy through agriculture. Unfortunately, rapid industrialisation leads to increased use of dyes and consequently places high risk of toxicity on the entire ecosystem (Sarkar et al., 2017). In the same vein, agricultural practices are accompanied with lots of waste generation. Industrialisation and agricultural practice without adequate environmental management policy put in place, especially in developing countries result to immense pollution of the environment. Therefore, the need to provide feasible treatment for industrial effluent, and recyclable strategy for agricultural waste materials into useful products is of great concern.

Synthetic dye consuming industries such as textile, pulp and paper, leather, tannery, paints, food, pharmaceutical and electroplating industries are major contributors to environmental pollution, specifically pollution of ground and surface water due to their discharge of untreated coloured wastewater into the environment. These coloured effluents contain mainly synthetic dyes that are difficult to sequester from wastewater due to their extreme solubility in water and complicated aromatic structure which make them more stable and non-biodegradable (Zaharia et al., 2009; Saini, 2017). Textile effluent discharge into surface water brings about discolouration of the water thereby making the water unfit for domestic, agricultural and recreational purposes. The extent of pollution and colouration of the surface water is visibly captured in Figure 1.1, a case of pollution of Juan river in Northern China by effluent from nearby chemical plant. This pollution of water has adverse effect on the growth of aquatic life because light penetration needed for photosynthesis activity is reduced. Human exposure to dye contaminated water has also been attributed to public health problems like dermatitis, skin irritation, allergy, mental confusion, cancer, mutation among others (Suteu et al., 2007; Saini, 2017).

World Bank reported textile effluent as being responsible for 20% of water pollution globally (Sarkar et al., 2017). Coloured effluents have been a serious problem to the environment also here in South Africa, especially in places like Western cape province and KwaZulu Natal coastal region where there is large concentration of Industries (Roes-Hill et al., 2017). This problem is not peculiar to South Africa only. Alex Scott (2015) reported a case of pollution of Noyyal river; a major source of water for residents and farms in southern city of Tirupur, India. Tirupur city has over 300 textile factories responsible for more than half of \$1.25 billion worth of textile export to the United States of America. Pollution from these industries has been linked to illness among residents and loss of productivity of nearby farms in Tirupur.



Figure 1.1: River of Blood: China's Jian River turns red after chemical dump.

Source: [Internet]- [https://www.huffpost.com/entry/jian-river-blood-china\\_n\\_1158679?slideshow=true#gallery/5bb105f4b09bbe9a593be5/0/](https://www.huffpost.com/entry/jian-river-blood-china_n_1158679?slideshow=true#gallery/5bb105f4b09bbe9a593be5/0/) accessed 2019/11/15.

Already, there is a government regulation on reducing contaminants in water to a permissible level (South African Water Act of 1998), in order to make the water reusable or safely discharged into the environment due to water shortage or adverse effect emanating from exposure to such water on human and aquatic life. This regulation further agrees with section 24 of the Constitution of the Republic of South Africa, 1996, which states that 'everyone has the right to an environment that is not harmful to their health or wellbeing'. Unfortunately, the level of compliance by industries to this regulation is low because existing methods of wastewater treatment are complex and highly

expensive (Edokpayi et al, 2020). Also, most existing wastewater treatment plants are not capable of treating wastewater they receive to a harmless and tolerable state in South Africa (Saving Water South Africa, 2011).

### 1.3 Motivation

We live in water shortage and water pollution generation. The need to conserve limited fresh water available and to preserve it from pollution majorly through industrialisation and rapid population growth is of great concern which require urgent attention. Hence, the motivation for this study, in providing feasible treatment for industrial wastewater with regards to dye-consuming industries like textile industry. Several methods of dye removal from aqueous solution/wastewater have been implemented. These methods could be chemical, biological and physical such as oxidation process, photochemical, ozonation, microbial cultures, bioremediation, membrane filtration, and ion exchange (Salleh et al., 2011). Often, the effectiveness of these methods depends on the type of dye present in wastewater, therefore their particular application could be limited (Zaharia et al., 2009). These existing methods have also suffered drawback due to their high cost and low regeneration.

As a result of the limitations of existing methods of removal of hazardous dye from wastewater, the utilisation of low cost, eco-friendly agricultural wastes materials have been researched with great success as an effective substitute for existing methodology for expelling dyes from wastewater. Therefore, this current study seeks to explore the use of local, low-cost, eco-friendly, agricultural wastes or plant materials (*Litchi chinensis* peel and *Dicerocaryum eriocarpum* seed) as biosorbents for sequestration of hazardous dye from wastewater. This will further contribute to cost effective treatment of dye wastewater and make it reusable or safely discharge into water bodies. This will eventually alleviate public health concern of dye-water contamination. Agricultural plant/waste materials like DE seeds and Litchi peel; used in this study are also converted to useful products thereby reducing problem of their disposal or pollution of the environment by these plant/waste materials.

### 1.4 Objectives

#### 1.4.1 Main Objective

The main objective of this study is to explore the potential of locally available agricultural waste materials for the sequestration of hazardous dyes from aqueous solution.

#### 1.4.2 Specific objectives

The specific objectives of the study are to:

- 1) Characterise the various biosorbents by Fourier transform infrared spectroscopy (FTIR), Scanning electron microscopy (SEM), Energy dispersive X-ray spectroscopy (EDS), Brunauer, Emmett, Teller (BET) surface area analysis and, X-ray diffraction (XRD).
- 2) Determine the effects of experimental parameters such as contact time, pH, adsorbent dosage and adsorbate concentration, temperature, particle size, effect of matrix on the removal efficiency of dye by the biosorbents.
- 3) Describe the kinetics, mechanisms and thermodynamics of the adsorption process using various adsorption-based models.
- 4) Determine the regeneration and reuse of the spent biosorbents.

### 1.5 Research questions

- 1) What properties of biosorbents are responsible for dye adsorption?
- 2) What experimental conditions can enhance the adsorption efficiency of biosorbents?
- 3) What is the mechanism, adsorption isotherm and thermodynamics of adsorption process of dye sequestration?
- 4) How regenerable and reusable are the spent biosorbents?

### 1.6 Description of plant materials

#### 1.6.1 *Dicerocaryum eriocarpum* (DE)

DE is a perennial herb which creeps along the ground in the Kalahari, with beautiful, bright mauve flowers that magnificently compliment the dull desert soils. It is commonly found in the Democratic Republic of Congo, Zambia, Zimbabwe, Namibia, Botswana and South Africa (Hoveka, 2017). It grows in the Limpopo, Northern Cape and North West Provinces of South Africa. As described by Hoveka (2017), DE occurs mainly in desert areas, but it also grows on sandy soils in grasslands, riverbanks and on dunes slopes at altitudes of 900-1200 mm. It is also known as devil's thorn because of its circular fruit having two central sharp projections. Leaves are opposite, egg-shaped in outline and attached at the broad end; they are about 22 mm long, with rounded teeth along the margins (Figure 1.2). Flowers are bright mauve, usually with dark spots in the throat and lower lip. These trumpet-shaped flowers are solitary, 22-24 mm long, supported by pedicels that are 14-25 mm long. It flowers in summer, mainly from December to April. Fruits are circular in shape, hairy, 12-22 mm long and 11-19 mm wide, with two central spines that are 4-5 mm long. The fruit bears seeds that are oblanceolate,  $\pm$  5.5 mm long and 2.2 mm wide (Hoveka, 2017).

Many uses of *Dicerocaryum eriocarpum* has been established. Khoisans people of Southern Africa use it to make soap and shampoo; and in traditional foot spa treatments (Luseba et al., 2007). Its antibacterial and anti-inflammatory properties make it suitable for treatment of certain

health conditions in Boswana and Namibia. Special preparation of leaves, flowers and roots can be used as remedy for malaria, sexually transmitted diseases, birth canal, abdominal pain and measles in children (Luseba et al., 2007). The leaves are edible to the Venda people of Limpopo province, South Africa. Indigenous farmers also found the plant useful for treatment of wounds and retained placentas in livestock (Luseba et al., 2007; Moreki et al., 2012). However, not so much has been documented about the seeds of *Dicerocaryum eriocarpum* and its uses. In this study, DE seed was processed and used as biosorbent for sequestration of hazardous dye from aqueous solution.



Figure 1.2: *Dicerocaryum eriocarpum* plant

Source: [Internet]- <http://pza.sanbi.org/dicerocaryum-eriocarpum/> accessed 2019/06/12.

### 1.6.2 *Litchi chinensis* (LC)

LC originated from China but now widely grown in countries like India and other countries in Southern Asia, the Indian Subcontinent, United State and South Africa. It requires a tropical climate that is frost-free and is not below the temperature of  $-4^{\circ}\text{C}$  ( $25^{\circ}\text{F}$ ), a climate with high summer heat, rainfall, and humidity. *Litchi chinensis* cultivation is best on a well-drained slightly acidic soil rich in organic matter and mulch (Ibrahim and Mohamed, 2015).

It is a tropical and evergreen tree (Figure 1.3) that is averagely about 49-92 ft tall. It has a grey-dark bark and brownish branches. *Litchi chinensis* has similar foliage to the *Lauraceae* family. The leaves are about 10-25 cm long with leaflets in 2-4 pairs. *Litchi chinensis* tree bears fleshly

fruits that grow into maturity at about 80 to 112 days depending on climate, location and cultivar. The shape of the fruit could be round or oval; up to 5cm long and 4cm wide. This fruit is covered by a thin tough skin with sharp protuberances all over it. This skin is green when immature and ripens to become a red or pink-red skin. The skin is inedible but can be easily removed to expose a layer of edible white fleshy part with a floral smell and a fragrant, sweet flavor. This fleshy, edible part of the fruit is called Aril; surrounding one dark brown inedible seed that is 1 to 3.3 cm long and 0.6 to 1.2 cm wide (0.39-1.30 by 0.24-0.47 in) (Pooja and Bhupendra, 2016). The skin which can be easily peeled off in order to consume the sweet fleshy part of the fruit eventually turns to agricultural waste. The peels were processed and used in this study as biosorbent for sequestration of hazardous dye from aqueous solution.



Figure 1.3: *Litchi chinensis* fruit tree

Source: [Internet]- <https://en.wikipedia.org/wiki/Lychee/> accessed 2019/06/12.



## CHAPTER TWO: LITERATURE REVIEW

### 2.1 Dyes: sources and properties

Clothes and other products like plastics, paints, foods and drugs, papers and cosmetics are ever in increasing demands. They are produced in different attractive colours which make them marketable and appealing to end-users. These varieties of colour are achieved through application of a substance known as “DYE”. Dyes are chemical compounds that attach themselves to fibres or surface shells to impart colour (Vital et al., 2016). Archaeological evidence has proved that the practice of dyeing has been widely carried out for over 5,000 years especially in India and Phoenicia (Booth, 2000). Dyes could be obtained from natural and synthetic sources. Those dyes used in ancient times were obtained from natural sources such as plants, insects, animals and minerals; with very little or no processing (Nagia and El Mohamedy, 2007). However, the greatest source of natural dyes has been from plant materials such as roots, berries, bark, leaves, wood, fungi and lichen but only a few have ever been used on a commercial scale. Examples of such natural dye are woad, indigo, saffron and madder (Hunger, 2003).

On the other hand, synthetic dyes are artificial or man-made. They are derived from coal and petroleum products or sometimes in combination with mineral derivatives. The first man-made organic aniline dye- mauveine, was accidentally discovered in 1856 as result of a failed attempt at total synthesis of quinine. Other synthetic dyes have since been produced, such as fuchsine, safranine, and induline (Zolinger, 1987; Zolinger, 2003). These dyes are cheaper when compared to the cost of natural dyes. They can be manipulated to produce variety of colours, have good levelling and high colour fastness (Rosa et al., 2018).

### 2.2 Emergence of synthetic dyes

The art of fabric colouring has been practiced by mankind since 3500 BC. In the year 1856, William Henry Perkin; a teenage English chemist in his laboratory researched for a better cure for malaria. He accidentally produced the first synthetic dye- Mauveine (a synthetic form of quinine that is derived from the bark of cinchona tree). During his experiment using coal tar to create this new form, he however noticed a rich purple hue. This was immediately sent to dye houses where it was successfully used as textile dye. Perkin thereafter left the Royal College of Chemistry in London and started synthetic dyes manufacturing (Hubner, 2006).

Following Perkin’s discovery, the use of natural dyes became a thing of the past as most textile industries in Europe and North America embraced synthetic dyes. In today’s world, there are more than 10,000 commercial dyes available and over 700,000 tons are produced annually (Owamah et al., 2013). Synthetic dye is preferable because it comes cheaper, can be produced in large

quantity and can be manipulated to variety of bright colours. The colours also could stick to fabric fast and do not fade easily (Rosa et al., 2018). The increased demand for synthetic dyes have contributed to becoming one of the main sources of severe environmental pollution today (Kant, 2012).

### 2.3 Classification of synthetic dyes

'Dye can be defined as a coloured substance that has an affinity to the substrate to which it is applied to' (Booth, 2000). According to Rehman et al. (2020), 'Dyes are complex unsaturated organic substances that absorb light and give colour to the visible region'. Chromogene-chromophore conjugate system (electron acceptor), resonance of electron (delocalized  $\pi$ -electron of aromatic ring) and solubility in water are the main features of synthetic dyes. Chromogene is an aromatic ring of benzene, naphthalene or anthracene, which binds chromophore (e.g., azo ( $-\text{N}=\text{N}-$ ), methine ( $-\text{CH}=\text{}$ ), carbonyl ( $=\text{C}=\text{O}$ ), etc.) in double conjugated links (Swan and Zaini, 2019). The colour imparting ability of dye is due to electromagnetic absorption of the conjugate system while their solubility in water is enhanced by the presence of electron donor-ionisable functional groups known as auxochrome (e.g., amino ( $-\text{NH}_2$ ), carboxyl ( $-\text{COOH}$ ), hydroxyl ( $-\text{OH}$ ), etc) (Swan and Zaini, 2019). They intensify the colour and confer the binding capacity of dye onto fibres (Saini, 2017). Application of dyes to fabric are usually in aqueous solution and sometimes require a mordant to improve its fastness (Benkhaya et al., 2020).

Classification of dyes are based on their (i) solubility in water- acidic/anionic dye, basic/cationic dye and non-ionic dye; (ii) chemical composition- azo, anthraquinone, carotenoid, acridine, quinoline, indamine, diphenyl methane, xanthene sulphur, indigoid, amino- and hydroxy ketone, phthalocyanine, inorganic pigment(Saini, 2017); (iii) type of application- acid, basic, mordant, reactive, direct, disperse, sulphur, pigment, vat, azo dyes (Saini, 2017). Major classification with regards to their industrial application are briefly discussed below and examples of these dye class with their chemical structures are presented in Table 2.1.

i. Acid Dyes: These are water-soluble anionic dyes. Structurally, they have one or more sulfonic acid or other acidic group substituent. Ability to stick to fibre is due to salt formation between anionic group on the dye and the cationic group on the fibre (Benkhaya et al., 2017). They are best used for dyeing wool, silk, nylon, modified rayon, modified acrylic, and polyester fibres in neutral to acid bath. Most synthetic food colour fall under this category of dyes.

ii. Basic Dyes: These are water soluble cationic dyes. Dyeing process with basic dye often requires addition of mordant like acetic acid to the dye bath for maximum uptake of dye onto the fibre. They are typically used on acrylic fibre, wool and silk (Benkhaya et al., 2017).

iii. Direct Dyes: These are water soluble and are often used for cotton, wool, silk, nylon and leather. Electrolytes (salts like sodium chloride, sodium sulphate or sodium carbonate) are added to the dye bath to control the rate of absorption. They are also used as pH indicators and biological stains (Burkinshaw and Salihu, 2017).

iv. Disperse Dyes: these are non-ionic dyes, insoluble or sparingly soluble in water (Clark, 2011). Dyeing process here is carried out in a pressurized dye bath and temperature of about 130°C in the presence of dispersing agent. Disperse dye were developed to dye acetate fibres such as polyester, acrylic, aramid, modacrylic, nylon, and olefin (Benkhaya et al., 2017).

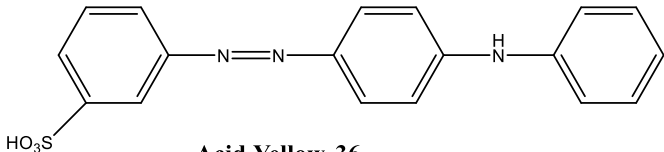
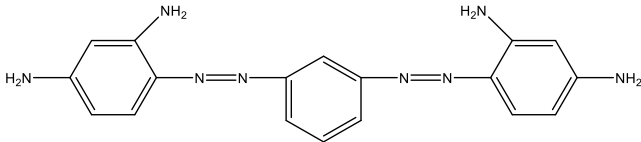
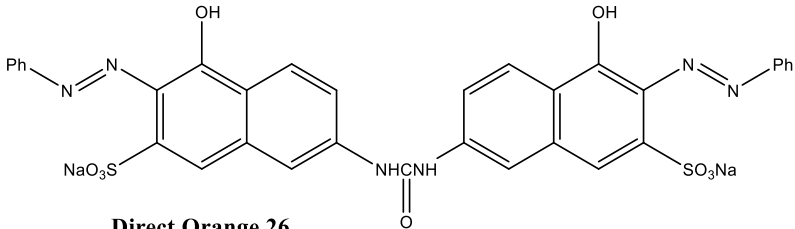
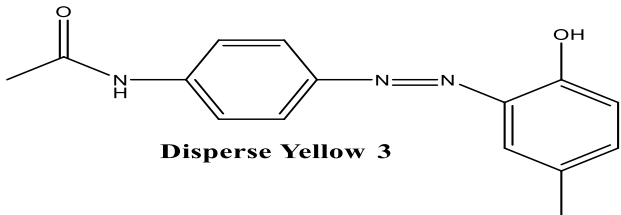
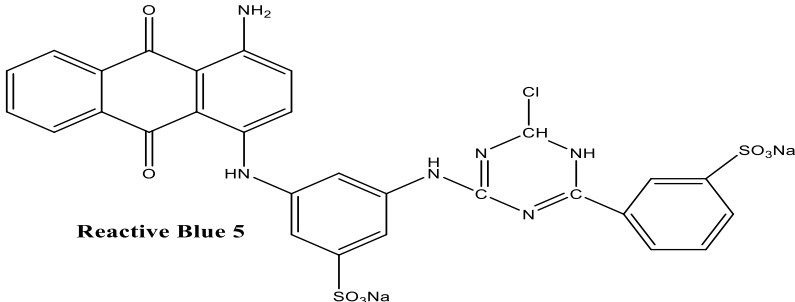
v. Reactive Dyes: These are used on cotton, flax, viscose rayon, silk, wool, and nylon and are often used with disperse dyes. The existence of covalent bond that attaches reactive dye and natural fibre make them permanent and more lasting on fabric (Farouk and Gaffer, 2013).

vi. Sulphur Dyes: This is a low-cost insoluble dye. It is applied by heating fabric in a solution of organic compound usually a Nitrophenol derivative and sulphide or polysulphide. They come in mostly dark shades of black, brown, and navy blue and mostly used for cotton material (Clark, 2011).

vii. Vat Dyes: This is insoluble in water and becomes soluble when reduced in an alkali. It can be made water insoluble again by oxidizing the dyed fabric. These are used to dye cotton, sportswear, prints, drapery fabrics, and cotton polyester blends (Burkinshaw and Salihu, 2017).

viii. Azoic Dyes: These are produced directly within the fibre by treating the fibre with diazoic and coupling component. The reaction under suitable conditions like low temperature produce a wide insoluble coloured molecule with the fibre (Gao et al., 2012). Although dyes under this group are widely used in textile industries because of their unique effectiveness but the toxic nature of the dye and its harmful effect on the environment is of great concern (Gao and Cranston, 2008). It was estimated that 130 of 3,200 azo dyes in use can undergo degradation to form carcinogenic aromatic amines (Yaneva et al., 2012). Common example of dye under this group is Congo red (Figure 2.8). Congo red is a benzidine-based anionic disazo dye; with commercial trade name like Direct Red 28, Benzo Congo Red, Direct Red 28. It turns blue in acidic solution and remains red in alkaline solution. It is used as an indicator and as a biological stain. Congo red is the first

synthetic azo dye produced for dyeing cotton. It has been widely used in textile, tannery, printing and dyeing, paper, rubber and plastics industries, and consequently found in their effluents (Purkait et al., 2007; Mittal et al., 2009; Ahmad and Kumar, 2010; Wang et al., 2011). Treatment of such effluents is problematic because congo red is highly resistant to bio and photo-degradation due to its complex aromatic structure, physicochemical, thermal, and optical stability properties (Smaranda et al., 2011; Rao and Rao, 2016). It is toxic to plant and animal; also has carcinogenic and mutagenic effect in humans (Sarkar et al., 2017).

Acid Dye	 <p style="text-align: center;"><b>Acid Yellow 36</b></p>
Basic Dye	 <p style="text-align: center;"><b>Basic Brown</b></p>
Direct Dye	 <p style="text-align: center;"><b>Direct Orange 26</b></p>
Disperse Dye	 <p style="text-align: center;"><b>Disperse Yellow 3</b></p>
Reactive Dye	 <p style="text-align: center;"><b>Reactive Blue 5</b></p>

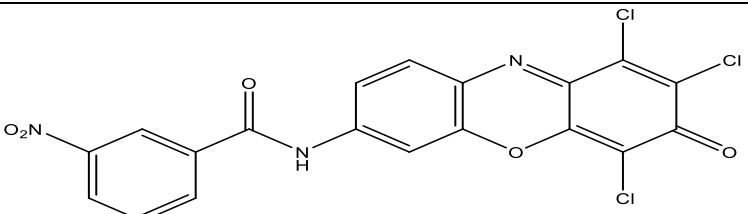
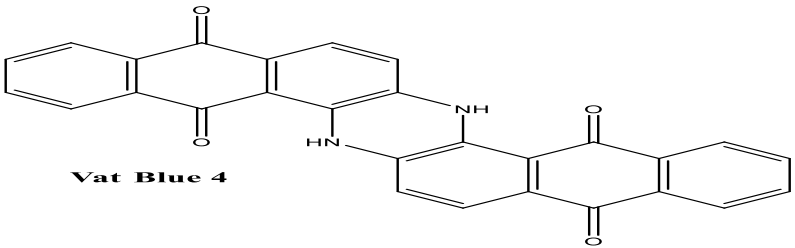
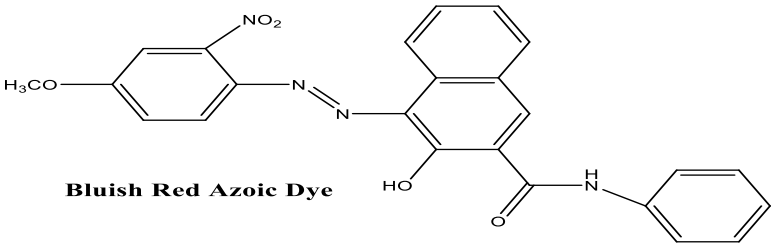
Sulphur Dye	 <p style="text-align: center;"><b>Sulphur Red 7</b></p>
Vat Dye	 <p style="text-align: center;"><b>Vat Blue 4</b></p>
Azoic Dye	 <p style="text-align: center;"><b>Bluish Red Azoic Dye</b></p>

Figure 2.1: Examples of dye classes and their chemical structures

## 2.4 Environmental impact of dye effluent

According to Cloete et al. (2010), textile industries are among industries responsible for consumption of about 80 % of fresh water in South Africa and in the same way, they are the largest consumer of dyestuff. Production of textile is generally accompanied by generation of lots of wastewater rich in dyestuff and other chemicals. This is so because about 15-20 % of dyestuff do not bind to the fabric and are washed off as effluent (Benkhaya et al., 2017). Almost half of dyestuff like reactive dye are lost into wastewater during textile production due to poor affinity of its hydrolysed form for fibres (Hassaan and El Nemr, 2017). These dyestuffs in effluent are potential hazards when discharged to land or water bodies causing severe harm to the entire ecosystem (Kant, 2012).

Sadly, it is very easy for dye consuming industries (cosmetics, food, pharmaceutical and textile) to shy away from hazardous effect of synthetic dyes on the environment because most dyes are known by their trade names and not their real chemistry (Sarkar et al., 2017). They are often traded with captivating names like Allura red AC, Direct black 38, Acid orange 5, Acid red 88, Direct blue 15, Brilliant black BN, Basic red 18, Mordant red 19 etc. These dyes are majorly reactive azo dyes which constitute over 70 % of more than 900,000 metric tons of global annual

production of synthetic dyes (Kanagaraj et al., 2015; Balapure et al., 2015). Azo dyes are complex natured, non-biodegradable aromatic compounds. Azo dyes and their degradation products have been found to have carcinogenic and mutagenic effect on living organisms.

Textile effluents are characterized by dense coloration due to significant amount of dyes present, high temperature and pH. These effluents are often discharge into the environment without treatment. This in turn causes adverse change in physico-chemical properties of soil and water, thereby reducing soil productivity and deterioration of water bodies respectively (Hassaan et al., 2017). Discharge of dye-contaminated wastewater brings about coloration, increased turbidity, temperature, pH, BOD, COD and TOS of the receiving water of the environment (Sen et al., 2016; Croce et al., 2017; Berradi and El Harfi, 2017). Coloration of surface water reduces its aesthetic value hence, making it unsuitable for recreation, agricultural and domestic purposes. It also prevents the penetration of sunlight needed for photosynthetic activity in water thereby leading to death of aquatic plants (Liang et al., 2017). It also interferes with the oxygen transfer mechanism at air-water interface. Depletion of dissolved oxygen in water is the most serious effect of textile effluent as dissolved oxygen is highly essential for respiration of fishes and other aquatic lives. Studies have established that dye effluent can reduce the level of dissolved oxygen in water and inhibit the reproduction of aquatic organisms (Cundari et al., 2019; Edokpayi et al., 2019). Due to non-biodegradability of azo dyes and other group of dyes, they get accumulated in sediments, fishes and other aquatic lives (Saini, 2017). Human exposure to dyes could be through feeding on marine lives, use of dye contaminated water and inhalation. Azo dyes and their degradation product like toxic amines are carcinogenic and mutagenic in human (Hassaan and El Nemr, 2017). They are absorbed into gastro-intestinal tract, skin and lungs causing allergies, eye and skin irritation, hypertension, damage of DNA, nuclear anomalies, bladder cancer, splenic sarcoma, hepatocarcinomas etc. (Sarvajith et al., 2018; Berradi et al., 2019).

Saini (2017) reported that dyes which are produced from recognized carcinogenic substances such as benzidine and other aromatic compounds are the most problematic dyes. The azo dyes such as direct black 38, azodisalecylate and their breakdown derivatives like benzidine, its derivatives, many anilines nitro semis, dimethyl amines etc. are known to cause cancer in human and animals (Saini, 2017). The summary of the few commonly used dyes relevant to this study and their hazardous effect on human is presented in Table 2.1.

## **2.5 Review of dye sequestration methods**

Dye effluents contain synthetic dyes which are hazardous to the environment. Due to the environmental and health concerns associated with the dye effluents, several methods of dye removal from wastewater have been employed. These methods are chemical, biological and

physical methods. Often, effectiveness of these methods depend on the dye types in wastewaters, therefore their particular application could be restricted (Zaharia et al., 2009). Reviews of various methods of treatment of industrial wastewater targeted at removing hazardous dyes, in order to make the water reusable or safely discharge into the environment are discussed below.

Table 2.1: Commonly used dyes and their hazardous effects

Type of dye	Application	Hazardous effect	References
Congo red	Used to dye cottons	Carcinogenic and mutagenic effect	Wekoye et al., 2020
Acid violet 7	Used in food, paper, cosmetic and textile industries	Chromosomal aberration, acetylcholinesterase activity inhibition, membrane lipid peroxidation	Mansour et al., 2010; Sarkar et al., 2017
Malachite green	Used as dye staff in silk, leather and paper. Used as antimicrobial in aquaculture	Carcinogenic and mutagenic effect, chromosomal fractures, teratogenicity and respiratory toxicity. Significantly alters biochemical parameters of blood in fish. Histopathological effects of MG include multi-organ tissue injury	Srivastava et al., 2004; Sarkar et al., 2017
Methylene Blue	Used in medication and Biological staining. used for printing calico, dyeing, printing cotton, tannin and dyeing leather	Skin, eye irritation. GIT irritation with symptoms like nausea, vomiting and diarrhea. Also cause methemoglobinemia, cyanosis, convulsions, tachycardia, and dyspnea.	Makeswari et al., 2016
Rhodamine B	Wide application in paint, textiles, paper and leather industries	Carcinogenic and mutagenic	Jain et al., 2007; Kooh et al., 2016
Crystal violet	Used in ink, paper and textile industries. Also used in medication and biological staining	Mitotic poison, potent carcinogen and clastogene promoting growth of tumour	Mani and Bharagava, 2016
Methyl orange	Used as pH indicator Used in food and textile industries	Eye and skin irritation. respiratory disorder. Mutagenic and carcinogenic	Chaukura et al., 2017
Reactive brilliant red	Extensively used in textile due to its attractive color and high fastness	Inhibit function of human serum albumin, may attach to body protein or enzyme, causing malfunctioning	Li et al., 2010
Disperse red 1 and disperse red 13	Used as textile dyes	Mutagenic to salmonella and human beings too. May affect the activity and composition of microbial communities	Chequer et al., 2015; Mahmood et al., 2016
Reactive Black 5 (sulfonated azo dye)	Used as dye staff	Inhibit nitrogen use efficiency of plant, lower the urease activity, mutagenic and carcinogenic effect	Topac et al., 2009; Dave et al., 2015



### 2.5.1 Chemical Methods

Chemical methods involve processes such as oxidation, ozonation and photocatalysis. Oxidation process involves conversion of dye into less toxic compound or biodegradable organic compound using oxidizing agents like chlorines, Fenton reagents, ozone, hydrogen peroxide, UV/ozone etc. (Saini, 2017). The effectiveness of this process is dependent on the oxidizing reagent ( $\bullet\text{OH}$ ) radicals generated. These radicals attack the chromophores, leading to the production of organic peroxide radicals and its finally converted to  $\text{CO}_2$ ,  $\text{H}_2\text{O}$  and inorganic compounds (Antoniadis et al., 2010). The most common oxidising agent in use is Fenton's reagent containing Iron ( $\text{Fe}^{2+}$  and  $\text{Fe}^{3+}$ ). Fenton's reagent is inexpensive and easy to handle compared to other reagents. The removal efficiency of this process depends on the production of the oxidant, hydroxyl radicals which show higher removal percentage at higher dyes concentration. This method as reported in literature was found to be relatively effective for Malachite Green dye with 99 % removal efficiency (Hameed and Lee, 2009) and for Crystal violet dye with 98.2 % removal efficiency (Su and Wang, 2011). However, the limitation of this process is that these reagents are poisonous; causing secondary contamination to the biological treatment system used for the post treatment than the original textile dyes (Arslan-Alaton et al., 2008). Also, industrial application of this process is not feasible due to excess amount of ferric hydroxide sludge generated and the hazards associated with its disposal (Sharma and Kaur, 2016).

Ozonation is a very effective treatment process for decolourization of textile effluent as ozone ( $\text{O}_3$ ) attacks the nitrogen conjugated double bonds which are often responsible for the colour (Gao et al., 2012). The decomposition rate of ozone is influenced by solution pH and initial dye concentration. Ozone rapidly decomposes to yield hydroxyl radical in basic medium but can directly react with organic substrates as an electrophile in acidic medium (Turhan et al., 2012). This process is advantaged because it does not form sludge due to complete disintegration of dyes (Sharma et al., 2013). However, ozone has a very short half-life, and require a high voltage to run a continuous process thus, increases the operational cost (Robinson et al., 2001; Tushar and Dawood, 2014). According to literature, ozonation has been found to have good removal of reactive dyes, moderately in removal of basic dyes and poor result was achieved with disperse dyes. Approximate value of 98 % removal efficiency was achieved for Rhodamine-B dye with ozonation method (Thao and Nguyen, 2017).

Photocatalysis is used in the removal of organic contaminants such as dyes from wastewater. Photocatalyst selection depends on dye properties as some dyes are resistant to photo-degradation process (Kabra et al., 2004). Photocatalysis has feasible applications in wastewater treatment as it can operate at ambient temperature and pressure thus reduce total operating cost (Chong et al., 2010). Also, complete mineralization of organic pollutant to carbon dioxide, water

and inorganic compounds is achievable (Rashed et al., 2017). In contrast, some photocatalyst undergo degradation and produce toxic products. Previous studies have successfully employed photocatalytic process in the removal of dyes like congo red (Shaban et al., 2017), safranin-T (Abukhadra et al., 2018) and Basic red 46 (Elhadj et al., 2020).

### 2.5.2 Biological Methods

Biological methods can be grouped into Aerobic and Anaerobic processes. Aerobic process is carried out with microorganisms such as algae, bacteria and fungi. Bacteria are classified as mono-oxygenase or di-oxygenase enzymes and they are utilised as catalyst for the incorporation of oxygen into the aromatic ring of organic compounds such as azo dyes and reactive dyes (Dos-Santos et al., 2007). Researchers have investigated bacteria decolourization of dye such as Blue Bezaktiv dye BB 150 by lyophilised *bacterial consortium* (Khouni et al., 2012). Bio-removal of methylene blue was carried out with bacteria isolated from contaminated soil with 82 % removal efficiency (Eslami et al., 2017). Some algae species have been tested for bio-decolourization of textile effluent. 106 *Chlorella sp.*, *Cosmorium sp.* and *Euglena sp.* have been tried out for the removal of Malachite green dye and found to have 92 %, 91 % and 87 % removal efficiency respectively (Khataee et al., 2009).

Treatment of dye effluent with fungi is mostly preferable to bacteria and algae. This is because fungi have high capacity for biodegradation of dyes as they can produce extracellular ligninolytic enzymes like laccase, manganese peroxidase and lignin peroxidase which are required to breaking down complex organic compounds (Tan et al., 2013). For example, white-rot fungi such as *Dichomitus*, *squalens*, *Daedalea flavida*, *Irpex flavus* and *Polyporus sanguineus* have been widely used in the decolourization and degradation of textile effluent containing chromophoric groups of dyes (Chander and Arora, 2007). Removal of acid red B by *Pichia sp.* (Qu et al., 2012) and azo dyes by *Candida tropicalis* (Tan et al., 2013) have been reported in literature. Bio-removal of Methylene blue has also been carried out with *Aspergillus fumigates*, dead fungal sp. with 80 % removal efficiency (Abdallah and Taha, 2012). The utilization of Algae, bacteria and fungi for decolourization and degradation of dyes from textile wastewater have the advantages of cost effectiveness and the ability to completely mineralize dyes without producing toxic by-products (Dawkar et al., 2010). However, this process is not applicable for real textile wastewater treatment because it is a very slow process and provides a suitable environment for the growth of microorganisms (Toor, 2010). Sometimes the effluent temperature does not favour the activity of microorganism in effluent treatment. Hence, scaling up is a major challenge.

Anaerobic process takes place in the absence of oxygen. Under this process, complex organic compound is decomposed so that they can be further treated either aerobically or by other dye

removal methods (Balamurugan et al., 2011). The biodegradation involves decolourization stage where the dye azo linkage of nitrogen double bond is broken down by microorganisms, followed the second stage where degradation of the aromatic amines occurs (Vander et al., 2005). Researchers investigated the use of bacteria for dye removal under anaerobic conditions such as removal of Methyl orange and Naphthol green B by *Shewanella oneidensis* MR-1 (Cao et al., 2013) and Reactive red by *Halomonas variabilis* and *Halomonas glaciei* (Balaamurugan et al., 2011). The disadvantage of this process is that post treatment under aerobic conditions is needed and it produces toxic by-products. Thus, a combination of anaerobic and aerobic process is required for the sequestration of dyes (Tushar and Dawood, 2014).

### 2.5.3 Physical methods

These include membrane filtration (micro-filtration, nano-filtration, ultra-filtration and reverse osmosis) and adsorption. However, physical methods suffer problems like excess sludge production and disposal. They are effective only when effluent volume is small.

#### Membrane filtration

This method is employed to check organic contaminants and microorganisms present in wastewater. The common membrane filtration types are:

**Micro-filtration:** It is mostly employed for treatment of dye baths containing pigment dyes and for following rinsing baths (Ramesh et al., 2007; Saini, 2017). Micro filtration is effective for removal of turbidity, suspended solids, colloids from effluents or macromolecules with particle size of 0.1 to 1 micron. Membranes used here are made from polymers such as Poly (Ether Sulfone), Poly Tetrafluoroethylene (PTFE), Poly (Vinylidene Fluoride), Poly (Vinylidene Difluoride), Poly (Sulfone), Polypropylene, Polycarbonate, etc. Ceramic, glass, carbon, zirconia coated carbon, alumina and sintered metal membranes are used for operation that requires extraordinary chemical resistance and high temperature (Saini, 2017).

**Ultra-filtration:** This technique has 31-76 % removal efficiency for dyes in wastewater and often used as pre- treatment for reverse osmosis. However, it can effectively eliminate macro molecules and particles. The treated wastewater cannot be reused for sensitive processes, such as textile dyeing (Ramesh et al., 2007) but suitable for rinsing, washing, etc. Membranes here are made from polymers such as nylon-6, polytetrafluoroethylene (PTFE), polyvinyl chlorides (PVC), polysulfone, polypropylene, acrylic copolymer, etc (Saini, 2017).

**Nano-filtration:** this method is mostly combined with adsorption for the remediation of coloured effluents from the textile industry since nano filtration components are very sensitive to fouling by

colloidal material and macromolecules. Membranes used here are usually made from cellulose acetate, aromatic polyamides, Inorganic materials like carbon-based membranes, ceramics, zirconia, etc. These can remove organic compounds with low-molecular weight, large monovalent ions, divalent ions, hydrolysed reactive dyes, and dyeing auxiliaries (Saini, 2017).

Reverse osmosis: This is a pressure driven membrane process also known as hyper filtration (Vijayageeta et al., 2014). This technique is effective for the removal of hydrolysed reactive dyes, most types of ionic compounds, chemical auxiliaries in one step (Ramesh et al., 2007). The influent must be cautiously pre-treated because this technique is very sensitive to fouling like Nano filtration. Reverse osmosis membranes are usually made from cellulose acetate, aromatic polyamides, and some inorganic materials (Saini, 2017).

## 2.6 Adsorption

Adsorption is a process by which ions, atoms or molecules of the adsorbate in an aqueous solution adhere to the surface of the adsorbent. The adsorbate can be gas, liquid or solute in the aqueous solution while adsorbent is the solid or liquid unto which the adsorbate molecules accumulate. Adsorption process can be physical and chemical adsorption. In physical adsorption (Physisorption), the adsorbates get accumulated on the surface of the adsorbent and bonded by physical forces such as Vander Waals forces, hydrophobicity, hydrogen bond, polarity, static interaction, dipole–dipole interaction,  $\pi$ - $\pi$  interaction. In chemical adsorption (Chemisorption), the adsorbate is chemically bonded to the adsorbent's surface by exchange of electrons (Artioli, 2008; Tushar and Dawood, 2014). The efficiency of adsorption process depends on the physical and chemical properties of the adsorbate and adsorbent. Properties such as molecular weight, molecular structure, molecular size, polarity and solution concentration of the adsorbate and particle size, surface area, surface charge of the adsorbent (Yagub et al., 2014).

Adsorption process is superior compared to other available methods of wastewater treatment because it is highly efficient, simple to design, easily operated and sensitive to toxic substances (Feng et al., 2011; Felista et al., 2020). Selection of adsorbent is based on the adsorption capacity, surface area, availability, and operational cost. Industrial waste materials such as metal hydroxide sludge, fly ash, red mud, activated carbon, coal ash, peat and clay have been used as adsorbent for decolorization process (Vital et al., 2016). Adsorption process using commercial activated carbon as adsorbent is found to be very efficient for effluent treatment.

Activation of adsorbent may either by physical activation or chemical activation. Reagents such as organic and inorganic acids, bases, zinc chloride are mostly used under different preparatory conditions for chemical activation (Tay et al., 2009). Alkali hydroxides and zinc chloride are not

suitable reagents for activation due to their corrosive natures and the harmful impact of their disposal to the environment (Gurten et al., 2012). The production of activated carbon thus depends on the reagent used, precursor properties, impregnation ratio, activation time and temperature. Advantage that chemical activation has more than physical activation is that it is a single step process i.e. carbonization and activation are carried out at the same time at relatively low operating temperature and higher yield (Tay et al., 2009; Fathy et al., 2012). In physical activation, carbonaceous materials are exposed to carbon dioxide, air mixture or steam under a very high temperature, thereby improving the porosity of the activated materials. After activation, many pores, particularly micropores, were generated due to the oxidation of partial carbon atoms by carbon dioxide and steam (Liu et al., 2012). Activated carbon is preferably produced in granular and powder forms to allow for large surface area in its application as adsorbents. Activated carbon is widely applied for various treatment in oil and gas, food, chemical industries, solvent recovery, air pollution control and in hydrometallurgy industry for the recovery of gold and silver (Sugumaran et al., 2012).

#### 2.6.1 Review of adsorption process

Despite enormous use of activated carbon in wastewater treatment, commercial activated carbon remains an expensive material (Akar et al., 2009). Recent research interests are focusing on the use of agricultural biomass as adsorbent for removal of hazardous dye from industrial effluent. Agricultural wastes usually have high molecular weight due to the presence of lignin, cellulose and hemicelluloses components (Salleh et al., 2011; Tushar and dawood, 2014). These solid wastes are biodegradable and available in large quantities with little or no value and often cause a disposal problem. Better waste management plan is provided by recycling these agricultural wastes into useful products; thereby solving their disposal problem. Few of the agricultural wastes that have been used as bio-sorbent for removal of synthetic dye from industrial effluent are: sesame hull (Feng *et al.*, 2011), rice husk (Abbas, 2013), cassava peel (Schwante *et al.*, 2016), corncob and corn husk (Malik *et al.*, 2016), Orange peel (Ashok et al., 2016), mango peel (Jawad *et al.*, 2017), Coconut shell (Aljeboree et al., 2017), pine (Schorr et al., 2018), Palm flower (Magdalena et al., 2018), Marula seed husk (Edokpayi et al., 2019) amongst others.

Various study has been carried out using agricultural plant waste materials as biosorbent for sequestration of dyes in wastewater. Edokpayi et al. (2019) carried out a study to explore the potential use of an agricultural waste- Marula seed husk to decontaminate methylene blue (MB) from aqueous solution. Maximum adsorption capacities of 28.25 mg/g (313 K), 29.32 mg/g (333 K) and 33.00 mg/g (343 K) were evaluated from the experiment. This experimental result proved Marula seed husk as suitable adsorbent for bioremediation of dyes from aqueous solution/wastewater. An agricultural waste- rice straw was used as an adsorbent material for

removal of Malachite green dye from aqueous solution. Rice straw was recorded to consist of cellulose (37.4 %), hemicellulose (45 %), lignin (5 %) and silica ash (13.1%). Experimental result revealed that unmodified rice straw showed less adsorption of about 9% while, rice straw modified with citric acid showed more adsorption of 26 % for Malachite Green dye (Gong et al., 2018). Ashok et al. (2016) researched on the utilization of orange peel as adsorbent for the removal of dyes from wastewater and to establish it as a standard wastewater treatment process for textile dyeing industry. The materials were obtained and treated for the removal of dyes at different doses. Batch adsorption experiment was carried out for finding the effects of adsorbent's dosage, agitation speed, pH and retention time on the removal of dyes from the wastewater. The experiment showed good dye removal percentage of 88.04 at pH of 10, dosage of 2.5 g/L, retention time of 120 minutes and rpm of 90.

Malik et al. (2016) also investigated the potential of corn husk as biosorbent for adsorption of methylene blue (MB) dye from synthetic dye effluent. The influence of operating conditions like contact time, initial dye concentrations, adsorbent doses, pH on dye removal were examined. The influence of pH of the solution was found to be the greatest on adsorption process as maximum dye removal of 90 % was achieved at pH 6.2 within 15 min of contact time. These experimental results favour the adsorption process for corn husk-based adsorbent. *Parkia speciosa* pod also showed extremely high potential in dye (Coomassie Brilliant Blue R-250) removal application especially for wastewater treatment. The optimum adsorption of 83.4 % was obtained with the optimal conditions of pH 5.0, dosage of 0.10 g and the contact time of 70 min. Close agreement was found between both the experimental and predicted values. Therefore, it was suggested that *Parkia speciosa* pod could be a potential natural dye adsorbent (Ngoh et al., 2015). The potential of Rice Husk on the removal of four types of dyes pollutant which were methylene blue, Congo red, brilliant green and crystal violet from wastewater was investigated. Results showed that the highest removal efficiency was (95.81, 93.44, 96.62 and 96.35) % for brilliant green, Congo red, crystal violet and methylene blue dyes respectively from aqueous solution. These results further established Rice Husk as an efficient adsorbent for dyes sequestration (Abbas, 2013).

Various biosorbent have been used in previous research, for sequestration of congo red from aqueous solution. Wekoye et al. (2020) successfully investigated the potential of utilization of dried cabbage waste powder as an agricultural waste biosorbent for congo red removal from aqueous solution. The results of the batch experiment conducted, and other experimental parameters favoured congo red removal with adsorption efficiency of 90 %. Two novel biosorbents were prepared from shrimp shell and their adsorption potential of congo red from aqueous solution were investigated by Zhou et al. (2018). The experimental results obtained showed that modified shrimp shell powder had higher adsorption capacity (288.2 mg/g) than raw

shrimp shell powder. It was concluded that shrimp shell powder exhibited enough advantage of large adsorption capacity, low cost, simple processing method and high specific gravity. This made shrimp shell to be considered a suitable biosorbent for the removal of dye from wastewater.

In addition, Edokpayi et al. (2015) used mucilaginous leaves prepared from *Dicerocaryum eriocarpum* for the adsorption of lead (II) ion from aqueous solution. Batch experiments were conducted on laboratory synthesised wastewater under optimized conditions of contact time, adsorbent dosage, pH and initial  $Pb^{2+}$  concentration at 298 K. 95.8 % and 96.4 % removal efficiencies were obtained from solutions of 10 mg/L and 12 mg/L of lead (II) ion concentrations respectively. The results obtained proved that mucilaginous leaves from DE plant can be used as adsorbent for lead (II) ion removal from wastewater. A study conducted by Odiyo et al. (2017) investigated coagulation efficiency of *Dicerocaryum eriocarpum* (DE) leaves in the removal of turbidity from raw water. Mucilage from DE leaves was extracted with deionized water, potassium chloride and sodium chloride solutions. The result obtained from the experiment showed higher coagulation efficiency of 99 % with modified mucilage extracts than unmodified extract. Reduction in turbidity of the treated water sample established modified DE leaves as suitable coagulant for water treatment. Chanda et al. (2019) also aimed at describing the removal of aniline blue from aqueous matrices using *Litchi chinensis* peel as an eco-friendly adsorbent. The experimental results showed that Langmuir adsorption capacity was found to be 5.2 mg/g. They concluded that *Litchi chinensis* can remove aniline blue from aqueous solution. Following established successes of utilization of *Litchi chinensis* seeds and *Dicerocaryum eriocarpum* leaves, this novel study further seeks to investigate the adsorption efficiency of *Litchi chinensis* peel and *Dicerocaryum eriocarpum* seed in sequestration of congo red and other selective dyes from wastewater.

Adsorption process has been proven as a very effective method of dye sequestration in effluent treatment (Ahmad and Kumar, 2010; Sharma et al., 2011; Farias et al., 2018). The shortcomings of adsorption process as clearly pointed in Table 2.2 has been overcome. Problem of expensive activated carbon adsorbent has been solved by recent research focusing on the use of agricultural wastes/plant materials as biosorbents over expensive activated carbon. Challenges of disposal of adsorbent has also been surmounted by ability to reuse spent biosorbent through recovery of used biosorbent by desorption or regeneration experiments. Plant materials with low surface area could also be chemically modified to increase the surface area for better adsorption capacity.

Table 2.2: Summary of dye sequestration methods

Dye Sequestration method	Advantage	Disadvantage
Adsorption	Simple to design and operate. High adsorption capacity for all dyes. No toxic substance is generated.	Expensive adsorbent. Disposal problem of adsorbent. Low surface area for some adsorbents.
Membrane filtration	Good removal capacity for all dyes with high quality effluent.	Not suitable for large scale effluent treatment. Production of sludge. High pressure needed. Clogging of pores. Membrane fouling.
Oxidation (Fenton reagent)	Effective process and cheap reagent.	Sludge production and disposal problem.
Ozonation	No sludge production.	Very short half-life (20 min) and costly operational process.
Photocatalysis	Economically feasible and inexpensive operational cost.	Some photocatalyst get degraded into toxic by-products.
Aerobic degradation	Efficient in the removal of azo dyes and low operational cost.	The process is very slow. Provide suitable medium for microorganism's growth.
Anaerobic degradation	By-products can be utilised as energy sources.	Further treatment is needed under aerobic conditions. Methane and hydrogen sulfide are produced as by-products.

Source: Srinivasan and Viraraghavan, 2010; Pang and Abdullah, 2013; Tushar and Dawood, 2014

### 2.6.2 Modification of adsorbent

Modification brings about increase in adsorption efficiency of adsorbent towards various types of pollutant due to chemisorption of pollutant onto adsorbent surface (Wang et al., 2016). It also reduces the amount of adsorbent required for adsorption process (Anbia et al., 2016). Adsorbent could be treated with chemicals like inorganic or organic acids, surfactant, oxidizing agents, metal salt (Girish, 2018). However, the structure of adsorbent could readily be destroyed by modifying with strong inorganic acid such as sulphuric acid and hydrochloric acid. Also, the cost of these



modifiers, toxicity and complicated modification techniques could limit their applications (Zhang et al., 2019). Therefore, it is important to find an appropriate, mild, eco-friendly chemical for adsorbent's modification without compromising on the dye removal efficiency.

Citric acid is an example of a non-toxic organic acid that is cheap and naturally abundant in biomass. Structurally, citric acid contains –OH and –COOH linking groups which are not only effective for loading citric acid on adsorbent but also good chelating groups for removal of pollutants like organic dyes and heavy metals from wastewater (Zhang et al., 2019). This explains why citric acid will moderately modify any adsorbent without causing secondary pollution (Zhou et al., 2018). Recent research has reported modification of adsorbents with citric acid for adsorption of various dyes (Wang et al., 2017; Yan et al., 2018; Ren et al., 2018; Zhao et al., 2018; Zhang et al., 2019). The common fact is that they all achieved higher removal with modified adsorbents than raw ones. As stated in experimental results of Zhang et al. (2019), congo red (CR) removal on raw Bentonite (RB) was 54 % after 450 min while that of citric acid modified Bentonite (CAB) was 87 % after 120 min. By comparing the CR removal efficiency of RB and CAB, one can conclude that the modified CAB had faster reaction kinetics, hence can be considered significantly cost effective on industrial level applications (Toor et al., 2015; Tarmizi et al., 2017).

Therefore, citric acid was carefully chosen in this study to modify raw *Litchi chinensis* peels and raw *Dicerocaryum eriocarpum* seeds to obtain citric acid modified biosorbents, which were thereafter used alongside with raw ones; for the adsorptive sequestration of congo red (and some selective dyes) from aqueous solution. The effects of experimental parameters such as contact time, adsorbent dosage and size, adsorbate concentration, temperature, and pH were systematically studied.

## **2.7 Experimental parameters affecting adsorption of dye**

There are physico-chemical parameters affecting adsorption of dye in aqueous solution. The effects of these factors when taken into consideration will not only help optimum adsorption of dyes from aqueous solution but also help in development of industrial scale treatment process for effluents. Some of these factors are briefly discussed below:

### **2.7.1 Effect of contact time**

This explains the amount of time adsorbent is in contact with dye solution while other parameters are kept constant. Generally, when adsorbent is agitated in dye solution, a sharp and steady increase is noticeable in the rate of adsorption at the initial stage. Afterwards, it reaches a state of equilibrium where little/no increase or even decrease is observed in the rate of adsorption. for

instance, Wanyonyi et al. (2014) recorded rapid increase in the uptake of congo red dye of over 64 % within the first 5 min of contact time, after which removal rate increased further and plateaued at about 90 min, achieving removal efficiency of 96 %. This behavioural pattern is as a result of strong affinity of adsorbent for dye molecule due to the presence of several adsorption sites on the adsorbent's surface at the initial stage. Thereafter, the adsorbent site gets saturated with the dye at increasing contact time. Also, repulsive forces between dye molecules and the adsorbent may contribute to the observed moderate rates of adsorption after the first 2-3 hours (Khan et al., 2015; Corda and Kini, 2018).

### 2.7.2 Effect of pH

Tushar and Dawood (2014) described the pH of a solution as a measure of molar concentration of hydrogen ions. Solution is said to be acidic when the solution pH is less than 7, basic when the solution has pH greater than 7, and neutral at pH 7. Solution pH strongly influences the efficiency of adsorption process, since variation in pH brings about variation in the degree of ionisation of the adsorptive molecule and the surface properties of adsorbent (Nandi et al., 2009). Usually, low pH solution leads to an increase in the removal percentage of anionic dye because of the electrostatic attraction between anionic dye and the positive surface charge of the adsorbent. At higher solution pH, there exists electrostatic repulsion between the negatively charged surface of the adsorbent and dye molecules, thus decreasing the adsorption efficiency or removal percentage of anionic dyes (Salleh et al., 2010). Examining previous studies, the optimum solution pH on the removal of anionic dyes such as Acid blue 15 by pomelo skin (Foo and Hameed, 2011), congo red by nut shells charcoal (Kaur et al., 2013), congo red by crab shell powder (Rao and Rao, 2016) and Reactive black 5 by macademia seed husk (Felista et al., 2020) were between pH 2-4. Conversely, high pH solution favours removal of cationic dye because the positive charge on the solution interface decreases and the adsorbent surface appears negatively charged (Salleh et al., 2010). From previous studies, the optimum solution pH on the removal of cationic dyes such as basic red 46 by pine tree leaves (Deniz and Karaman, 2011), methylene blue by *Ricinus communis* leaves (Makeswari et al., 2016) and methylene blue by marula seed (Edokpayi et al., 2019) were observed between pH 9-11.

### 2.7.3 Effect of adsorbent dosage

Most previous study has established that the effectiveness of varied adsorbent doses on dye removal determines the most economical minimum dosage. Generally, the dye removal percentage increases with increasing adsorbent dosage (Salleh et al., 2010). Increase of adsorbent dosages could bring about adsorption of larger amount of dye because of the availability of more active sites on the surface of the adsorbent (Ologundudu et al., 2016; Chanda et al., 2019). Previous study showed that the amount of congo red dye removal by activated

carbon was increased from 41-99.2 % with the increase of adsorbent dose from 0.1-20 g/L (Lafi et al., 2019). Also, the amount of congo red dye removal by pine bark was increased from 23.4-100 % with the increase of adsorbent dose from 1-10 g/L (Litefti et al., 2019).

#### 2.7.4 Effect of temperature

Temperature plays a very vital role in adsorption process because change in temperature either increases or decreases the adsorption efficiency of the adsorbent. Adsorption process is said to be endothermic when increase in temperature brings about increase in adsorption efficiency of the adsorbent. This may be due to fact that increase in temperature speeds up the migration of dye molecules and, also increases the number of active sites of the adsorbent due to bond rupture (Firas, 2013). However, the decrease of adsorption efficiency with increasing temperature indicates that the adsorption process is an exothermic one. This may be due to the fact that increasing temperature decreases the adsorptive forces between the dye species and the active sites on the adsorbent surface (Salleh et al., 2011). Experimental result showed that adsorption of methylene blue on treated rice husk adsorbent was an endothermic process (Lin et al., 2013), while adsorption of methylene blue on black tea waste adsorbent was an exothermic process (Lin et al., 2020). The amount of congo red dye removal by cabbage waste powder was increased from 64.81-85.21 % with temperature increases from 25-75°C, and an endothermic reaction (Wekoye et al., 2020).

#### 2.7.5 Effect of dye concentration

Influence of dye concentration on adsorption of dye from aqueous solution is of great importance. In general, increase in the initial dye concentration results to decrease in the dye removal efficiency which may be due to the saturation of adsorption sites on the adsorbent surface (Dawood and Sen, 2012). The amount of dye adsorption  $q_t$  (mg/g) increases with increasing contact time at all initial dye concentrations as reported by various researchers (Purkait et al., 2007; Sen et al., 2011; Foo and Hameed, 2011). This is so because the initial dye concentration provides the driving force to overcome the resistance to the mass transfer of dye between the adsorbate and the adsorbent phases (Tushar and Dawood., 2014).

### 2.8 Characterisation methods of plant materials

The functional group in adsorbent is found to be responsible for its several physical and chemical properties (Bandosz, 2009). Various methods or instrumentation are available for characterisation of the surface functional groups of plant material used as adsorbent in order to understand their properties or improve their applications (Moreno-Castilla, 2004; Shen et al., 2008; Calvino-Casilda et al., 2010). Examples of such characterisation methods used in various literatures for identification of properties of adsorbents are briefly described below:

### 2.8.1 Fourier Transform Infrared Spectroscopy (FTIR)

Infrared spectroscopy is commonly used for structural analyses of organic compounds. FTIR spectroscopy has the capability to detect specific bonds in a material by selective absorption of infrared radiation by various bonds within the compound thereby revealing the functional group present (Duran-Valle, 2012). FTIR is mainly used as a qualitative technique for the analysis of the chemical structure of materials and sometimes, as quantitative technique (Bandosz, 2009). Kowanga et al. (2016) performed FTIR analysis on *Moringa oleifera* seeds powder to determine the functional groups present. The results revealed the presence of amino, carboxyl, hydroxyl and carbonyl groups on the biomaterial which are responsible for biosorption of metals from aqueous solution.

### 2.8.2 Scanning Electron Microscopy - Energy Dispersive X-ray Spectroscopy (SEM-EDS)

Energy-dispersive X-ray spectroscopy (EDS) is usually coupled with scanning electron microscopes (SEMs). The combination of these two equipments for analysis allows for microscopy image of the surface of the test material and a pictorial diagram of the elemental composition of the material under investigation. This technique is mainly used to study the content and dispersion of dyes/metals on the surface of a carbonaceous material (Duran-Valle, 2012). Rapo et al. (2020) characterised powdered eggshell waste material using SEM-EDS analysis. The microscopy image displayed the surface morphology and EDS displayed the elemental distribution of major elements like calcium, magnesium, sulphur and phosphorous in the eggshell.

### 2.8.3 Brunauer, Emmett, Teller Technique (BET)

This technique was developed in 1938 and named after Stephen Brunauer, P.H. Emmett and Edward Teller. The Brunauer, Emmett and Teller (BET) technique is commonly used for determining the surface area of powders and porous materials. Nitrogen gas is generally employed as the probe molecule and is exposed to the material under investigation at liquid nitrogen conditions (*i.e.* 77 K). The surface area of the material is calculated from the measured monolayer capacity and knowledge of the cross-sectional area of the Nitrogen gas being used as a probe. The cross-sectional area of Nitrogen is taken as 16.2 Å<sup>2</sup>/molecule (Zielinski and Kettle, 2013). Study conducted by Lafi et al. (2019) on adsorption of congo red from aqueous solution presented surface area of raw coffee waste as 2.9 m<sup>2</sup>/g and that of activated carbon prepared from coffee waste as 219.69 m<sup>2</sup>/g. This reveals that activation of biomaterial increases its surface area, thereby improving its adsorption efficiency.

#### 2.8.4 X-Ray Diffraction (XRD)

XRD technique is used to estimate crystalline or amorphous degree in carbonaceous material (Pradhan and Sandle, 1999; Biniak et al., 2010) and also used to characterize the inorganic material (Pastor-Villegas et al., 1999). The information about the test material is obtained from the distribution of scattered radiation using X-rays. The observed diffraction pattern may then be converted to structural data. The degree of graphitization is a significant parameter because it shows the transition extent of carbon material from turbostratic to graphitic structure, and determines some properties of the material (Hussain et al., 2000; Zou et al., 2003). XRD characterisation of crab shell powder used for biosorption of congo red from aqueous solution revealed amorphous nature of the adsorbent material (Rao and Rao, 2016).

#### 2.8.5 Thermo Gravimetric Analysis (TGA)

Thermal analysis method is widely used for the characterization of materials. This technique is done by heating a sample in a carrier gas in order to induce thermal decomposition. By heating, the oxygenated groups are thermally decomposed, releasing CO, CO<sub>2</sub>, and H<sub>2</sub>O at different temperatures. The groups can be identified by decomposition temperature, type of gas released and can be quantified by the areas of peaks (Duran-Vale, 2012). Dipa et al. (2015) showed through TGA that the adsorbent's material has very high resistant to weight loss.

### 2.9 Adsorption Kinetics

Adsorption kinetic describes the solute uptake rate and evidently this rate controls the residence time of adsorbate uptake at solid-solution interface (Reddy et al., 2010). The most common models used for adsorption kinetics are Lagergren pseudo-first order, pseudo-second order kinetic models.

#### 2.9.1 Pseudo-first order

Pseudo-first order rate expression based on solid capacity is generally expressed as follows (Lagergren, 1898):

$$\frac{dt}{dq} = k_1 (q_e - q_t) \quad (2.1)$$

Where  $q_t$  and  $q_e$  are amounts of dye adsorbed (mg/g) at time  $t$  (min) and at equilibrium, respectively,  $k_1$  is the rate constant of adsorption ( $\text{l min}^{-1}$ ). Mathematically, it can be expressed as follows:

$$q_t = (1 - e^{-k_1 t}) \quad (2.2)$$

$$\log(q_e - q_t) = \log q_e - \frac{k_1}{2.303}t \quad (2.3)$$

Where  $k_1$  is first order constant;  $q_e$  (mg/g) is the amount of adsorbate adsorbed at equilibrium and at time  $t$ ;  $q_t$  is the amount of adsorbate adsorbed at time ( $t$ ). The slope and intercept of the plot of  $\log(q_e - q_t)$  vs.  $t$  give the values of  $k_1$  and  $q_e$  respectively. A linear plot of  $\log(q_e - q_t)$  against time ( $t$ ) with high correlation coefficient shows that the adsorption process is a pseudo first order process, which indicates a case of physisorption (Hameed, 2009).

### 2.9.2 Pseudo-second order

This is mathematically expressed as follows:

$$\frac{t}{q_t} = \frac{1}{k_2 q_e^2} + \frac{t}{q_e} \quad (2.4)$$

Where,  $k_2$  [(g/mg)/h] is the second order constants  $q_e$  (mg/g) and  $q_t$  (mg/g) the amount of dye adsorbed at equilibrium and at any time respectively. The slope and intercept of the plot of  $t/q_t$  vs.  $t$  give the values of  $q_e$  and  $K_2$  respectively (Ho and McKay, 1999). A linear plot of  $t/q_t$  against  $t$  with high correlation co-efficient indicates conformity to pseudo second order (Achmad *et al.*, 2012), which indicates a case of chemisorption (Qiu *et al.*, 2009). Kinetic adsorption data for most adsorption system is better represented by a pseudo-second order model. Experimental findings reported in literatures that conform to pseudo second order are kinetic of adsorption of Direct Red 23 unto uncaria gambir extract (Achmad *et al.*, 2012), Congo red and Reactive black-5 unto coffee waste (Wong *et al.*, 2020) and Methylene blue on black tea (Lin *et al.*, 2020).

### 2.9.3 Intra-particle diffusion

Intra-particle diffusion model is usually important to further ascertain the probable adsorption mechanism of dye unto adsorbent (Sen *et al.*, 2011). This model basically involves three steps which are, film diffusion, pore diffusion and, intra-particle transport. The slowest step among the three is called as the rate determining step (Corda and Kini, 2018). It can be mathematically expressed according to Weber and Morris, (1963) by the relationship:

$$q_t = k_p t^{0.5} + C \quad (2.5)$$

Where  $q_t$  is the amount of dye adsorbed (mg/g) at time  $t$  (min),  $k_p$  is the intra-particle diffusion rate constant (mg/g min) and  $C$  is the intercept (mg/L). The intercept gives an idea about the thickness of the boundary layer. The higher the value of  $C$ , the greater is the thickness (Corda and Kini, 2018). The calculated value of the slope of the initial linear portion is the intra-particle rate

constant. Adsorption of Malachite green onto CO<sub>2</sub> activated carbon gave good results for intra-particle diffusion model (Yu et al., 2017).

## 2.10 Adsorption Isotherms

Adsorption isotherm plays an important role in understanding the mechanism of adsorption. It explains adsorption capacity of an adsorbent i.e. how adsorbent interacts with the adsorbate. This interaction takes place on the surface of the adsorbent which may be considered as a monolayer or multilayer surface (Yagub et al., 2014). An adsorption isotherm represents plot of the concentration of the adsorbate adsorbed by the adsorbent against the concentration of the adsorbate remaining in solution at equilibrium (Goldberg and Criscenti, 2008). Major isotherm models presented in the literatures are as follows:

### 2.10.1 Langmuir Isotherm

The Langmuir isotherm is of the assumption that adsorption takes place at specific homogeneous sites within the adsorbent. This implies that, once the adsorbate molecules occupies a site, the adsorbent surface becomes saturated and reaches a state of equilibrium where no further adsorption can take place. The saturated monolayer curve is expressed by the Langmuir model's linear equation stated below, which has been successful for monolayer adsorption (Langmuir, 1916):

$$\frac{1}{q_e} = \frac{1}{q_{\max}} + \left( \frac{1}{K_L q_{\max}} \right) \frac{1}{C_e} \quad (2.6)$$

Where  $C_e$  is the equilibrium concentration (mg/L),  $q_e$  is the amount adsorbed at equilibrium (mg/g) and  $q_{\max}$  and  $k_L$  are Langmuir constants related to adsorption efficiency and energy of adsorption respectively (Ramathai et al., 2009). The constants  $q_{\max}$  and  $k_L$  can be calculated from the intercept and slope of the plot of  $1/q_e$  vs  $1/C_e$ . A positive plot of  $1/q_e$  against  $1/c_e$  shows conformity to the Langmuir isotherm indicating that adsorption takes place on smooth surfaces. Studies conforming to Langmuir isotherm in literature include adsorption of congo red onto acid functionalized walnut shell (Ojo et al., 2017), methylene blue onto modified pomelo peel (Ren et al., 2018) and Rhodamine B onto acid treated banana peel (Oyekanmi et al., 2019).

### 2.10.2 Freundlich Isotherm

Freundlich isotherm model is of the assumption that adsorption takes place on heterogeneous adsorbent's surface through a multilayer adsorption mechanism (Freundlich, 1907). The Linear form of Freundlich equation is expressed as:

$$\text{Log } q_e = \text{log } K_F + 1/n \text{ log } C_e \quad (2.7)$$

Where  $q_e$  is the amount of dye adsorbed (mg/g),  $C_e$  is the equilibrium concentration of the dye in solution (mg/L), and  $K_F$  and  $n$  are constants incorporating all factors affecting the adsorption capacity and intensity of adsorption, respectively. A plot of  $\text{log } q_e$  vs  $\text{log } C_e$  gives a linear with a slope of  $1/n$  and intercept of  $\text{log } K_F$ . A positive plot of  $\text{log } q_e$  against  $\text{log } c_e$  shows conformity to the Freundlich isotherm indicating adsorption on rough surfaces. Studies conforming to Freundlich isotherm are adsorption of methylene blue unto citric acid modified peanut shell (Wang et al., 2015), Rhodamin B unto rice husk ash (Nguyen and Dang, 2016) and Congo red unto pine bark (Litefti et al., 2019).

### 2.10.3 Temkin Isotherm

Temkin isotherm model considers the effect of indirect adsorbent–adsorbate interaction on adsorption and postulates that the heat of adsorption of all the layer would decrease linearly with coverage because of these interactions (Temkin and Pyzhev, 1940). Temkin model expresses the fall in the heat of adsorption as linear rather than logarithmic as stated in Freundlich expression (Teles de Vasconcelos and Gonzalez, 1993). The linear form of Temkin equation is expressed as:

$$Q_e = B_1 \ln K_T + B_1 \ln C_e \quad (2.8)$$

The  $K_T$  equilibrium binding constant ( $\text{Lmg}^{-1}$ ),  $B_1$  Temkin constant related to the heat of adsorption. Temkin constants  $B_1$  and  $K_T$  were calculated from the slope and intercept of  $q_e$  vs  $\ln C_e$ .

### 2.10.4 Dubinin-Radushkevich Isotherm

The Linear form of Dubinin-Radushkevich isotherm (Dubinin et al., 1947) is

$$\ln q_e = \ln q_D - B \epsilon^2 \quad (2.9)$$

Where,  $q_D$  is the theoretical saturation capacity (mg/g),  $B$  is a constant related to the mean free energy of adsorption per mole of the adsorbate ( $\text{mol}^2/\text{J}^2$ ) and  $\epsilon$  is polanyi potential which is related to the equilibrium as follows,

$$E = R_T \ln (1 + 1/C_e) \quad (2.10)$$

The constants  $q_D$  and  $B$  are calculated from the slope and intercept respectively from the plot of  $\ln q_e$  vs  $\epsilon^2$ .



The mean free energy of adsorption  $E$  is calculated from  $B$  using the equation:

$$E = 1/(2B)^{1/2} \quad (2.11)$$

Based on this energy of adsorption, one can predict whether an adsorption is physisorption or chemisorption. If the energy of activation is  $< 8 \text{ kJmol}^{-1}$ , the adsorption is physisorption and if the energy of adsorption is  $8\text{-}16 \text{ kJmol}^{-1}$  the adsorption is chemisorption in nature (Srivastava et al., 2004).

### 2.11 Adsorption thermodynamics

Thermodynamic parameters such as enthalpy change ( $\Delta H^{\circ}$ ), Gibb's free energy ( $\Delta G^{\circ}$ ) and entropy change ( $\Delta S^{\circ}$ ) are used to determine the feasibility and spontaneity of a reaction process (Singh et al., 2020). A process is said to be spontaneous if it shows a decreasing value of  $\Delta G^{\circ}$  and  $\Delta H^{\circ}$  with increasing temperature. Also, endothermic adsorption process shows a positive  $\Delta H^{\circ}$  value while exothermic process has negative  $\Delta H^{\circ}$  value (Wong et al., 2020). Thermodynamic parameters are calculated from the equations below:

$$\Delta G^{\circ} = \Delta H^{\circ} + T\Delta S^{\circ} \quad (2.12)$$

$$\ln K_o = \frac{\Delta S^{\circ}}{R} - \frac{\Delta H^{\circ}}{RT} \quad (2.13)$$

Where  $K_o$  is the equilibrium constant,  $R$  is the universal gas constant ( $8.314 \text{ J/mol K}$ ) and  $T$  is the temperature ( $\text{K}$ ) (Van't Hoff, 1884). According to Abd El-Latif et al. (2010), adsorption of methylene blue dye onto oak sawdust was found to be spontaneous and endothermic. Also, adsorption process of congo red onto Litchi seeds powder was found to be spontaneous and exothermic (Edokpayi and Makete, 2021).

## CHAPTER THREE: RESEARCH METHODOLOGY

### 3.1 Research design

The principal objective of this research is to explore the potential of locally available agricultural plant materials for the sequestration of hazardous dyes from aqueous solution by adsorption method. Adsorption has been established as the most suitable method of waste-water treatment considering both cost and effectiveness (Kumar et al., 2011). Agricultural plant materials have porous structure, very high free-surface volume, and lignocellulosic (plant-derived) resources. These properties make agricultural plant materials show sorption characteristic for a wide range of pollutants in waste-water treatment (Malik et al., 2016). Adsorption capacity of both raw and modified *Litchi chinensis* peel (LC) and *Dicerocaryum eriocarpum* seed (DE) were evaluated. Experimental procedure for this research followed six major segments (Figure 3.1) which are: (i) Sample collection, preparation and modification (ii) Characterisation of both raw, modified and spent plant materials. (iii) Determination of point of zero charge (iv) Biosorption study, which investigated the effect of experimental parameters such as agitation time, temperature, adsorbent dosage, adsorbate concentration and, pH. (v) Evaluation of equilibrium adsorption data for isotherms, kinetics and, thermodynamic studies of adsorption process. (vi) Desorption study was evaluated to determine the recovery and reusability of adsorbents. The results obtained from these segments were analysed/interpreted using equations, models, graphs, tables, and discussed in the later chapter.

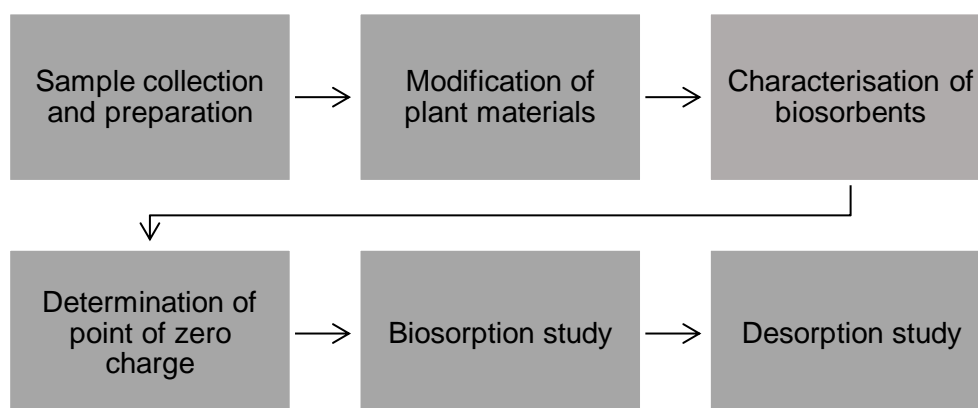


Figure 3.1: Methodology design

### 3.2 Preparation of adsorbent

DE seeds were collected from villages in Vhembe District, Limpopo province of South Africa where DE plants are predominant. *Litchi chinensis* peels were also gathered from Litchi fruits purchased at Tshakuma fruit market in Vhembe district. These plant materials were washed several times with distilled water to remove adhering impurities. The plant materials were thereafter dried in the oven at temperature of 50°C for 72 hours. The dried plant materials were

grinded using Retsch RS 200 pulverizer. The pulverised plant materials were sieved with King-test VB 200/300 sieve shaker to obtain fine particulate powder of sizes  $<125\ \mu\text{m}$  and  $>125\ \mu\text{m}$  (Figure 3.2). The powdered plant waste materials were then stored in airtight containers and termed as raw Litchi peels powder (RL) and raw DE seeds powder (RDE).



Figure 3.2: Images of novel plant materials; (a) Litchi peels, (b) pulverised Litchi peels, (c) DE seeds, (d) pulverised DE seeds

### 3.3 Modification of adsorbent

Raw plant waste materials (RL and RDE) were modified with citric acid (chemical structure shown in Figure 3.3) similar to methods described by Yan et al. (2018) and Zhang et al. (2019). About 10 g of each raw plant material was dispensed into 250 mL shaker bottle containing 100 mL of 0.5 M citric acid. The mixture was agitated at 250 rpm in a water bath shaker at room temperature for 90 min. After time expiration, the slurry was poured into a stainless-steel tray and dried at  $50^{\circ}\text{C}$  in an oven for 24 hours. Afterwards, the temperature of the oven was raised to  $120^{\circ}\text{C}$  for 90 min to allow for thermochemical reaction between the acid and plant material. The dried material was soaked and washed several times with distilled water to remove excess citric acid. Presence of acid was confirmed by testing the filtrate with 0.1 M lead (ii) nitrate until no turbidity was observed. Lastly, the plant material was dried in an oven at  $50^{\circ}\text{C}$  for 48 h. The plant material was thereafter allowed to cool, grinded again and stored in an airtight container for adsorption experiments. The

modified plant waste materials are termed as citric acid modified Litchi peel powder (CL) and citric acid modified DE seed powder (CDE).

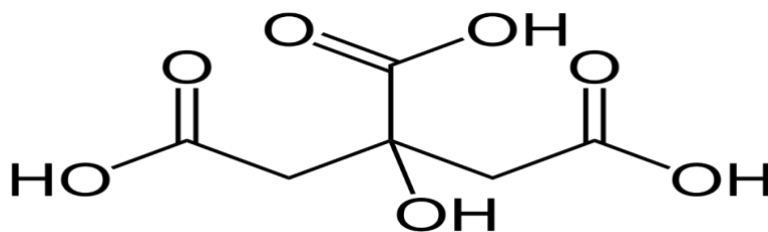


Figure 3.3: Chemical structure of citric acid ( $C_6H_8O_7$ )

### 3.4 Characterization of the adsorbent

#### 3.4.1 Fourier Transform Infra-Red (FTIR)

Perkin Elmer 100 FTIR spectrophotometer (Waltham, MA, USA) with accessories was utilised to investigate the functional groups responsible for the properties of raw and modified adsorbents before and after CR dye adsorption. This FTIR spectrophotometer is equipped with Alpha's Platinum ATR, (attenuated total reflection) single reflection diamond ATR module with spectral range  $7500\text{--}375\text{ cm}^{-1}$  and spectral resolution of  $<2\text{ cm}^{-1}$ . Following the procedure employed by Pazourková et al. (2014) and Ologundudu et al. (2016), the spectrophotometer was turned on and allowed to complete its automatic calibration and thereafter, measurement of samples were carried out. The sample area was wiped clean with cotton wool soaked in 70% ethanol and allowed to dry. With the use of a clean spatula, 0.5 g of the sample was dispensed into the sample area of the equipment which was afterward clamped to the ATR sampler. The start measurement was then selected and allowed about 15 secs to generate the spectra with the labelled peaks. The spectroscopy spectra were scanned over the wavelength range of  $4000\text{--}500\text{ cm}^{-1}$  to capture bands applicable to the sample (Ologundudu et al., 2016, Edokpayi et al., 2019).

#### 3.4.2 Scanning Electron Microscopy and Energy Dispersive X-Ray Spectroscopy (SEM-EDS)

Surface morphology and elemental composition of the raw and modified adsorbents before and after CR dye adsorption were analysed using a scanning electron microscope (TESCAN, VEGA 3 SBU, Brno, Czech) coupled with an energy dispersive X-ray spectrometry (EDS) system. This is important in order to understand the morphology of the surface and to observe any changes in the adsorbent brought about by modification and adsorption of CR dye. Following procedure described by Edokpayi et al. (2015), powdered sample of adsorbents were oven dried at  $105^\circ\text{C}$  for 6 h. The samples were sputtered with thin layer of carbon to form a conductive layer around the non-metallic sample and to prevent accumulation of electron beams. Prior to analysis, the samples were mounted on a metallic stub with a conductive carbon tape. Micrograph of the samples were obtained after irradiation with 20 kV beam of electrons under a vacuum. Analyses

of elemental composition of the biosorbents were carried out using Energy Dispersive X-ray Spectroscopy (EDS). Line spectra (peaks) were obtained, each corresponding to an element. The intensity of the characteristic lines is proportionate to the concentration of the element.

### 3.4.3 Brunauer, Emmet and Teller (BET) Technique

Textural characteristics of powdered biosorbents were determined with BET technique using Tristar II Micromeritics, (USA) analyser. Samples were degassed under vacuum at 50°C overnight. Surface area, total pore volume and average pore diameter were measured using Nitrogen gas (N<sub>2</sub>) at 77 K. Distribution of the pore size and pore volume were determined using Barrett-Joyner-Halenda (BJH) model (Barrett et al., 1951) and t-plot respectively (Lippens and De Boer, 1965). Nitrogen molecule cross-sectional area is assumed to be 0.162 nm<sup>2</sup>. The micropore corresponds to volume adsorbed in the pore less than 2 nm, mesopore corresponds to volume adsorbed in pores between 2 and 50 nm and, macropore corresponds to volume adsorbed in the pore greater than 50 nm. The mesopore surface area was calculated by subtraction of BET surface area and micropore surface area. The Dubinin-Radushkevich (DR) method was used to calculate the micropore volume. The micropore size distribution calculated by density functional theory (DFT). The total volume was calculated by converting the amount of nitrogen gas adsorbed at a relative pressure of 0.989 to the equivalent liquid volume of the adsorbate. The mesopore volume is calculated by subtracting the micropore volume to the total volume (Das et al., 2015).

### 3.4.4 X-Ray Diffraction

X-Ray Diffraction reveals the amorphous or crystalline nature of the adsorbents. It also reveals change that has occurred due to modification, also as a result of adsorption of dye onto the surface of the adsorbent. pAnalytical XPERT-PRO diffractometer (USA) was used for XRD analyses of raw and modified samples of adsorbent before and after CR dye adsorption. The samples were grinded into fine particulate powder (< 90 µm) after which they were loaded on the glass sample holder using razor slide to remove any excess and the shutters were closed. Precautions were taken to ensure a tight packing on the glass slit and to avoid manual contamination of the samples (Marquis, 2013). The X-ray diffraction was scanned with the goniometer using the Ni filtered CuK $\alpha$  radiation ( $\lambda=1.5406 \text{ \AA}$ ) source at an accelerated voltage of 45 kV and a current of 40 mA.

## 3.5 Determination of point of zero charge

To understand the adsorption mechanism, it is necessary to determine the point of zero charge of the adsorbent. Point of zero charge indicates the pH at which the adsorbent is neutral. However, beyond this pH, the adsorbent becomes either positively or negatively charged (Achmad et al., 2012). The point of zero charge (pH<sub>ZPC</sub>) of the adsorbents were analysed according to the method

explained by Ojo *et al.* (2017) and Edokpayi *et al.* (2019). Set up of 7 shaker bottles were made each containing 40 mL of 0.01 M NaCl. The pH of NaCl solution in each bottle was adjusted to initial pH ( $pH_0$ ) 2, 4, 6, 7, 8, 10 and 12 using 0.1 M HCl and 0.1 M NaOH solutions. The pH of solution was measured using pH meter- Thermo Orion VersaStar. 0.15 g of adsorbent was added to each bottle and agitated in water bath shaker at 30°C for 24 hours. After 24 hours, the samples were centrifuged at 2800 rpm for 10 min. The final pH ( $pH_f$ ) of the supernatant was measured. The point of zero charge was estimated by plotting a graph of change in pH ( $\Delta pH = pH_0 - pH_f$ ) against initial pH ( $pH_0$ ). The point of zero charge of the adsorbent is the point of intersection on the x-axis where  $pH_f = pH_0$ .

### 3.6 Preparation and calibration of dye solution

Analytical grade of Congo red used for the experiment was purchased from Fisher Scientific, United States of America. Structural formula of Congo red is shown in Figure 3.4 and its physicochemical properties as presented by Ojo *et al.* (2017) is shown in Table 3.1 below.

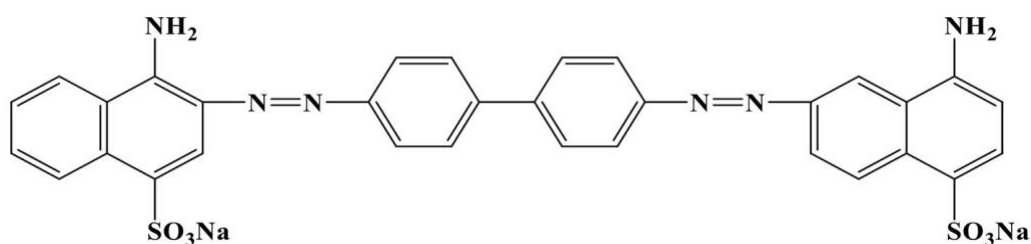


Figure 3.4: Chemical structure of Congo red.

Table 3.1: Physicochemical properties of Congo red dye

CAS No.	573-58-0
CA Index name	1-Naphthalenesulfonic acid, 3,30-[(1,10-biphenyl)-4,40-diylbis (2,1-diazenediyl)] bis [4-amino-, sodium salt (1:2)]
Molecular formula	$C_{32}H_{22}N_6Na_2O_6S_2$
Molecular weight	$696.66 \text{ g mol}^{-1}$
Molecular surface area	$557.6 \text{ \AA}^2$
Physical form	Brownish-red powder
Solubility	Soluble in water, ethanol; very slightly soluble in acetone; practically insoluble in ether, xylene
Density	$0.995 \text{ g cm}^{-3}$ at 25°C
Dye class	Azo
Melting point	>360°C
pH range	3.0–5.0
Color	Blue (pH 3.0) to red (pH 5.0)
pKa	4.1; 3.0
Absorption wavelength ( $\lambda_{max}$ )	497 nm; 488 nm

Stock solution of Congo red (CR) was prepared by dissolving 1 g of CR with de-ionized water in 1000 mL volumetric flasks. Various test solutions of desired concentrations were prepared by dilution of a known volume of stock solution with appropriate volume of de-ionized water. The wavelength for maximum CR absorption ( $\lambda_{\max}$ ) of 496 nm was predetermined by running a scan on CR dye solution between 400-1000 nm, using UV-Vis Spectrophotometer (Orion Aquamate 7000, Thermoscientific). Calibration curve linear through zero with correlation coefficient of 0.999 was obtained using 0, 10, 20, 30, 40 mg/L of CR solution as represented in Figure 3.5.

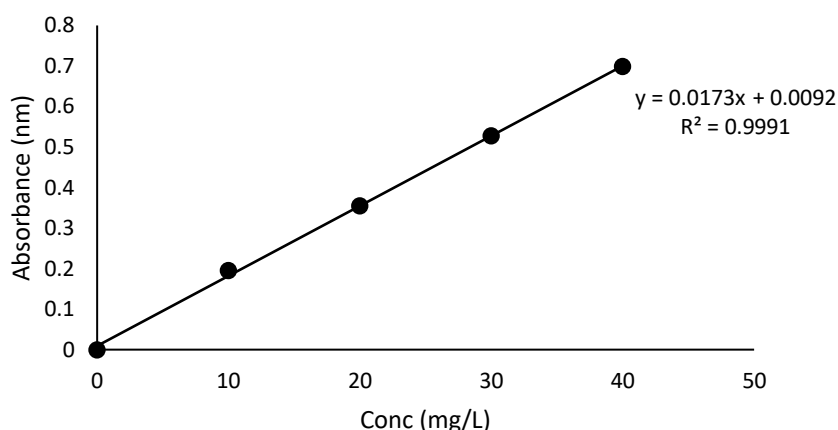


Figure 3.5: Calibration curve for aqueous solution of Congo red

### 3.7 Biosorption study

In this study, adsorption efficiency of (4) plant waste materials used as adsorbents were investigated. They are: (i) raw Litchi peel powder- **RL**, (ii) citric acid modified Litchi peel powder- **CL**, (iii) raw DE seed powder- **RDE** and, (iv) citric acid modified DE seed powder- **CDE**. Batch equilibrium study were conducted as described by Kooh et al. (2016) and experimental set up is shown in Figure 3.6. For each adsorption experiment, 40 mL of CR dye solution of 40 mg/L concentration was dispensed into 100 mL shaker bottles, each containing 0.05, 0.10, and 0.15 g of adsorbent. The sample was agitated in a water-bath shaker (Ecobath Labotech) at agitation speed of 200 rpm and temperature of 30°C. The samples were withdrawn from the shaker at different time interval. The adsorbent was separated from the solution by centrifugation for 10 min at 2800 rpm. Final concentration of the supernatant was estimated using UV-Visible Spectrophotometer at a wavelength of 496 nm. Batch experiments were carried out to investigate the effect of parameters like agitation time, adsorbent dose, adsorbent size, adsorbate concentration, temperature, and pH on the adsorption process. Effect of matrix and effect of the adsorbents on other dyes were also investigated following the same procedure. All experiments were carried out in triplicate and conducted at temperature of 30°C; except if otherwise stated.



Figure 3.6: Experimental set up for biosorption study

### 3.7.1 Agitation time

The effect of agitation time on removal of CR dye from aqueous solution using raw and citric acid modified adsorbents were investigated. Equilibrium time required for optimum adsorption of CR dye from aqueous solution was also determined. Three masses (0.05 g, 0.10 g and 0.15 g) of adsorbents dispensed into 100 mL shaker bottles containing 40 mL of 40 mg/L congo red solution were agitated in Eco-bath shaker controlled at 200 rpm and 30°C for 5, 15, 30, 45, 60, 90, 120, 150, and 180 minutes (Mann and Mandal, 2014). After expiration of each time, the samples were centrifuged at 2800 rpm for 10 min. The final concentrations of the supernatant were subsequently estimated using UV-Vis spectrophotometer.

### 3.7.2 Temperature

Temperature effect was carried out on CR dye sequestration from aqueous solution by varying the experimental temperature and alongside; determine the most suitable temperature for adsorption process. Experiments was conducted by agitating batch of 0.05, 0.10 and 0.15 g of adsorbent with constant dye concentration of 40 mg/L in a temperature-controlled shaker at 30°C, 200 rpm and equilibrium time. The temperature of the shaker was subsequently raised to 40, 50, 60, 70, 80 °C for other batch of experiments. The samples for each adsorbent were centrifuged and the residual dye concentration was determined using UV-Spectrophotometer.



### 3.7.3 Adsorbent dosage and adsorbate concentration

The effect of dosage of adsorbent, alongside with effect of adsorbate concentration on removal of CR dye from aqueous solution was monitored and optimised to determine the optimum dosage/mass for maximum adsorption. Different masses of 0.02, 0.04, 0.06, 0.08, 0.10, 0.12, 0.14, 0.16, 0.18, 0.20 g of adsorbents were agitated at 200 rpm, with 40 mL of 40, 60 and 80 mg/L CR dye solution at equilibrium time and optimum temperature. The samples were then centrifuged, and the final concentration of the supernatant were determined.

### 3.7.4 pH

Experimental analysis of pH effect was conducted to determine the pH condition that favours removal of CR dye from aqueous solution using all the four adsorbents. Seven shaker bottles containing 40 mL of 40 mg/L CR solution were set up. pH of each bottle was adjusted to 2, 4, 6, 7, 8, 10 and 12 using 0.1 M HCl and 0.1 M NaOH solutions. Adsorbent masses in batch of 0.05, 0.10 and 0.15 g were added to each bottle and agitated at optimum time and temperature. Samples were later centrifuged at 2800 rpm for 10 min. Final concentration of the supernatant were analysed using spectrophotometer.

### 3.7.5 Particle size of adsorbents

Adsorption efficiency of adsorbent sizes  $<125\ \mu\text{m}$  and  $>125\ \mu\text{m}$  were investigated and compared to determine effect of particle size of plant waste material on adsorption of CR dye from aqueous solution. Batch experiment was carried out for both sizes of adsorbents following the procedure explained in section 3.7. Adsorbent masses of 0.02, 0.04, 0.06, 0.08, 0.10, 0.12, 0.14, 0.16, 0.18 and 0.20 g of adsorbents were agitated (200 rpm) with 40 mL of 40 mg/L congo red solution at equilibrium time and optimum temperature. The samples were later centrifuged, and the final concentration of the supernatants were determined.

### 3.7.6 Effect of matrix

Natural surface water collected from Mutale river (Limpopo province, South Africa) was used to prepare 40 mg/L CR dye solution instead of deionised water used for other experiments. Following experimental procedure explained under biosorption study section 3.7, dye removal efficiencies of the adsorbents here were compared to experiment carried out using deionized water for CR dye solution preparation. This is important in order to examine the effect of change in water chemistry on the sequestration of CR dye from aqueous solution (Edokpayi et al., 2019).

### 3.7.7 Removal efficiency of adsorbents on other dyes

Apart from sequestration of CR dye (which is the major test dye in this study) from aqueous solution using RL, CL, RDE, CDE adsorbents, their removal efficiency was also tested on other

dyes like Rhodamine B, Methylene blue, Methylene orange, Crystal Violet and Malachite green. 0.15 g of adsorbent was agitated with 40 mL of 40 mg/L of each dye for 180 min. The temperature of the water-bath shaker was controlled at 30°C and agitation speed of 200 rpm. Each batch of samples were withdrawn from the shaker at every 15 min and centrifuged to separate the adsorbate from adsorbent. Final concentrations of adsorbates were determined using UV-Vis spectrophotometer.

After every batch experiment explained above, the amount of sorption  $q_t$  (mg/g) at time  $t$  (min) was calculated using the formula below (Ologundudu et al., 2016, Singh et al., 2020):

$$q_t = \frac{(C_o - C_t)}{m} \times V \quad (3.1)$$

Where  $C_t$  (mg/L) is the liquid phase concentration of dye at any time  $t$ ,  $C_o$  (mg/L) is the initial concentration of the dye in solution,  $V$  (L) is the volume of the solution and  $m$  (g) is the mass of the adsorbent.

The amount of equilibrium adsorption  $q_e$  (mg/g) was calculated using the formula:

$$q_e = \frac{(C_o - C_e)}{m} \times V \quad (3.2)$$

Where  $C_o$  and  $C_e$  (mg/L) are the liquid-phase concentrations of dye initial and at equilibrium.

The dye removal percentage was calculated using the formula:

$$\% \text{ of dye removal} = \frac{(C_o - C_f)}{C_o} \times 100 \quad (3.3)$$

Where  $C_o$  and  $C_f$  (mg/L) are the initial and final concentrations of the dye in solution respectively.

### 3.8 Adsorption kinetics

The mechanism and rate at which CR dye is adsorbed on the surface of the bio-sorbents was investigated by applying Lagergren pseudo first order, pseudo second order and, intra-particle kinetic models to data generated on biosorption study for the effect of time. The linearised equations for the pseudo first and pseudo second order kinetics are presented in equations (3.4) and (3.5) respectively below ((Lagergren, 1898):

$$\log (q_e - q_t) = \log q_e - \left( \frac{k_1 t}{2.303} \right) \quad (3.4)$$

$$\frac{t}{q_t} = \frac{1}{k_2 q_e^2} + \frac{t}{q_e} \quad (3.5)$$

where  $q_e$  and  $q_t$  are the amounts of dye adsorbed at equilibrium and at a given time  $t$ ;  $K_1$  and  $K_2$  are the rate constants of pseudo first and pseudo second order models.

The pseudo first order kinetic model was used to treat the experimental data obtained by plotting  $\log(q_e - q_t)$  against time. The values of  $K_1$  and  $q_e$  were determined from slope and intercept of the graph. The same way, pseudo second order kinetic model was applied to the experimental data by plotting  $t/q_t$  against time  $t$ . The values of  $q_e$  and  $K_2$  were calculated from the slope and intercept the graph. The linearity coefficients of the linear plots obtained were compared in order to determine the best fit kinetic model for the adsorption process. The results from the kinetic plots were also compared whether it favours chemisorption or physisorption mechanistic pathway (Edokpayi et al., 2015).

Intra-particle diffusion model is linearly expressed by equation (3.6) stated below (Vimonses et al., 2009; Zhou et al., 2018):

$$q_t = k_p t^{0.5} + C \quad (3.6)$$

Where  $q_t$  is the amount of dye adsorbed (mg/g) at time  $t$  (min),  $k_p$  is the intra-particle diffusion rate constant (mg/g min) and  $C$  is the intercept (mg/L) (Webber and Morris, 1963).

This model is further used to treat experimental data obtained by plotting a graph of  $q_e$  against  $t^{0.5}$ . The values of  $K_p$  and  $C$  can be determined from the slope and intercept of the graph. If the line of the curve passes through the origin, it is assumed that the internal diffusion is the only rate-controlling step of the reaction (Lin et al., 2020). The intercept gave an idea about the thickness of the boundary layer. The higher the value of  $C$ , the greater is the thickness (Corda and Kini, 2018). The calculated value of the slope of the linear plot is the intra-particle rate constant.

### 3.9 Adsorption isotherms

Adsorption isotherm describes the performance and interaction of the adsorbate with the adsorbent (Edokpayi et al., 2021). Equilibrium data obtained from biosorption study were analyzed using Langmuir, Freundlich and Temkin adsorption isotherm models in order to know the type of adsorption taking place on the surface of the adsorbents. The Langmuir model

assumes that the adsorption of adsorbate on an ideal adsorbent's surface occurs only at fixed number of sites and each site can only hold one (monolayer) adsorbate molecule (Mwangi et al., 2012). It also assumes that all available sites are equivalent and there is no interaction between adsorbed molecules on adjacent sites (Edokpayi et al., 2015). The linearised equation for Langmuir model is represented by the equation below (Langmuir 1916):

$$\frac{1}{q_e} = \frac{1}{q_{max}} + \left( \frac{1}{K_L q_{max}} \right) \frac{1}{C_e} \quad (3.7)$$

where  $C_e$  is the equilibrium concentration of the dye (CR) (mg/L),  $q_e$  is the quantity of Congo red dye adsorbed at equilibrium (mg/g),  $q_{max}$  is the maximum amount adsorbed (mg/g) and  $K_L$  is the Langmuir adsorption constant (L/mg). The plot of  $1/q_e$  against  $1/C_e$  was made and the values of maximum amount of congo red dye adsorbed ( $q_{max}$ ) and the Langmuir adsorption constant ( $K_L$ ) were calculated from the intercept and slope of the plot respectively. The conformity of the adsorption process to Langmuir model was determined using equation:

$$R_L = \frac{1}{(1 + K_L C_o)} \quad (3.8)$$

where  $R_L$  is the separation factor,  $C_o$  is the initial dye concentration (mg/L) and  $K_L$  is the Langmuir constant (L/mg).  $R_L > 1$  indicates an unfavourable,  $R_L = 1$  indicates linear,  $0 < R_L < 1$  indicates favourable and  $R_L = 0$  indicates irreversible monolayer adsorption process (Edokpayi et al., 2015; Inyinbor et al., 2015).

The Freundlich isotherm model describes a multi-site adsorption for heterogeneous surfaces and can be represented by the equation (Freundlich, 1907);

$$Q_e = K_F C_e^{\frac{1}{n}} \quad (3.9)$$

Taking the logarithm of equation 3.9 above, we obtain:

$$\log q_e = \log K_F + \frac{1}{n} \log C_e \quad (3.10)$$

Where  $q_e$  is the quantity of dye adsorbed at equilibrium (mg/g),  $C_e$  is the equilibrium concentration of dye in solution (mg/L),  $K_F$  is the adsorption capacity (L/mg) and  $1/n$  is the intensity of the adsorption showing the heterogeneity of the adsorbent site and the energy of distribution

(Olorundare et al., 2014; Edokpayi et al., 2015). A linear graph of  $\log q_e$  against  $\log C_e$  was plotted and the constants  $n$  and  $K_F$  were determined from the slope and intercept of the plot respectively. The value of  $n > 1$  also indicates favourable adsorption process.

Temkin isotherm assumes a linear decrease in the heat of adsorption of dye molecules on the adsorbent's surface and that this decrease is not logarithmic as stated in Freundlich expression (Temkin and Pyzhev, 1940). The linear form of Temkin model is expressed in equation (3.11):

$$Q_e = B_1 \ln K_T + B_1 \ln C_e \quad (3.11)$$

The  $K_T$  equilibrium binding constant ( $\text{Lmg}^{-1}$ ),  $B_1$  Temkin constant related to the heat of adsorption. Temkin constants  $B_1$  and  $K_T$  were calculated from the slope and intercept of  $q_e$  vs  $\ln C_e$ .

The linearised coefficients ( $R^2$ ) obtained from the three models were compared to determine the best fit adsorption isotherm model.

### 3.10 Adsorption thermodynamics

Thermodynamic study reveals energy changes that occur during adsorption process (Olakunle et al., 2017). Data obtained from effect of temperature on adsorptive removal of CR dye were employed in order to get sufficient data for thermodynamic study. Effect of temperature on adsorptive removal of CR from aqueous solution was monitored by varying the working temperature from 30 to 80°C. Spontaneity and feasibility of the adsorption process was determined by thermodynamic parameters such as Gibb's free energy change ( $\Delta G^\circ$ ), enthalpy change ( $\Delta H^\circ$ ) and, entropy change ( $\Delta S^\circ$ ). These thermodynamic parameters were calculated based on equations (3.12) and (3.13):

$$\ln K_o = \frac{\Delta S^\circ}{R} - \frac{\Delta H^\circ}{RT} \quad (3.12)$$

$$\Delta G^\circ = - RT \ln K_o \quad (3.13)$$

Where  $K_o$  equilibrium constant,  $R$  is the universal gas constant (8.314 J/mol/K) and  $T$  is the temperature (K) (Van't Hoff, 1884).

Equilibrium constant  $K_o$  has been expressed in literature as  $K_o = q_e/C_e$  (Inyinbor et al., 2015, Kooh et al., 2016; Ren et al., 2018; Singh et al., 2020). However, it is highly important to note that  $K_o$  determined through this expression is in the unit of L/g. This must be re-calculated as dimensionless to make it fit for thermodynamic equilibrium constant to be used for Van't Hoff plot.

It is re-calculated by multiplying with molecular weight of adsorbate (696.66 g/mol) and concentration of water (55.5 mol/L) (Zhou and Zhou, 2014). The Van't Hoff plot of  $\ln K_o$  against  $1/T$  should give a linear relationship with the slope of  $\Delta H^\circ/R$  and an intercept of  $\Delta S^\circ/R$ . Basically, a positive  $\Delta H^\circ$  value specifies endothermic nature of an adsorption process while a negative value implies exothermic reaction. A positive value of  $\Delta S^\circ$  indicates an increase in randomness at the solid/solution interface that occurs in the adsorption process besides reflecting the affinity of the adsorbent towards the adsorbate. Furthermore, a negative  $\Delta G^\circ$  value indicates a feasible and spontaneous adsorption process at the study temperatures and vice-versa.

### 3.11 Desorption Study/Regeneration

Desorption study is highly important especially when considering reusability of adsorbent and safe disposal of spent adsorbent into the environment. This brings about practical economic wastewater treatment, prevent accumulation of sludge and, alleviate secondary dye contamination of the environment. Desorption experiment as illustrated by Edokpayi et al. (2015), 0.15 g of adsorbent was dispensed into three 100 mL shaker bottles containing 40 mg/L CR dye solution. These were agitated in an eco-bath shaker controlled at 30°C and agitation speed of 200 rpm for 90 min. After time expiration, the adsorbents were recovered and washed with distilled water to remove the residual dye on the surface of the spent adsorbent. De-ionized water, 0.1 M HCl and 0.1 M NaOH were utilised as potential desorbing agents. 40 mL of the desorbing agents were measured into each 100 mL shaker bottle containing the spent adsorbent and agitated for 90 min at a speed of 200 rpm and 30°C. The mixtures were afterward centrifuged, and the supernatant were analysed to determine the final concentration of the solution after desorption. The percentage desorption was calculated using equation (3.14) stated below. Regeneration of biosorbent was thereafter investigated by repeating adsorption and desorption cycle several times in order to explore the reusability of the biosorbent (Lafi et al., 2019).

$$\text{Desorption \%} = \frac{\text{Desorbed dye concentration}}{\text{Initial adsorbed dye concentration}} \times 100 \quad (3.14)$$

### 3.12 Data interpretation

Experimental parameters such as pH, mass of adsorbent, agitation time, temperature and initial dye concentration were analysed using equations, graphs, tables, and charts. This was subsequently used to depict their relationship with percentage removal of dye on the adsorbents.

### 3.13 Quality assurance

Laboratory experiments were carried out with high level precision and accuracy especially during weighing, volume measurement, preparation of solutions and cleaning of glass wares. All solutions/reagents were prepared with deionised water to prevent contamination or interference

of ions; except if stated otherwise. Dyes solutions and other solution were freshly prepared for various experiments to maintain high standard and quality.

## CHAPTER FOUR: RESULTS AND DISCUSSION

### 4.1 Preamble

Following the detailed methodology stated in the previous chapter, the results of laboratory analyses carried out on sequestration of hazardous Congo red (CR) dye from aqueous solution through adsorption process are presented and interpreted in this chapter. The biosorbents used are prepared from two different plant materials which are *Litchi chinensis* peels and *Dicerocaryum eriocarpum* (DE) seeds. The prepared biosorbents are raw Litchi peel powder (**RL**), citric acid modified Litchi peel powder (**CL**), raw DE seed powder (**RDE**) and, citric acid modified DE seed powder (**CDE**). The results are for experimental analyses carried out which include characterisation of raw, modified and spent biosorbents, determination of point of zero charge, effect of experimental parameters, adsorption kinetics, isotherms, thermodynamic studies and, regeneration study.

### 4.2 Characterisation of adsorbents

#### 4.2.1 Fourier Transform Infrared Spectroscopy (FTIR)

The FTIR spectra of raw and modified Litchi biosorbents (RL, CL) and raw and modified DE biosorbents (RDE, CDE) before CR dye sorption are shown in Figure 4.1. The spectrum range of FTIR was collected between wave numbers 4000 and 500  $\text{cm}^{-1}$ . The spectra lines obtained at different band areas indicate that there are various functional groups on the surface of the adsorbents.

With reference to Figure 4.1 (A) which represents the FTIR spectra of RL and CL, the broad band observed at wave numbers 3500–3000  $\text{cm}^{-1}$  which peaks at 3270  $\text{cm}^{-1}$  represents O-H stretch of alcohol group (Duran-Valle, 2012). The medium peaks at 2911 and 2841  $\text{cm}^{-1}$  represent C-H stretch of aliphatic group (Wong et al., 2020). A strong medium peak at 1603  $\text{cm}^{-1}$  characterises C=C stretch of aromatic group (Olakunle et al., 2017). Short peaks at 1425 and 1362  $\text{cm}^{-1}$  represent presence of C-H groups, 1311 and 1230 ( $\text{cm}^{-1}$ ) correspond to C-O stretching (Coates, 2000). The strong sharp peak at 1007  $\text{cm}^{-1}$  is allocated to C-O stretch of carboxylate groups (Duran-valle, 2012). Decrease in the intensity of peaks was observed for the modified Litchi (CL) because the spectra moved to lower absorbance level. This observation reveals the effect of the acid modification and high temperature which brought about intermolecular bonds breakage and, thereby capable of enhancing dye adsorption (Bello and Ahmad, 2012; Kaur et al, 2013).

FTIR spectra of RDE and CDE shown in Figure 4.1 (B) display broad band peak at wave numbers 3323  $\text{cm}^{-1}$  which represents O-H stretch of alcohol group (Duran-Valle, 2012). The medium bands at 2937-2841  $\text{cm}^{-1}$  represent C-H stretch of the aliphatic group (Wong et al., 2020). Short peaks



at 1766, 1631, 1242  $\text{cm}^{-1}$  of the fingerprint regions correspond to C=O stretch of carbonyls, N-H stretch of primary amines and C-N stretch of aliphatic amines respectively (Coates, 2000). The strong sharp peak at 1019  $\text{cm}^{-1}$  is allocated to C-O stretch of carboxylate groups (Duran-Valle, 2012). The spectra of the modified biosorbent- CDE clearly showed little difference from raw biosorbent- RDE. CDE spectra showed band/peak shift to higher absorbance level and emergence of new peaks was also observed at wave numbers 2913, 2845  $\text{cm}^{-1}$  assign to C-H stretch of alkane/aliphatic group, and 1621, 1589  $\text{cm}^{-1}$  assign to C=C stretch of ester and carboxylate groups respectively (Ren et al, 2018). This appearance of new peaks indicates that carboxylate group were successfully introduced on CDE because of modification with citric acid.

Various functional groups available on the surface of these adsorbents have been reported to be appropriate for removal of dye (Inyinbor et al., 2015). The changes observed in FTIR spectra of modified biosorbents indicate that modification of biosorbents contributed to the observed band shifts, change in absorbance values and appearance of new peaks, thereby capable of improving CR dye adsorption (Bello and Ahmad, 2012).

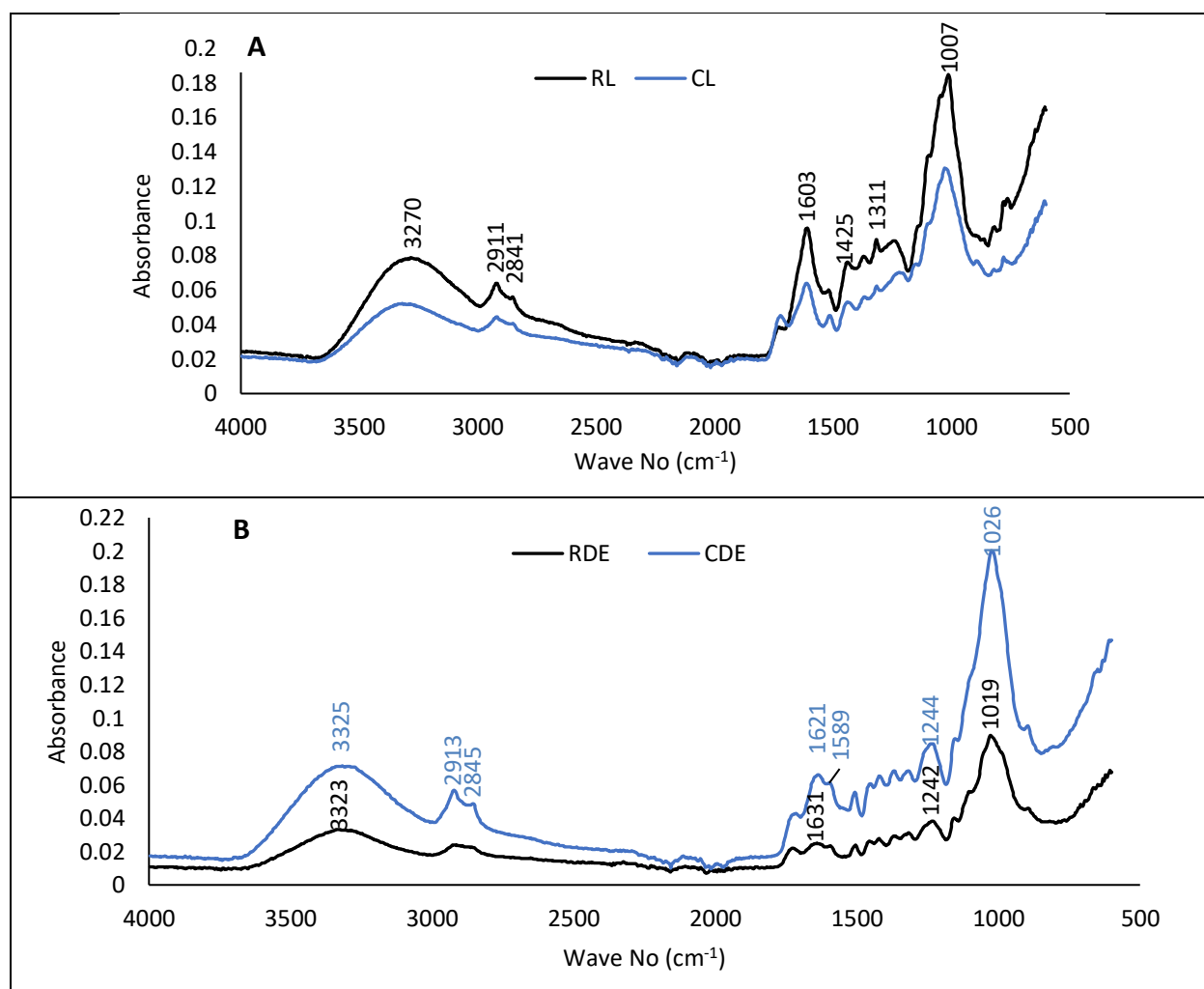


Figure 4.1: FTIR spectra of (A) RL and CL, (B) RDE and CDE

After CR dye adsorption, the spectra of spent raw Litchi (SRL) reveals a decrease in absorbance values of bands and peaks when compared to RL as presented in Figure 4.2 (A). The reduction of absorbance values suggested that the available sites of the biosorbent had been occupied by CR dye and is an indication of dye adsorption. With regards to Figure 4.2 (A and B), minor changes were observed in the spectra lines of spent raw and modified Litchi biosorbents (SRL and SCL) when compare to their raw forms. Likewise, the spectra of spent raw and modified DE biosorbents (SRDE and SCDE) as shown in Figure 4.3 (A and B) displayed little changes after CR dye adsorption when compared to their raw forms- RDE and CDE. Although SRDE showed spectra line pattern close to its raw form- RDE, however there is movement of peaks/band to higher absorbance values and, the peaks at 2158 and 2027  $\text{cm}^{-1}$  became more prominent. SCDE spectra pattern showed disappearance of peaks 2913 and 2845  $\text{cm}^{-1}$ .

The changes observed in the FTIR spectra like decrease in band intensities, appearance and disappearance of peaks, all suggests that these functional groups were utilized for dye adsorption (inyinbor et al, 2015). The slight changes indicate that removal of CR dye by the biosorbents is more of physical adsorption than chemical adsorption. Comparable result was reported by Elavarasan et al. (2018) in his study on the adsorption of methylene blue dye onto acid activated carbon prepared from *Mimusops elengi* Leaves.

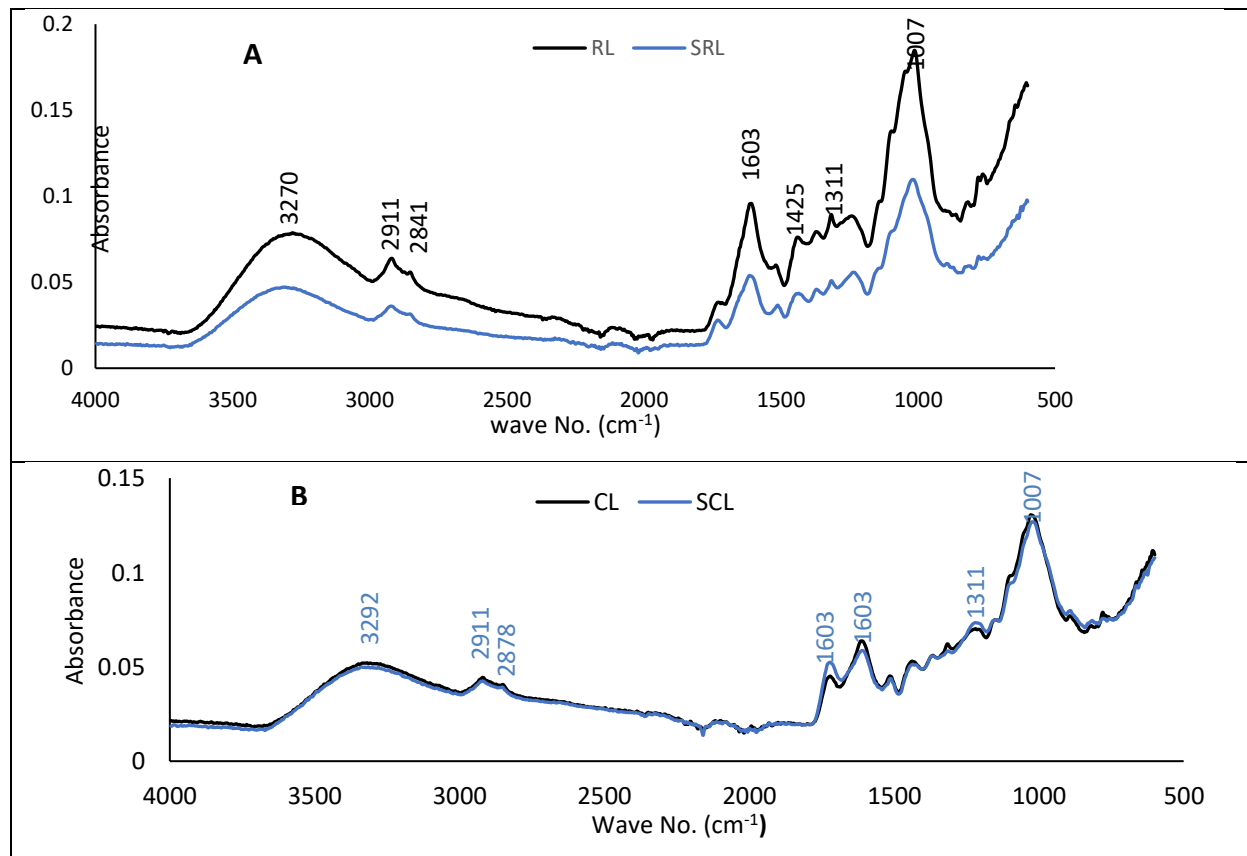


Figure 4.2: FTIR spectra of (A) RL and SRL, (B) CL and SCL

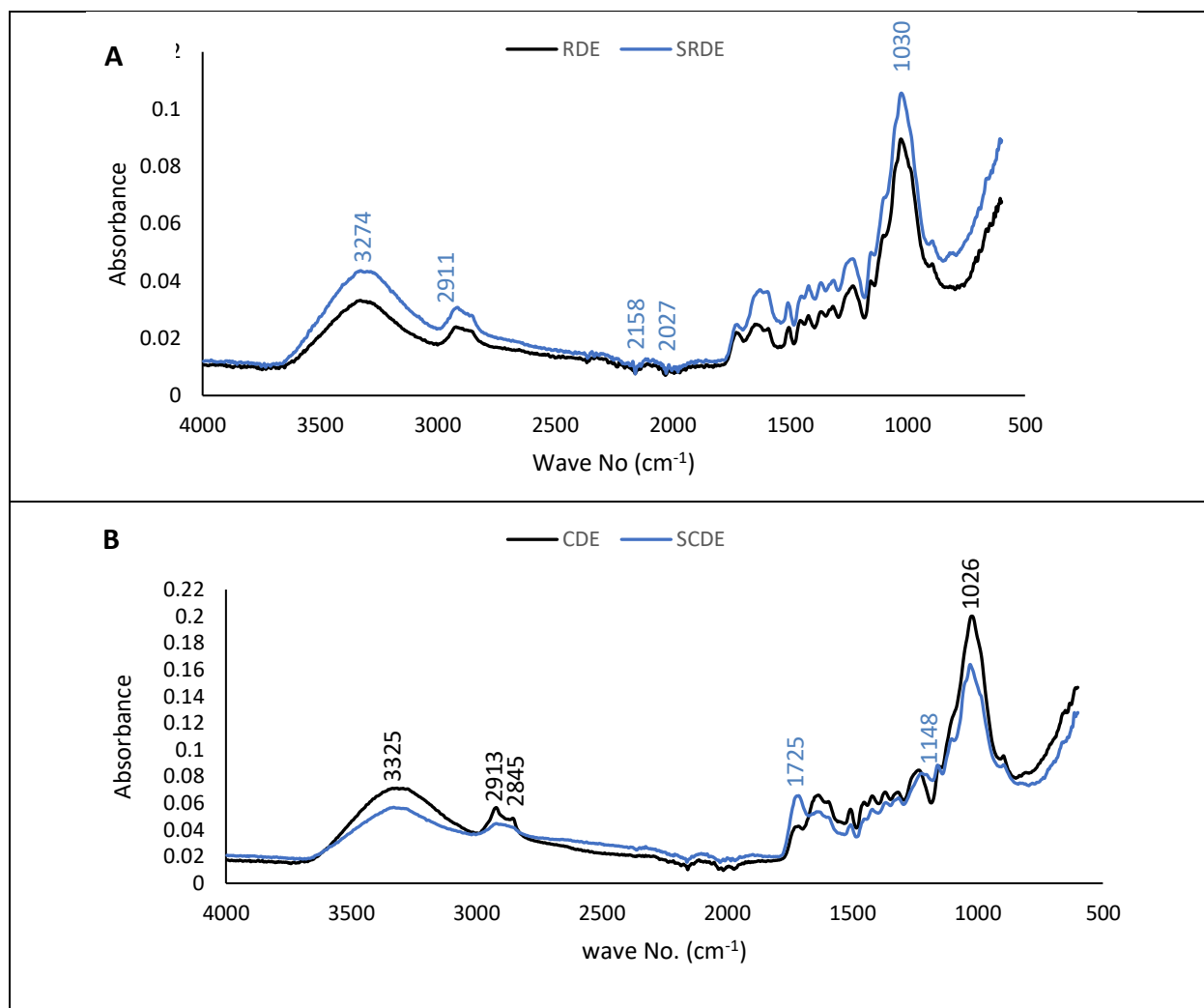


Figure 4.3: FTIR spectra of (A) RDE and SRDE, (B) CDE and SCDE

#### 4.2.2 Scanning electron micrograph (SEM)

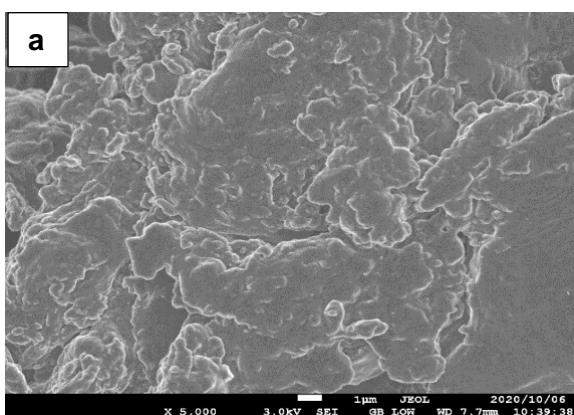
The micrographs of both raw (RL) and modified (CL) Litchi peels biosorbents before and after adsorption of CR dye are shown in Figures 4.4 and 4.5 respectively. Figure 4.4 (a–d) presents the micrographs of RL and CL before CR dye adsorption. The micrographs of RL (a, b) reveals a faded, free and, less flaky structured surface comparative to that of CL (c, d) which appeared sharp and more definite, flakier structured surface. This observation is more visible in the 10,000 magnification images (b and d). Likewise, Figures 4.6 and 4.7 reveal the micrographs of both raw (RDE) and modified (CDE) DE biosorbents before and after adsorption of CR dye respectively. Figure 4.6 (a–d) presents the micrographs of RDE and CDE before CR dye adsorption. The micrographs of RDE (a, b) reveal a compact and less flaky structured surface compare to that of CDE (c, d) which appears wider and more definite flaky structured surface.

The changes observed in the morphology of modified biosorbents (CL and CDE) can be attributed to the effect of thermochemical reaction between the modifying agent and plant material thus, aggregated particles of the plant material, thereby giving it a definite flaky structure. In addition,

the surface of modified biosorbents became sharper and more definite due to removal of impurities such as pectin, lignin, and viscous compounds from the plant material by citric acid treatment (Ren et al., 2018; Oyekanmi et al., 2019). This observation is relative to the effect of acid modification on biosorbents as reported in literatures by Inyinbor et al. (2015) on adsorption of Rhodamine B dye from aqueous solution using *Irvingia gabonensis* biomass and removal of Methylene blue dye from aqueous solution using citric acid modified Pomelo peels (Ren et. al., 2018).

After adsorption of CR dye, the morphology of spent raw and modified Litchi biosorbents (SRL, SCL) and spent raw and modified DE biosorbent (SRDE and SCDE) are presented in Figures 4.5 and 4.7 respectively. The SEM after adsorption reveals more definite and occupied morphology with flaky protuberances which can be attributed to adsorption of CR dye molecule onto biosorbent's active surfaces. This observation is also more obvious in the 10,000 magnification images (Figure 4.5, f and h and Figure 4.7, f and h).

RL



CL

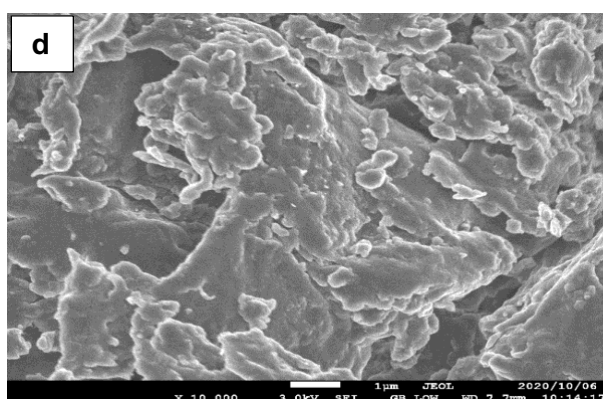
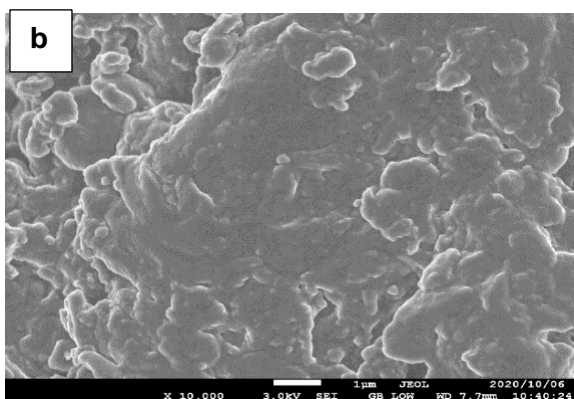
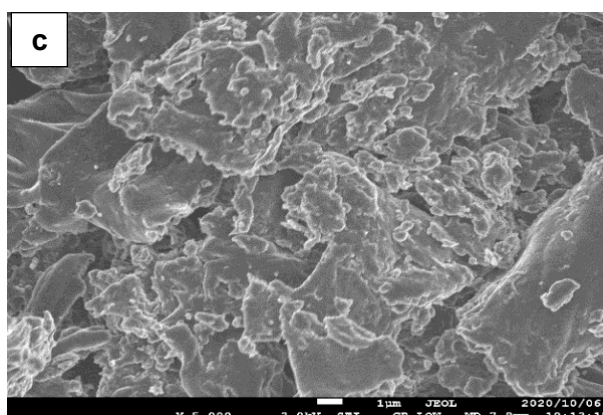
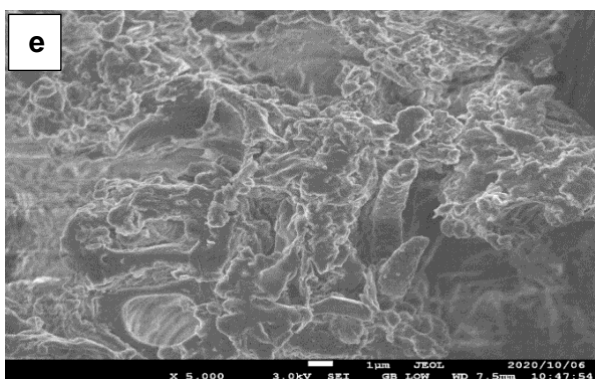


Figure 4.4: SEM of RL and CL before CR dye adsorption (a,c) X 5,000 and, (b,d) X 10,000

SRL



SCL

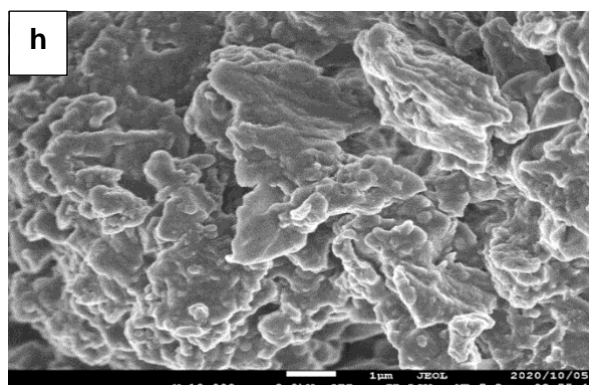
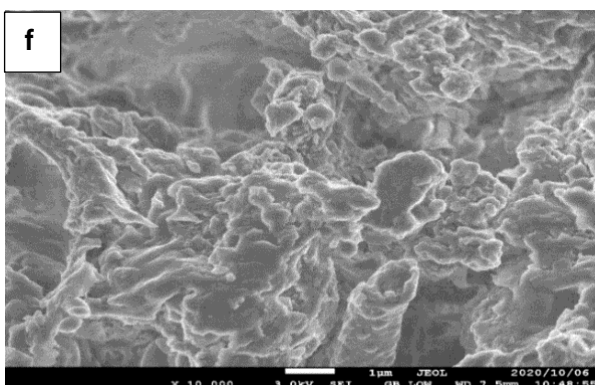
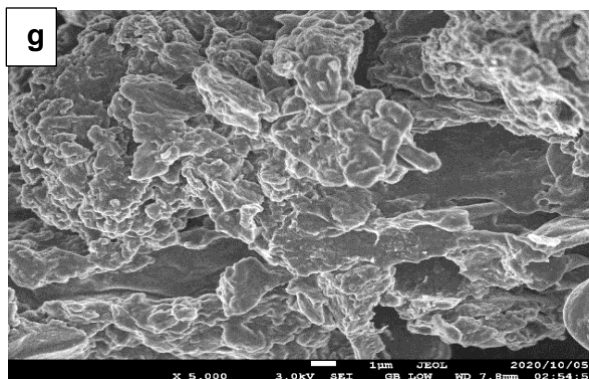
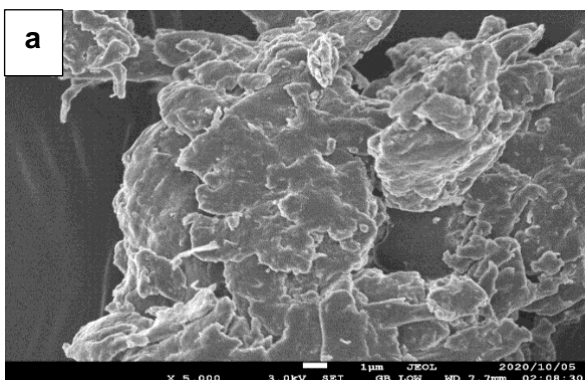


Figure 4.5: SEM of SRL and SCL after CR dye adsorption (e,g) X 5,000 and, (f,h) X 10,000

RDE



CDE

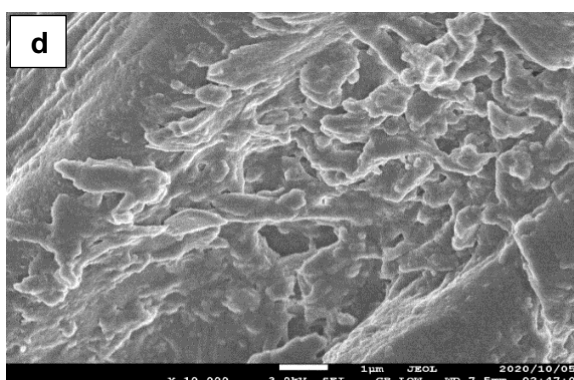
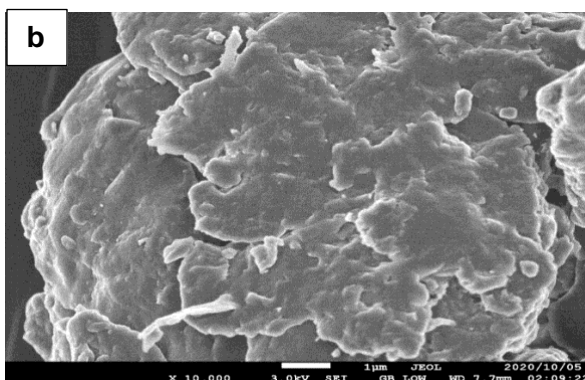
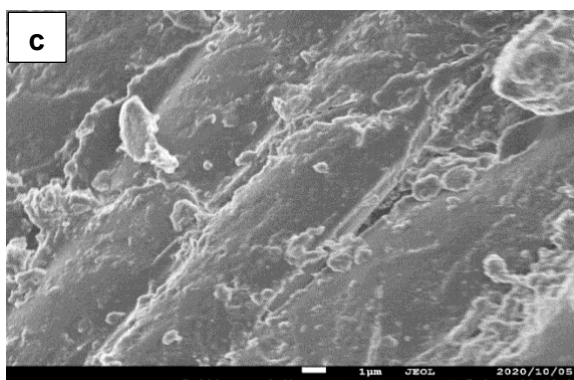
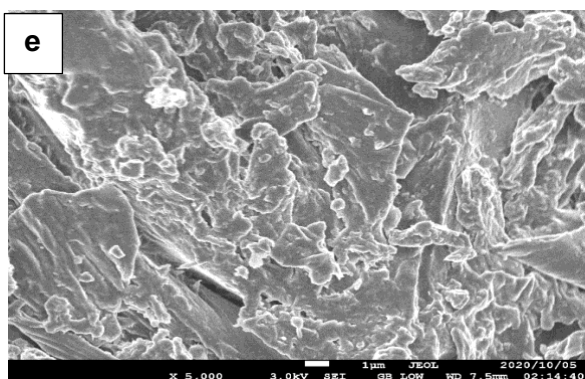


Figure 4.6: SEM of RDE and CDE before CR dye adsorption (a,c) X 5,000 and, (b,d) X 10,000

SRDE



SCDE

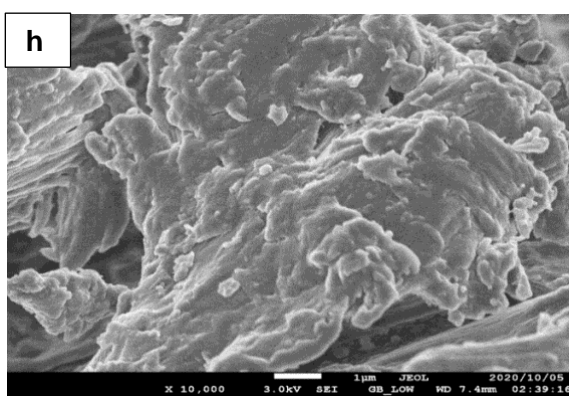
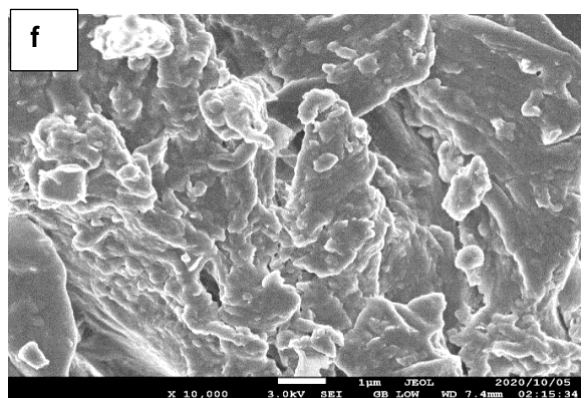
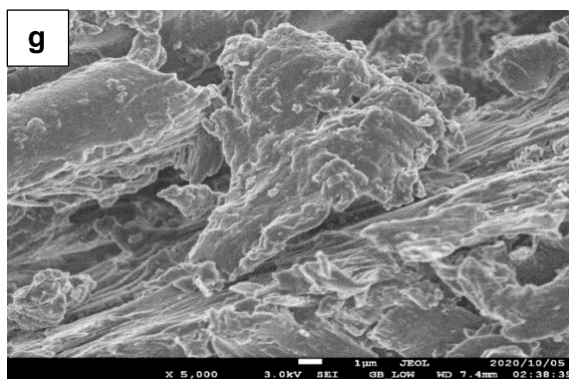


Figure 4.7: SEM of SRDE and SCDE after CR dye adsorption (e,g) X 5,000 and, (f,h) X 10,000

#### 4.2.3 Energy dispersive X-ray spectroscopy (EDS)

Energy dispersive X-ray spectroscopy (EDS) was coupled with scanning electron micrograph to investigate elemental composition of adsorbents before and after CR dye adsorption. The EDS line spectra of RL, CL and RDE, CDE obtained are as shown in Figures 4.8 and 4.10 respectively, and the quantitative results of elemental compositions are also presented in Appendix I (a, b, c, d). The major elements identified from EDS spectra were O and C amongst other elements which are in minute percentage. Atom percentage value of O (55.91) and C (14.40) were recorded for RL while atom percentage value of O (54.07) and C (24.25) were recorded for CL. Likewise, atom percentage value of O (28.44) and C (64.64) were recorded for RDE while atom percentage value of O (17.16) and C (76.21) were recorded for CDE. The observed increase in atom percentage of carbon and decrease in that of oxygen in quantitative results of modified as compared to that of raw biosorbents could be due to the thermochemical effect of modification (Olakunle et al., 2017). Chemical modification of adsorbents at high temperature distabilised the volatile contents of the adsorbents due to bond breakage and linkages thereby resulting in increased percentage of active carbon (Ojo et al., 2017). As rightfully stated by Bello et al. (2013), 'the higher the carbon content, the better the adsorbent for adsorption process'. Therefore, modified biosorbents are capable of higher dye removal efficiency than raw biosorbents.

Figures 4.9 and 4.11 present EDS spectra of spent raw and modified Litchi and DE biosorbents i.e. SRL, SCL and SRDE, SCDE and their respective elemental compositions are presented in Appendix I (c, d, g, h). After adsorption, it was observed that there is significant increase in weight and atom % of carbon and significant reduction in weight and atom % of oxygen for all adsorbents. This change thereby confirms that adsorption of CR dye onto the adsorbents had taken place, and that both forms of sorbent materials are suitable for the removal of CR dye from aqueous solution.

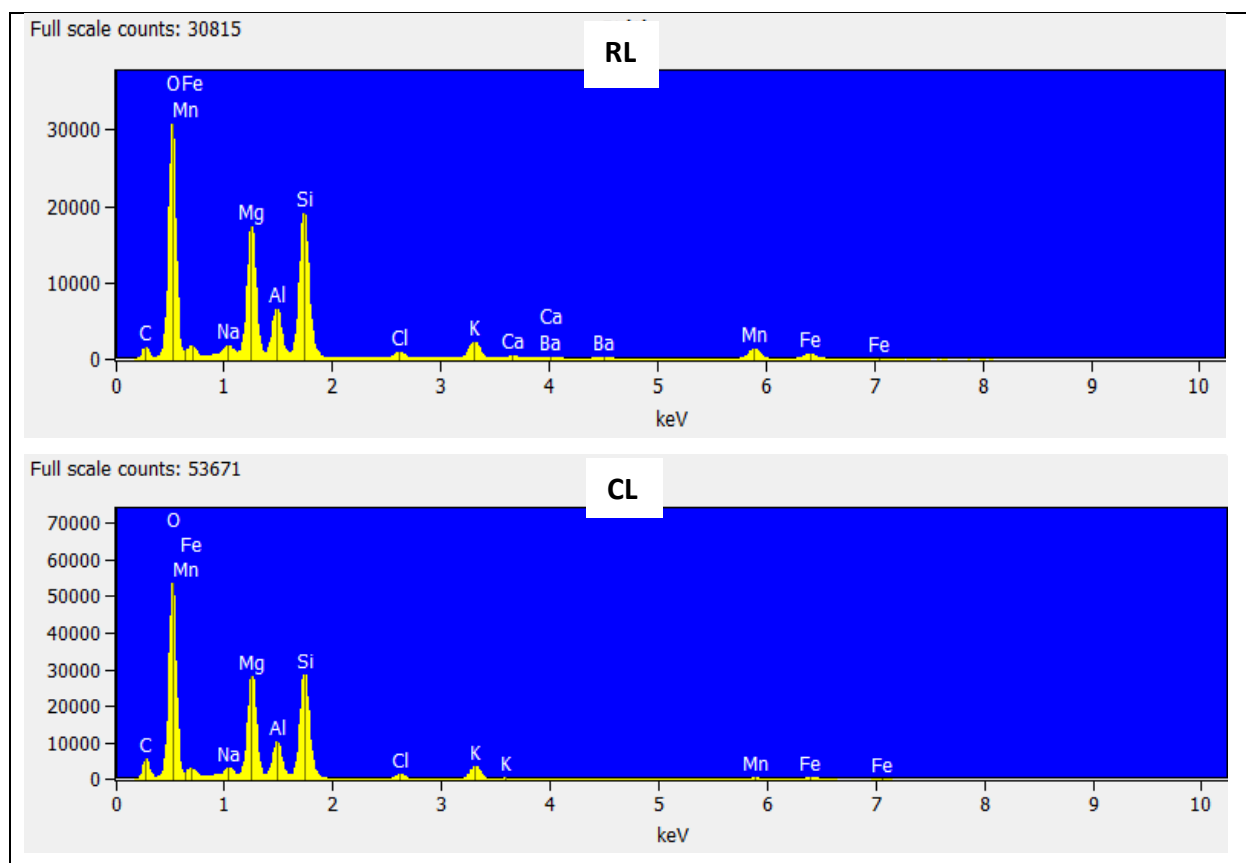


Figure 4.8: EDX spectra of raw Litchi (RL) and modified Litchi (CL)

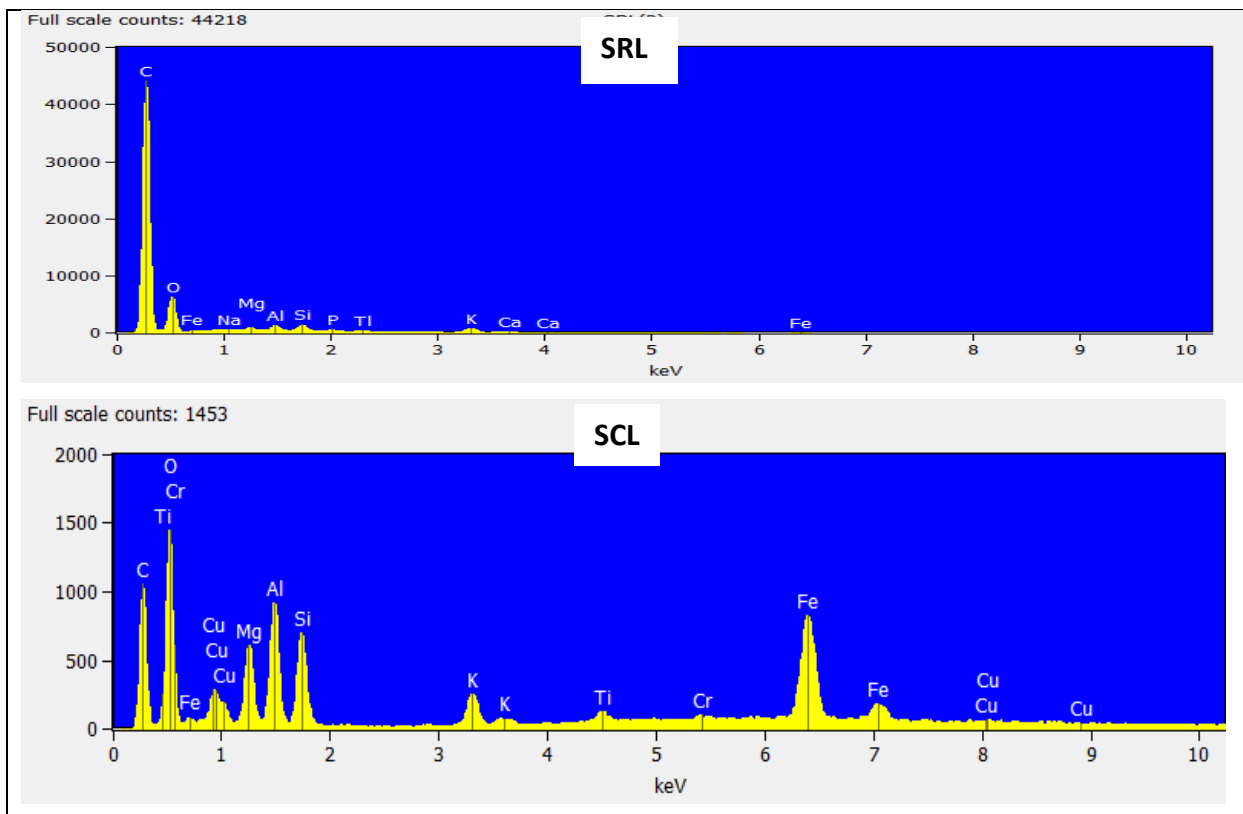


Figure 4.9: EDX spectra of SRL and SCL

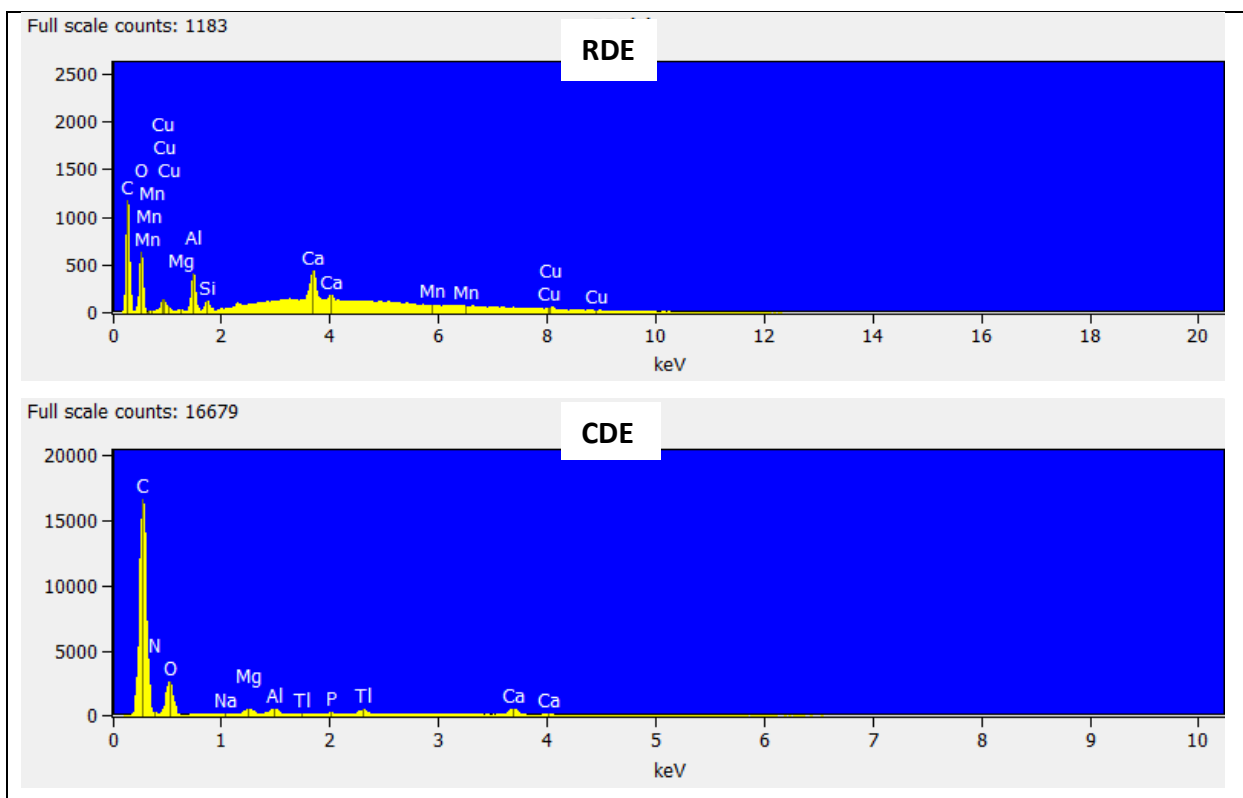


Figure 4.10: EDX spectra of RDE and CDE



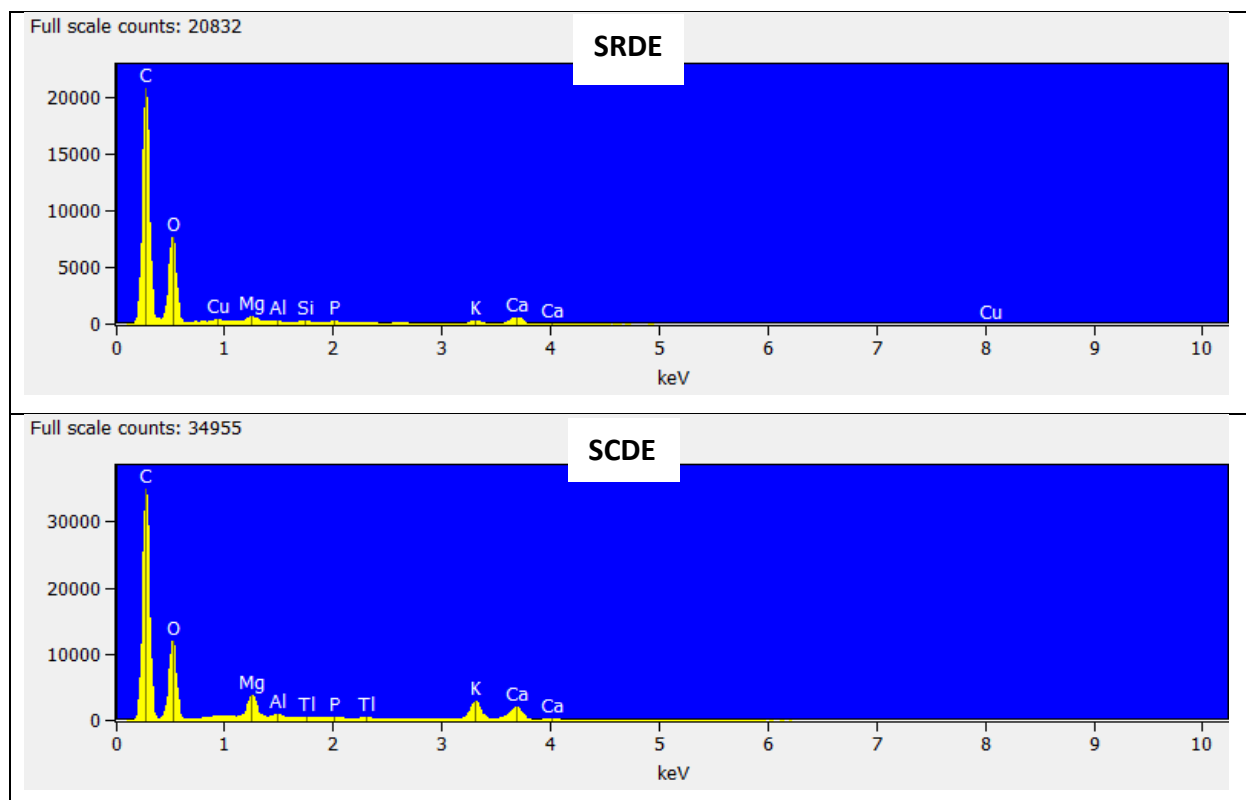


Figure 4.11: EDX spectra of SRDE and SCDE

#### 4.2.4 Brunauer, Emmett, and Teller Technique (BET)

Important characteristics such as surface area and porosity of biomaterials were investigated by Brunauer, Emmett and Teller (BET) method of analysis. Surface area and pore size distribution were analysed by N<sub>2</sub> adsorption and desorption studies. As presented in Table 4.1, BET surface area of raw (RL) and modified (CL) Litchi biosorbents showed low value of 0.4465 m<sup>2</sup>/g and 0.6278 m<sup>2</sup>/g respectively. Also, BET surface area of raw (RDE) and modified (CDE) DE biosorbents are 0.7750 m<sup>2</sup>/g and 0.9727 m<sup>2</sup>/g respectively. The low surface area value is an indication that both biosorbents are not microporous in nature hence, adsorption of CR dye may be through the active surfaces, pores and, functional group interaction which is more of Physiosorption (Inyinbor et al., 2015). Some previous research on adsorption of dye from aqueous solution using plant-based adsorbents have also reported low surface area values (Inyinbor et al., 2015; Sharma and Tiwari, 2016; Lin et al., 2020). The observed increase in surface area after acid modification can be credited to acidic washing of the cell wall which eliminated some polar functional groups on the surfaces of the biosorbents (Inyinbor et al., 2015). After adsorption of CR dye, there are reduction in BET surface area values of the spent biosorbents (SRL, SCL, SRDE and SCDE). This reduction in BET surface area value could be as a result of adsorption of CR dye, which now occupy active surfaces of the biosorbents.

Table 4.1: BET structure parameters of biosorbents

Biosorbents	BET surface area (m <sup>2</sup> /g)	Total pore volume (cm <sup>3</sup> /g)	Average pore diameter (Å)
RL	0.4465	-0.000022	86.899
SRL	0.3497	0.000273	336.486
CL	0.6278	0.000236	845.690
SCL	0.4263	0.000186	1701.820
RDE	0.7750	0.000021	370.593
SRDE	0.5519	0.000017	233.335
CDE	0.9727	0.000138	362.997
SCDE	0.6621	0.000211	222.988

#### 4.2.5 X-Ray Diffraction

X-ray Diffraction (XRD) analyses the crystalline and amorphous nature of the plant materials under investigation. The diffraction pattern of a crystalline material shows prominent or sharp peaks while that of an amorphous material shows broad or irregular peaks. The X-ray diffraction plots of both raw and modified Litchi peels powder (RL and CL) before adsorption, alongside their respective spent forms (SRL and SCL) after adsorption are presented in Figure 4.12. The diffraction plots of RL and CL displayed broad peaks at 2-theta angles 13°, 22° and 43° which are associated with organic functional groups present in the biosorbents (Lin et al., 2020). The diffraction pattern of RL revealed amorphous nature of the biosorbent as there were no prominent peaks in the diffraction pattern. Modified biosorbent (CL) showed some level of crystallinity due to short sharp peak displayed at 2 theta angle 27° which could be attributed to impact of modification at high temperature. This sharp peak was further intensified/elongated as noticeable in the diffraction pattern of the spent adsorbent (SCL) after adsorption of crystalline natured CR dye. This could be attributed to the adsorption of CR dye on the upper layer of the biosorbent's surfaces (Elavarasan et al., 2018). Moreover, diffraction pattern of both spent biosorbents (SRL and SCL) moved to higher intensities. This result suggests that dye adsorption might induce bulk phase changes of the biosorbents.

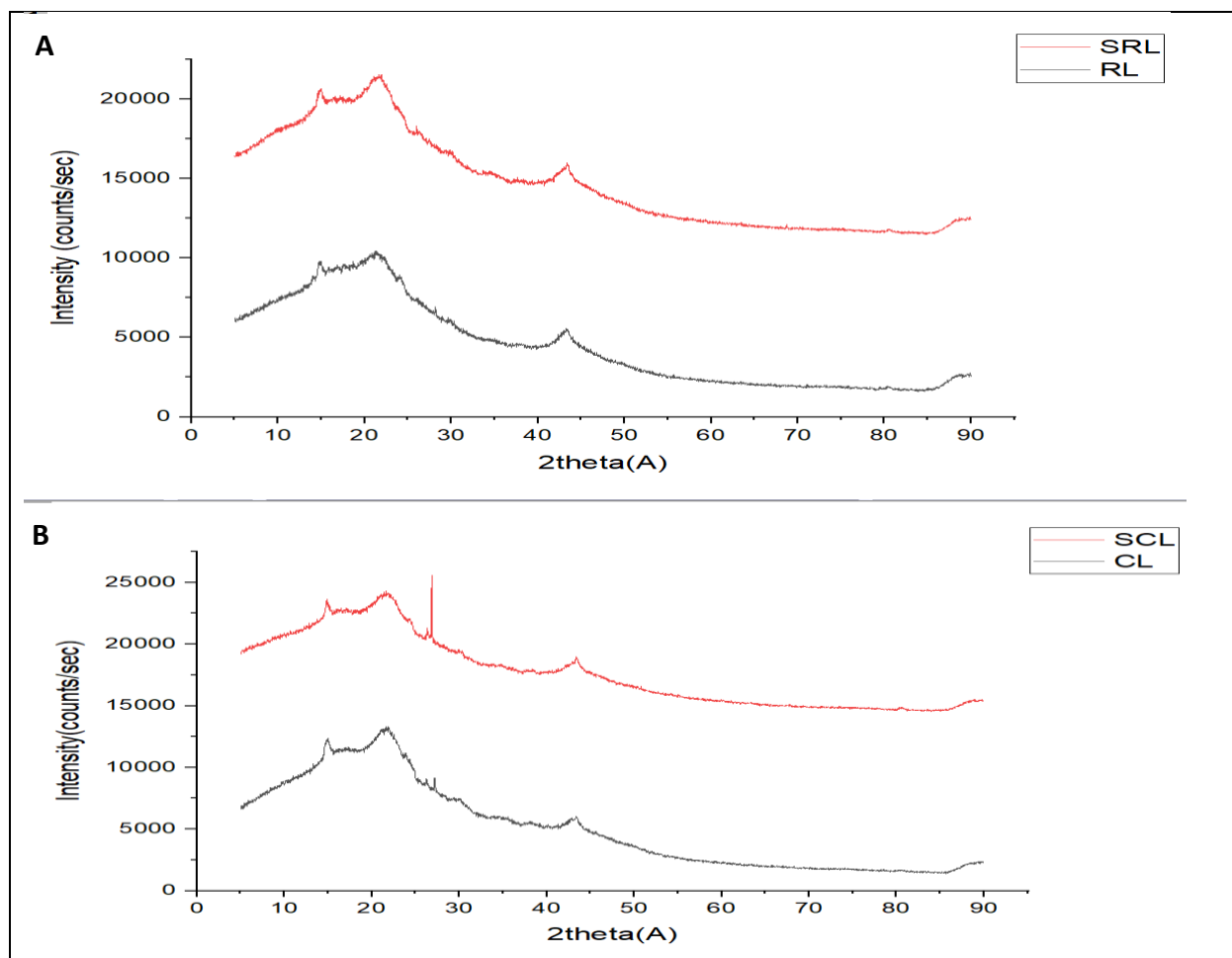


Figure 4.12: XRD plots of (A)- RL and SRL, and (B)- CL and SCL

X-ray diffraction plots for both raw and spent DE (RDE and SRDE), alongside modified DE and spent modified DE (CDE and SCDE) are presented Figure 4.13. The diffraction pattern of RDE displayed broad peaks at 2-theta angle 22° which is associated to organic functional groups (Lin et al., 2020). The diffraction pattern of RDE reveals some level of crystallinity due to sharp peak displayed at 2 theta angle 27°, which can be assigned to cellulosic content of plant material-based adsorbent (Edokpayi et al., 2019). Constriction of the intensity of sharp peak at 2 theta angle 27° of RDE is noticeable in the spectra of CDE at 2 theta angles 27° and 28° which could be due to resultant effect of acid modification at high temperature.

After the adsorption of CR dye ions, the adsorbents changed into amorphous state which is noticeable by total constriction of the intensity of sharp diffraction peaks of spent adsorbents (SRDE and SCDE). This has been attributed to the adsorption of CR dye on the active sites of the biosorbents surfaces (Elavarasan et al., 2018). Moreover, XRD pattern of spent biosorbents also displayed higher intensities of diffraction peaks. This result suggests that dye adsorption might induce bulk phase changes of the adsorbents. Study conducted by Kaur et al. (2013) on

removal of CR dye by biowaste materials as adsorbent also showed similar change of crystalline to amorphous state after adsorption of CR dye.

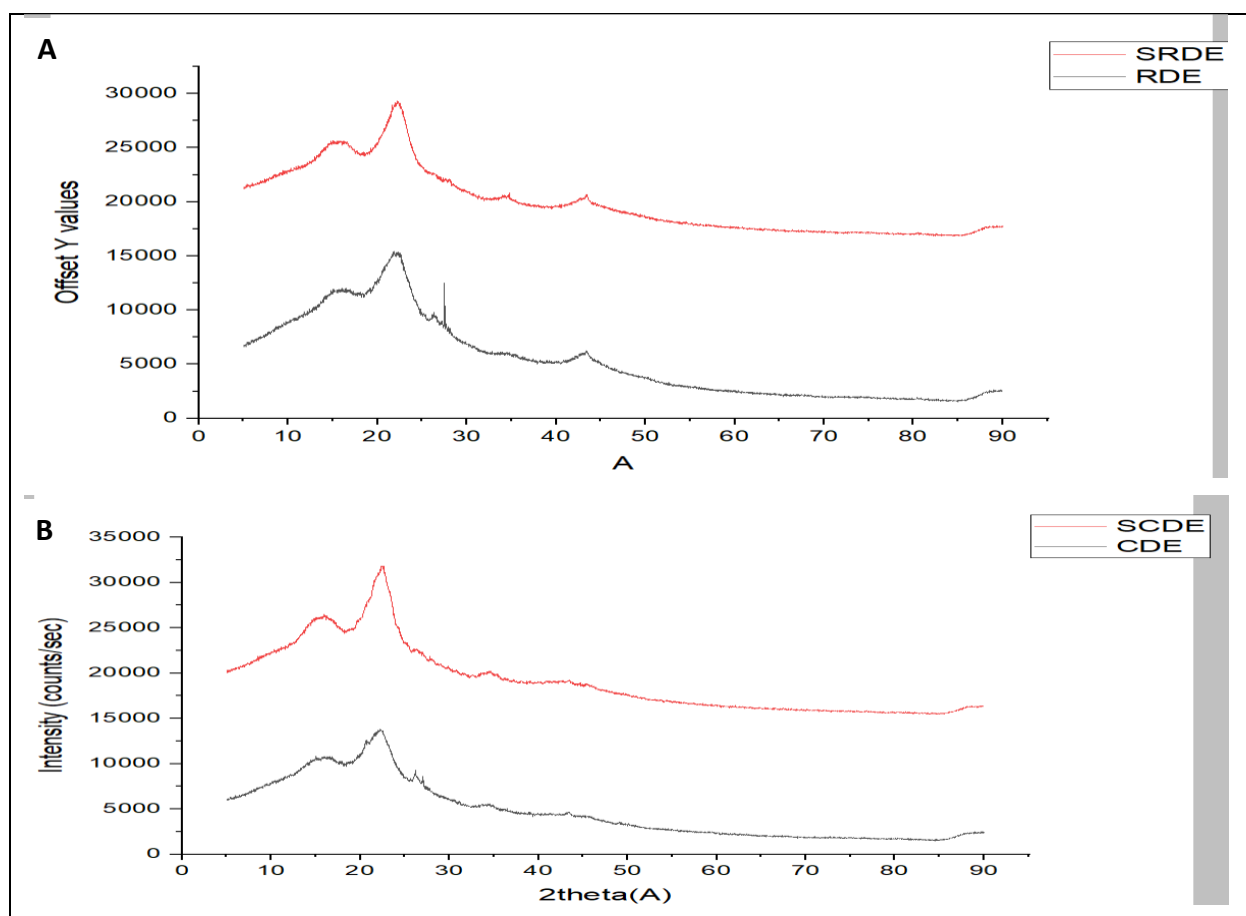


Figure 4.13: XRD plot of (A)- RDE and SRDE, and (B)- CDE and SCDE

### 4.3 Point of zero charge (PZC)

The plots of change in pH against initial pH are shown in Figures 4.14 and 4.15. Point of zero charge (point of intersection on x-axis) for RL and CL were determined to be 5.8 and 4.1 respectively while PZC for RDE and CDE are determined to be 6.2 and 2.8 respectively. When the pH of adsorption process is below PZC value, the adsorbent surface is positively charged (attracting anions) because more protons are donated by the acidic water than the hydroxide group. Conversely, above PZC value, the adsorbents' surface is negatively charged (attracting cations/repelling anions). For this study, PZC for biosorbents are all in the acidic region which means that the adsorbents would strongly attract anions at acidic pH.

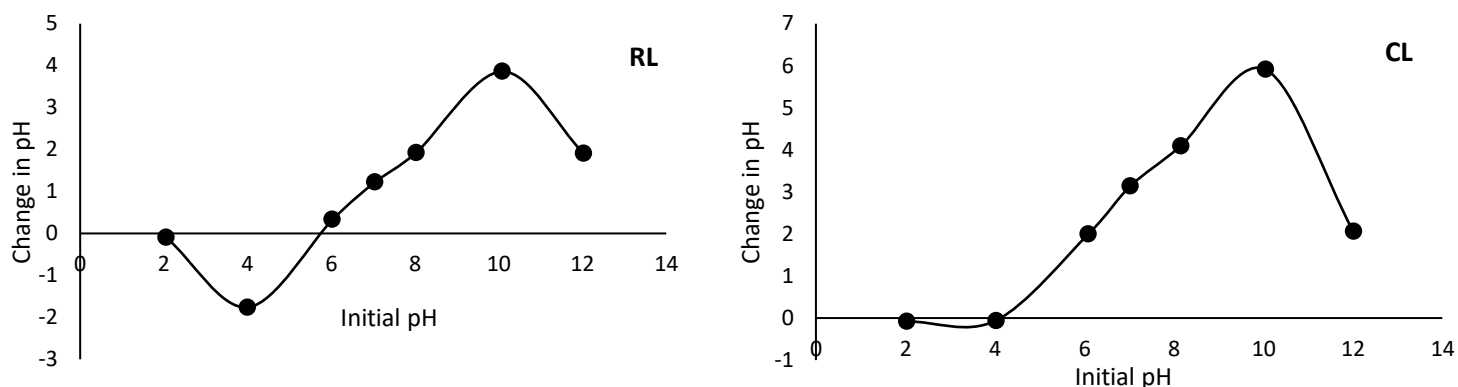


Figure 4.14: Point of zero charge for RL and CL

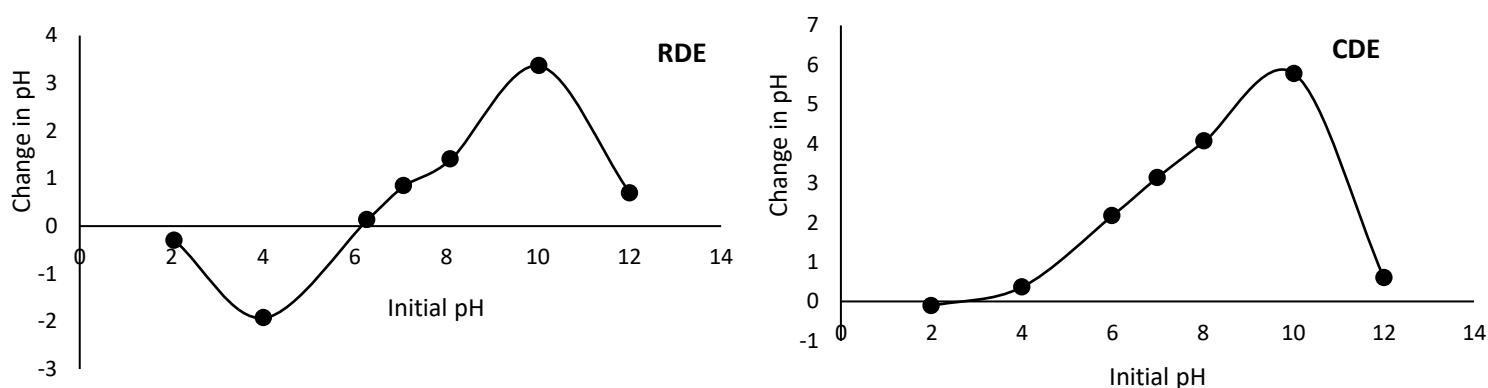


Figure 4.15: Point of zero charge for RDE and CDE

#### 4.4 Effect of experimental parameters on adsorption of Congo red from aqueous solution

##### 4.4.1 Effect of contact time

The effect of contact time on CR dye adsorption from aqueous solution using raw and modified Litchi biosorbents (RL, CL) and raw and modified DE biosorbents (RDE, CDE) were investigated, and the results are graphically presented in Figures 4.16 and 4.17 respectively. These plots clearly showed that the removal efficiency of CR dye by 0.05 g, 0.1 g and 0.15 g masses of adsorbents increased rapidly with increasing contact time and attained equilibrium at 90 minutes for RL, RDE, CDE and at 15 min for CL. It is important to note that all the masses of adsorbents showed the same level of consistency in attaining equilibrium. However, the modified Litchi (CL) attained equilibrium in 15 min; faster than other adsorbents which attained equilibrium at 90 min. Beyond these equilibrium times, there were no further reasonable or consistent increase in removal of CR from aqueous solution. Presence of virgin active sites on the surface of adsorbents at the early phase could be responsible for rapid removal efficiency of CR from the solution. In addition, increase in removal percentage with increased adsorbent dosage from 0.05 - 0.15 g was achieved because of more vacant active sites provided by larger mass of adsorbent. Little or no

increase in the adsorption efficiency that was observed after equilibrium was attained could be attributed to saturation of the biosorbent's surfaces with CR molecules (Toor et al., 2015; Tarmizi et al., (2017). Similar trend has been observed in some other studies on adsorptive removal of anionic dyes (Wanyonyi et al., 2014; Ojo et al., 2017; Felista et al., 2020, Edokpayi and Makete, 2021). However, these comparable studies recorded longer equilibrium time and higher doses of adsorbents.

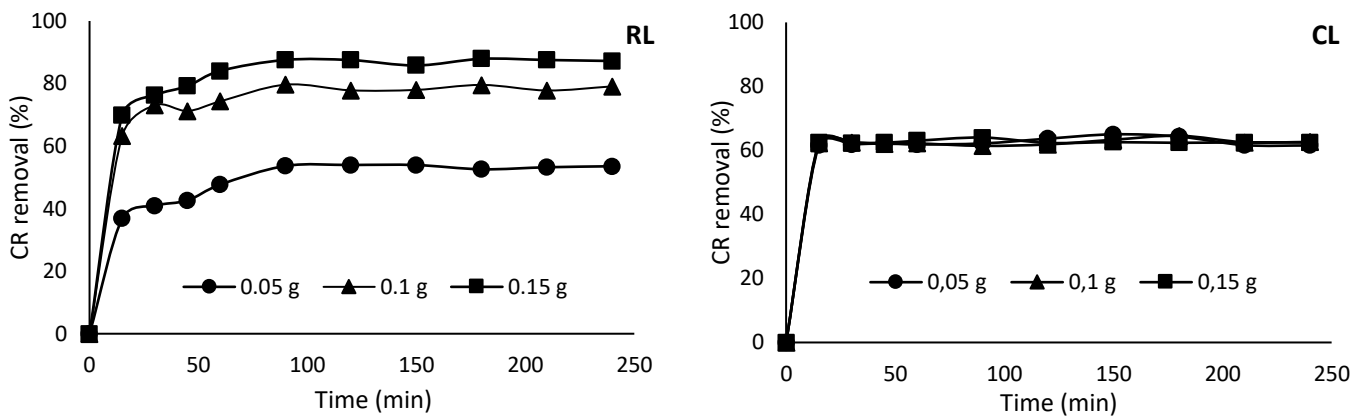


Figure 4.16: Effect of time on adsorption of CR dye onto RL and CL

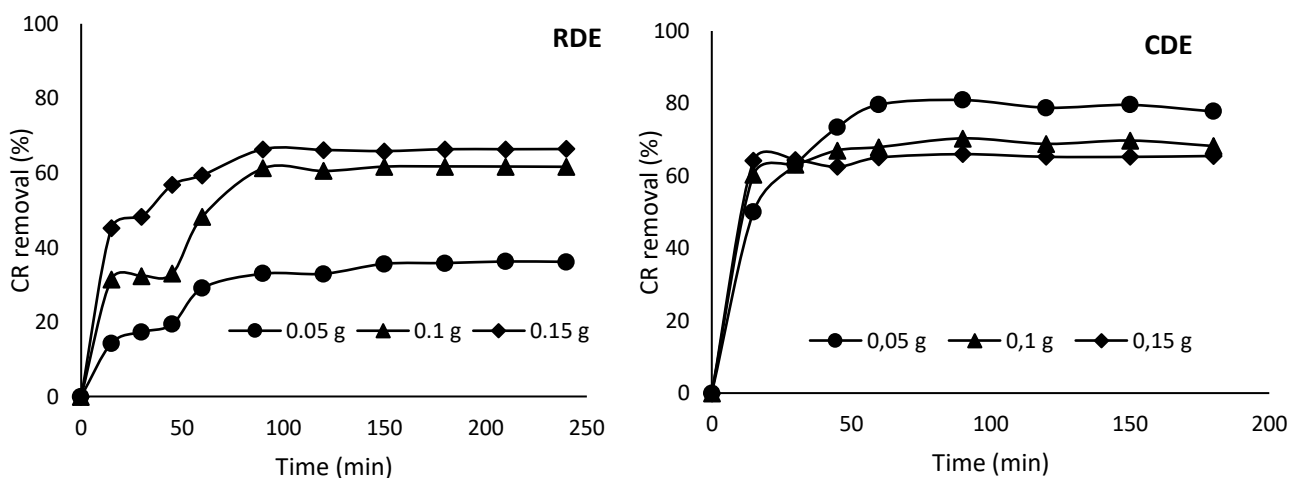


Figure 4.17: Effect of time on adsorption of CR dye onto RDE and CDE

#### 4.4.2 Effect of temperature

The relationship between adsorption of CR dye from aqueous solution using RL, CL and RDE, CDE biosorbents with varying temperature are shown graphically in Figures 4.18 and 4.19 respectively. During biosorption study, the effect of temperature was investigated by increasing the working temperature between 30 - 80°C. The results as displayed in the plots shows that increase in temperature did not favour adsorption of CR dye unto raw biosorbents (RL, RDE), implying an exothermic adsorption process. On the contrary, the result for modified biosorbents (CL, CDE) shows that increased temperature favoured CR dye removal from aqueous solution indicating an endothermic adsorption process. This increase in uptake of CR dye by modified biosorbents could be credited to increase in mobility of dye molecule due to higher temperature and more activation of adsorbent's active sites due to modification of the biosorbent. Study conducted by Olakunle et al. (2017) on adsorption of CR by activated cocoa pod husk showed the same trend with increasing temperature but novel modified biosorbents (CL and CDE) in this study exhibited higher removal efficiency.

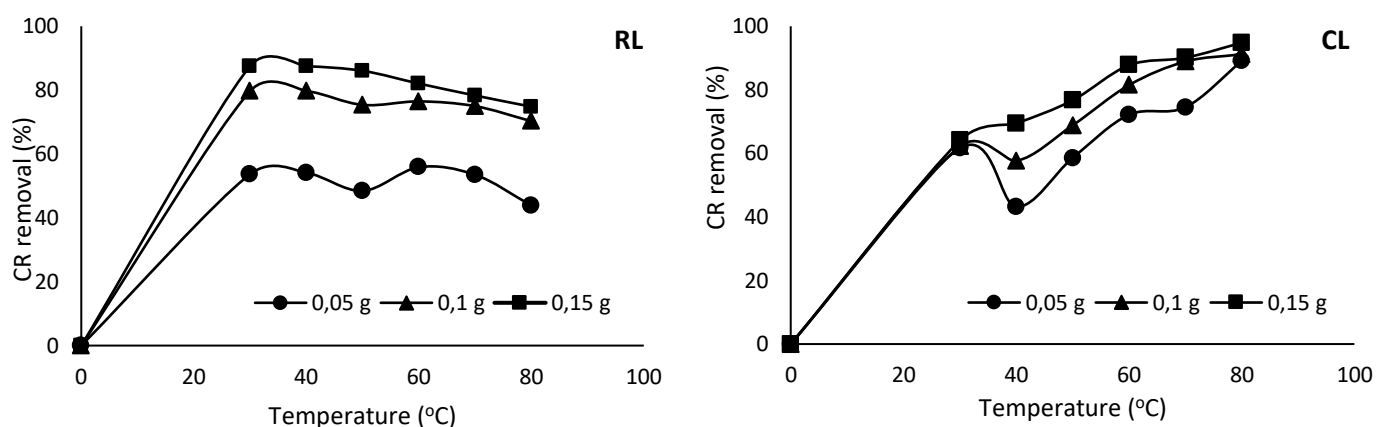


Figure 4.18: Effect of temperature on adsorption of CR dye onto RL and CL

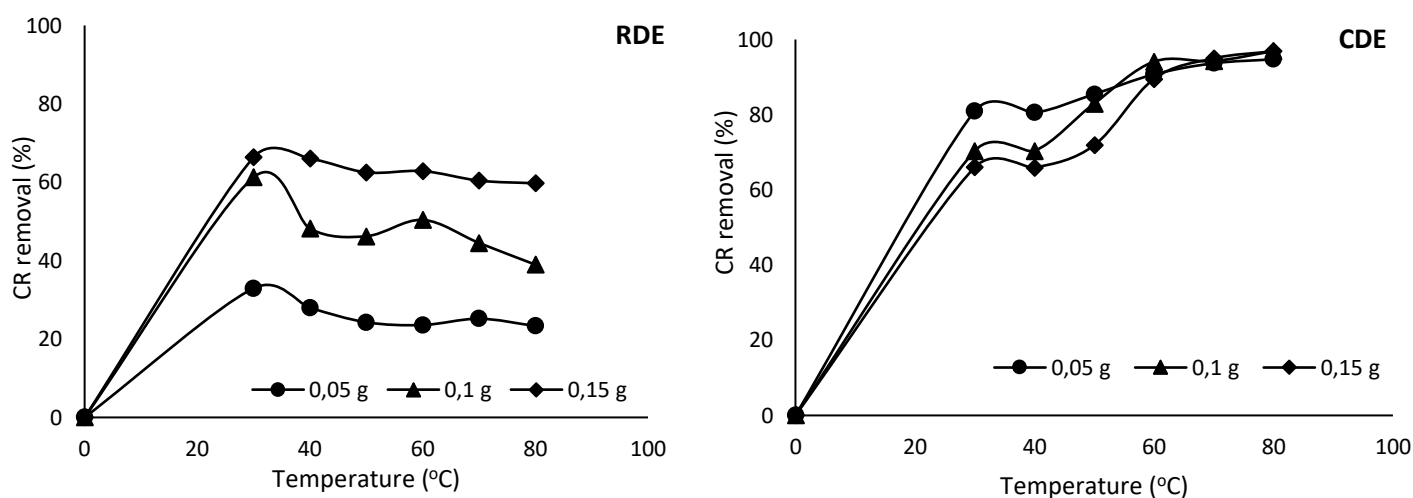


Figure 4.19: Effect of temperature on adsorption of CR dye onto RDE and CDE

#### 4.4.3 Effect of dosage and concentration

The effects of adsorbent dosage and initial CR dye concentration on the adsorptive removal of CR dye from aqueous solution using RL, CL and RDE, CDE biosorbents were investigated. Adsorbents' dosage of 0.5 g/L–5.0 g/L were used on different adsorbate concentration of 40, 60 and 80 mg/L and the results are presented in Figures 4.20 and 4.21. Experimental results as indicated in the plots showed that removal percentage of CR dye increased with increased adsorbent dosage. In general, lowest concentration of 40 mg/L recorded the highest CR dye removal efficiency compared to other concentrations (60 mg/L and 80 mg/L).

It is important to note that raw biosorbents (RL, RDE) reached state of equilibrium at adsorbent dosage of 4 g/L. However, this state of equilibrium was reached much faster by modified biosorbents- CL and CDE with lesser dosage of 1.5 g/L and 2.5 g/L respectively. At this state of equilibrium, similar removal efficiencies of CR dye were recorded regardless of the varying adsorbents dosage. The initial increase in removal efficiency with increased adsorbent dosage could be attributed to the corresponding increase in active site available for adsorption. The successive supplementary CR removal recorded could result from either aggregation or overlapping of adsorption sites (Edokpayi et al., 2019). Due to saturation of adsorbent site, very little or no removal was recorded after the state of equilibrium was reached.

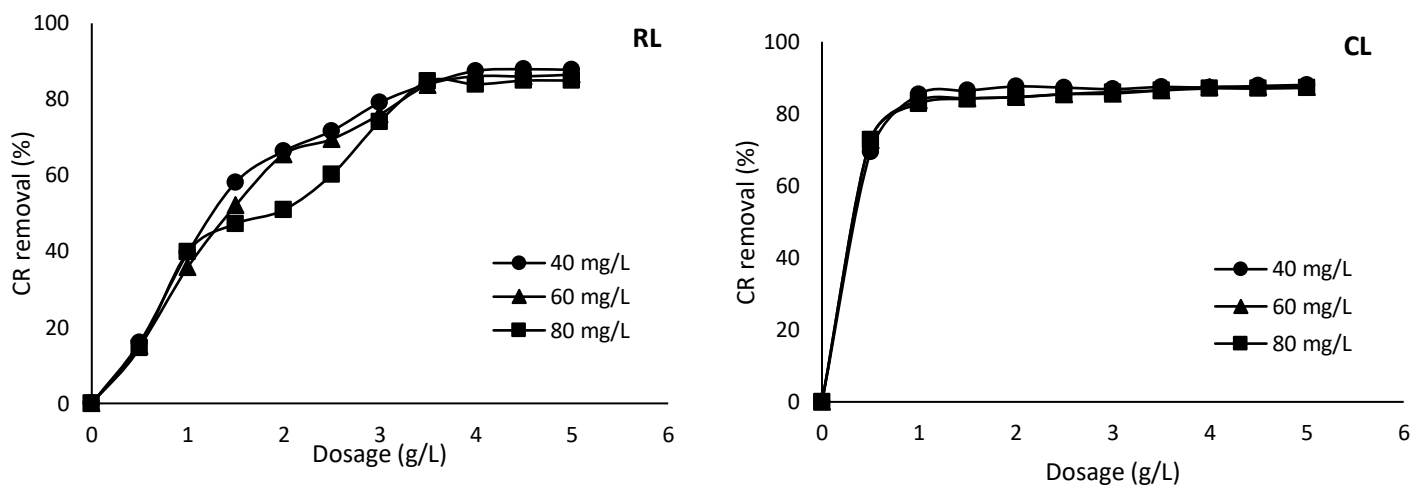


Figure 4.20: Effect of dosage and concentration on adsorption of CR dye onto RL and CL



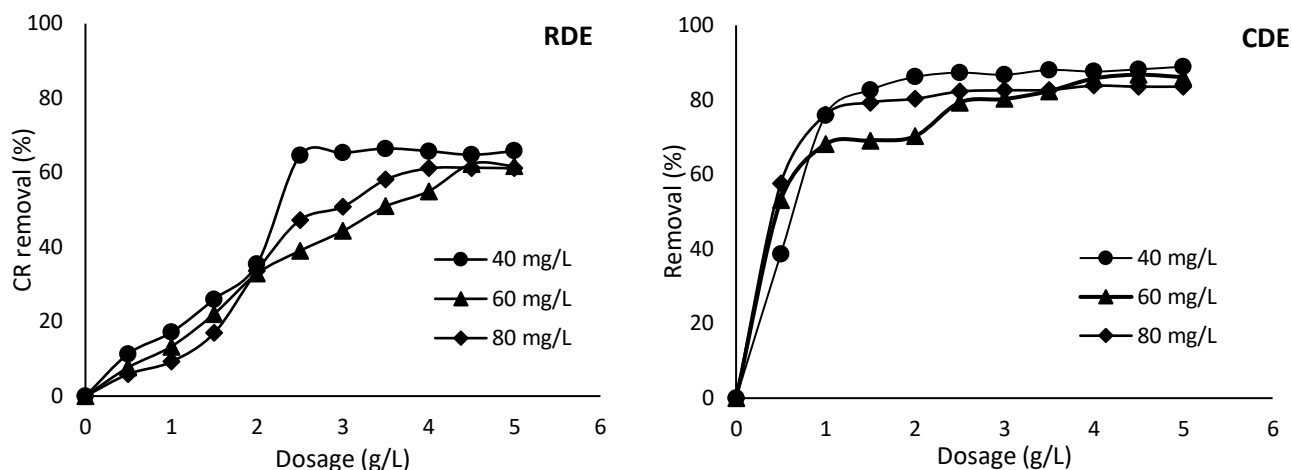


Figure 4.21: Effect of dosage and concentration on adsorption CR dye onto RDE and CDE

#### 4.4.4 Effect of pH

The pH of aqueous solution has been established as a significant parameter of an adsorption process because of its influence on the surface binding sites of the adsorbent and the ionization process of the dye molecule (Jain and Sikarwar, 2014; Lafi et al., 2019). The effect of pH on the adsorption of CR from aqueous solution by raw and modified biosorbents were investigated, and the experimental results obtained are graphically illustrated in Figures 4.22 and 4.23. CR dye is very sensitive to pH change as it turns blue at acidic pH and turns red at basic pH. This colour change in acidic medium is due to protonation, i.e. there is  $\pi$ - $\pi^*$  transition of azo group to higher wavelength (Lafi et al., 2019). The effect of pH was examined in the pH range between 2.0 and 10.0. The plots clearly show that for all adsorbents, maximum CR dye removal percentage was observed at pH 2. Further variation of pH above pH 2 resulted in drastic decline in the removal percentage of CR dye. This observation agrees with the result obtained for PZC in section 4.3, which suggested that CR dye removal efficiency would be best in acidic medium.

CR is an anionic dye which dissociate into  $R-SO_3^-$  in acidic medium. The maximum adsorption of CR dye at pH 2 could be attributed to the existence of strong electrostatic force of attraction between CR in its dissociated state and the positively charged surface of the adsorbent (Lafi et al., 2019). Further increase in pH of the aqueous solution led to increase in negatively charged site and decrease in positively charged site of the adsorbent. This brings about electrostatic repulsion between dye anions and negatively charged site of the adsorbent, thereby causing a decline in adsorption of CR dye (Olakunle et al., 2017; Zhou et al., 2018). Furthermore, the drastic decrease in adsorption of CR at higher pH could also be due to competition for adsorption sites between the increased negative ions ( $OH^-$ ) in solution and CR dye molecules (Ge et al., 2017). Comparable trends of CR dye adsorption using other biosorbents had been reported in literature (Munagapati and Kim, 2016; Ojo et al., 2017; Lafi et al., 2019; Felista et al., 2020).

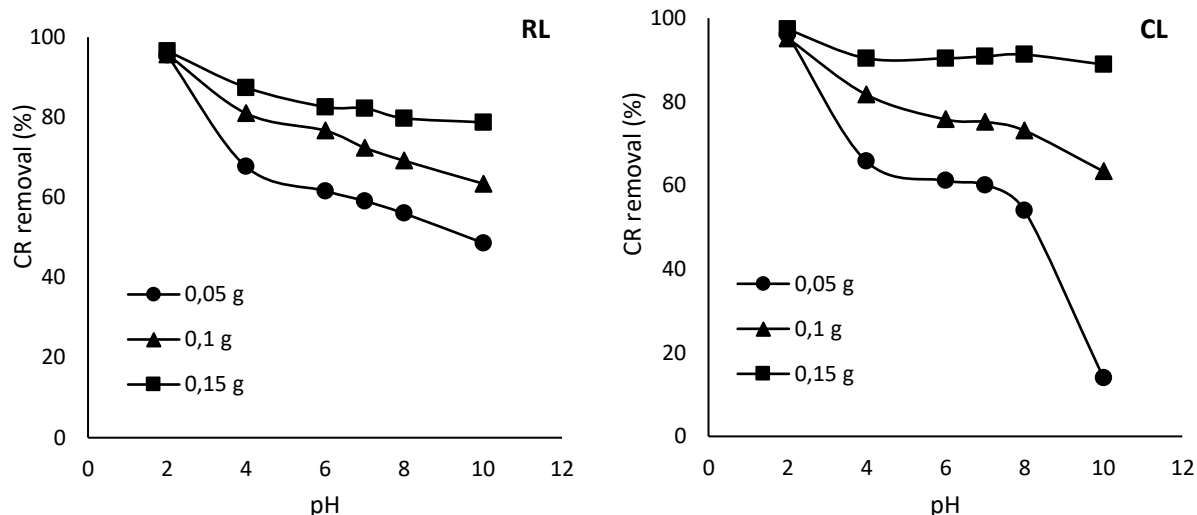


Figure 4.22: Effect of pH on the uptake of CR dye by RL and CL

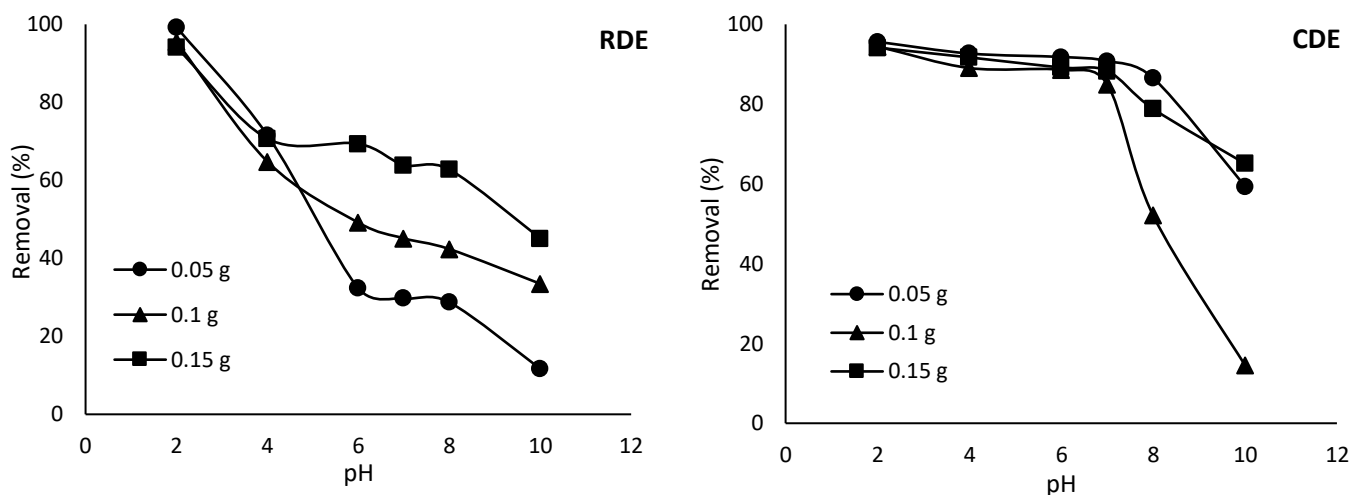


Figure 4.23: Effect of pH on the uptake of CR dye by RDE and CDE

#### 4.4.5 Effect of particle size of adsorbent

Particle size of an adsorbent is an important controlling parameter in the adsorption process because availability of surface area for adsorption is greatly influenced by particle size of the adsorbent. In this study, the effect of particle sizes of <125  $\mu\text{m}$  and >125  $\mu\text{m}$  adsorbents on CR dye adsorption from aqueous solution were investigated and the results are presented graphically in Figures 4.24 and 4.25. It can be deduced from the results that for all adsorbents, adsorption of CR dye is higher with particle size of <125  $\mu\text{m}$ . This could be attributed to the fact that pulverisation of particle sizes to smaller and fine particulate powder provides larger surface area for the same amount of adsorbent, and thereby increasing rate of adsorption (Ikenyiri and Ukpaka, 2016). This implies that powdered adsorbent material has larger surface area and achieved higher removal efficiency than granular material for adsorption process. This observation was consistent with studies conducted on adsorption of CR dye using cabbage waste (Wekoye et al., 2020) and Methylene blue dye using *ginkgo biloba* (Singh et al., 2020).

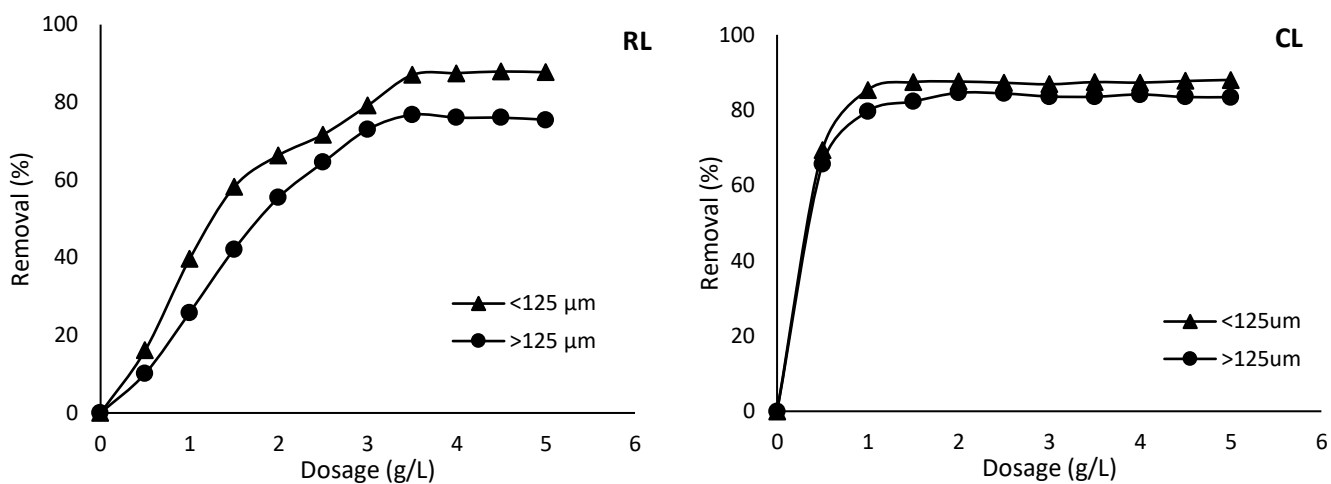


Figure 4.24: Effect of particle sizes of RL and CL on adsorption of CR dye

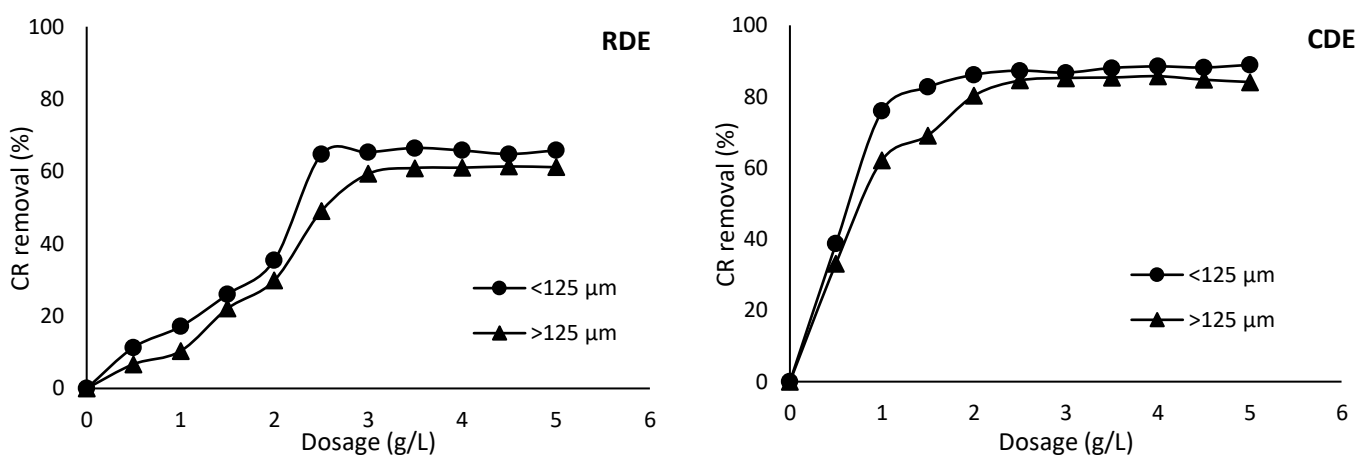


Figure 4.25: Effect of particle sizes of RDE and CDE on adsorption of CR dye

#### 4.4.6 Effect of matrix

The influence of change in water chemistry on adsorption of CR dye from aqueous solution was examined. Simulated CR dye wastewater was prepared with surface water collected from Mutale river, located in Limpopo province. Analysis of the characteristic of Mutale surface water is presented in Table 4.2. Assessment of biosorption experiments conducted with the wastewater and that of deionised water was made. The results as graphically illustrated in Figures 4.26 and 4.27 indicate that there was higher adsorption of CR dye in experiment conducted with natural water (Mutale river) than that of deionised water. Higher removal percentage in natural water could be due to catalytic effect of ions present in natural water on the adsorption process (Edokpayi et al., 2019). These ions tend to speed up uptake of CR dye from the aqueous solution onto the active sites of the biosorbents. This trend of higher removal efficiency in natural water agrees with the study conducted by Edokpayi et al. (2019), when they investigated influence of change in water chemistry on uptake of Methylene blue dye onto *Macademia nutshell*. This therefore ascertains that adsorption process using these novel biosorbents is realistic for

sequestration of dye from real wastewater and not just limited to simulated dye solution prepared in the laboratory.

Table 4.2: Characteristics of natural water from Mutale river

Parameter	Value
pH	6.9
Conductivity ( $\mu\text{S/cm}$ )	24
Turbidity (NTU)	14
Sodium (mg/L)	4.66
Calcium (mg/L)	2.15
Potassium (mg/L)	0.35
Magnesium (mg/L)	1.0
$\text{SO}_4^{2-}$ (mg/L)	3.35
$\text{Cl}^-$ (mg/L)	36.99

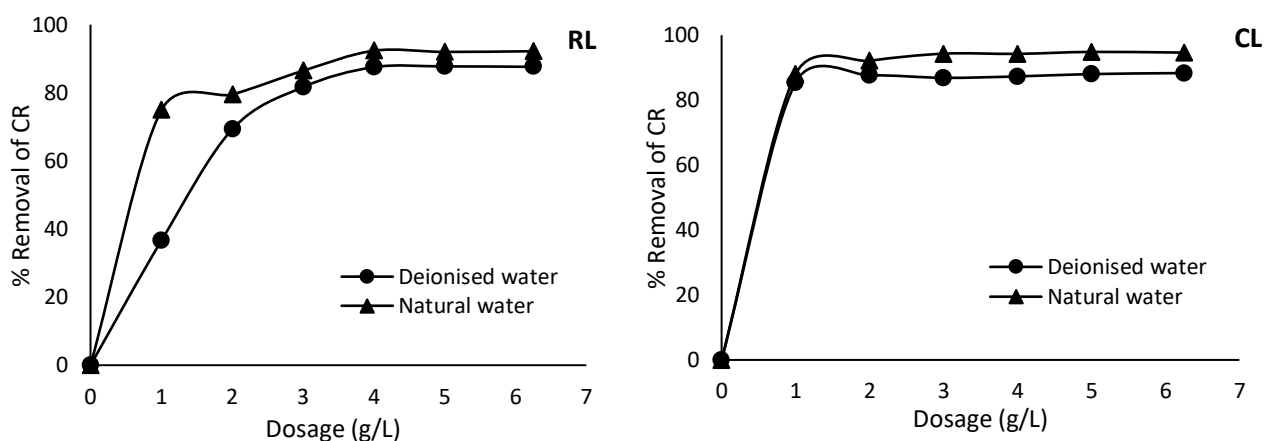


Figure 4.26: Effect of matrix on adsorption of CR dye onto RL and CL

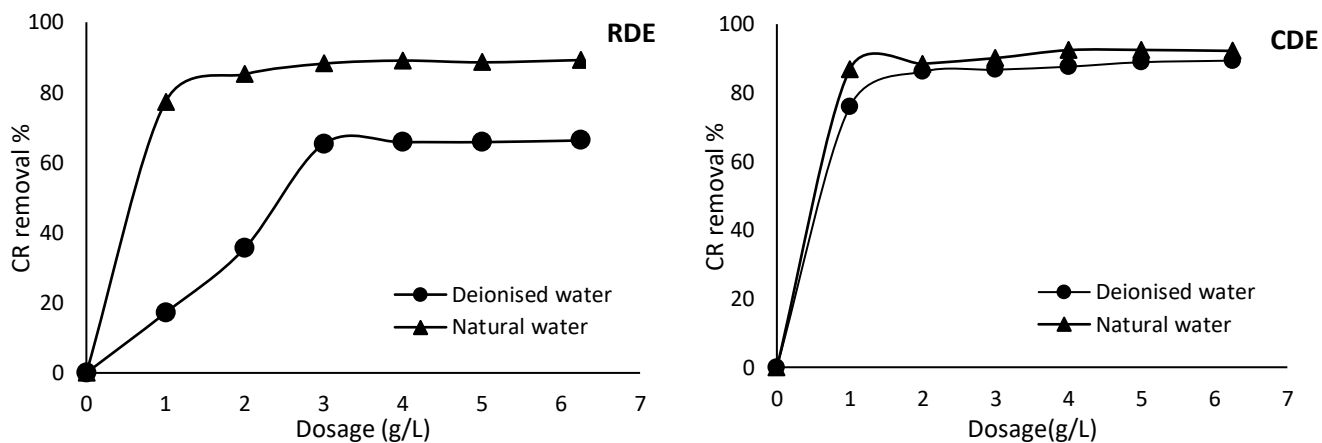


Figure 4.27: Effect of matrix on adsorption of CR dye onto RDE and CDE

#### 4.4.7 Removal efficiency of adsorbents on selective dyes

Effectiveness of the biosorbents on removal of other selective dyes from aqueous solution was explored here, to investigate if the biosorbents' potency is not limited to CR (anionic) dye. Five other dyes were selected in the group of anionic dyes such as methyl orange, erythrosine B and others are in the cationic group such as rhodamine B, methylene blue and malachite green. The results of the experiment conducted on these selective dyes are presented in a plot of removal efficiency against time as shown in Figures 4.28 and 4.29. It can be deduced from the plots that the biosorbents are effective not only for removing CR dye, which is the major dye in this study but also effective for the removal of other dyes. In consequence, higher removal percentage was recorded for dyes in the cationic group. This finding confirms the practicability of these novel biosorbents for effective adsorptive sequestration of any other dyes from aqueous solution.

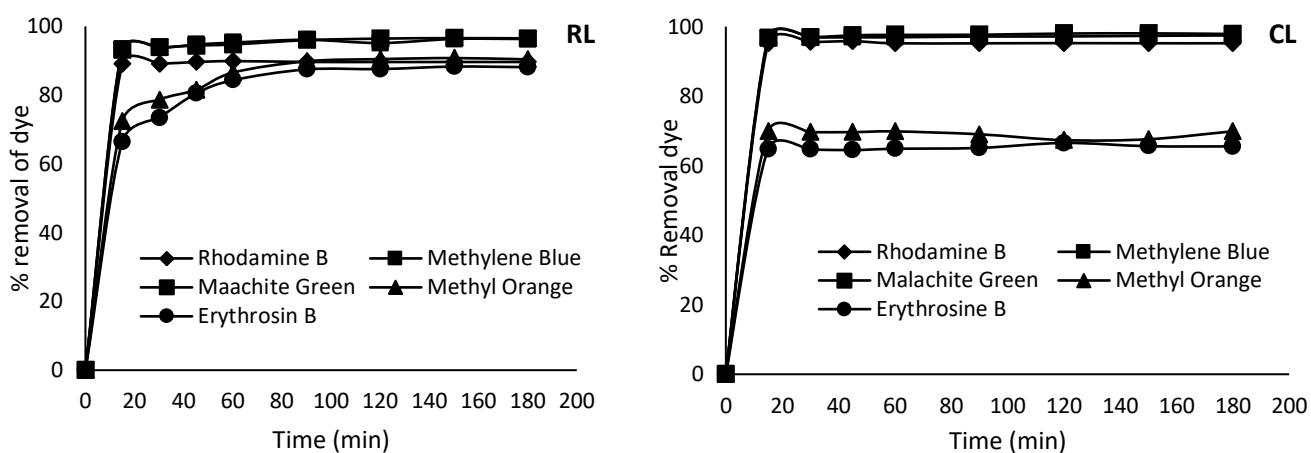


Figure 4.28: Removal efficiency of RL and CL on selective dyes

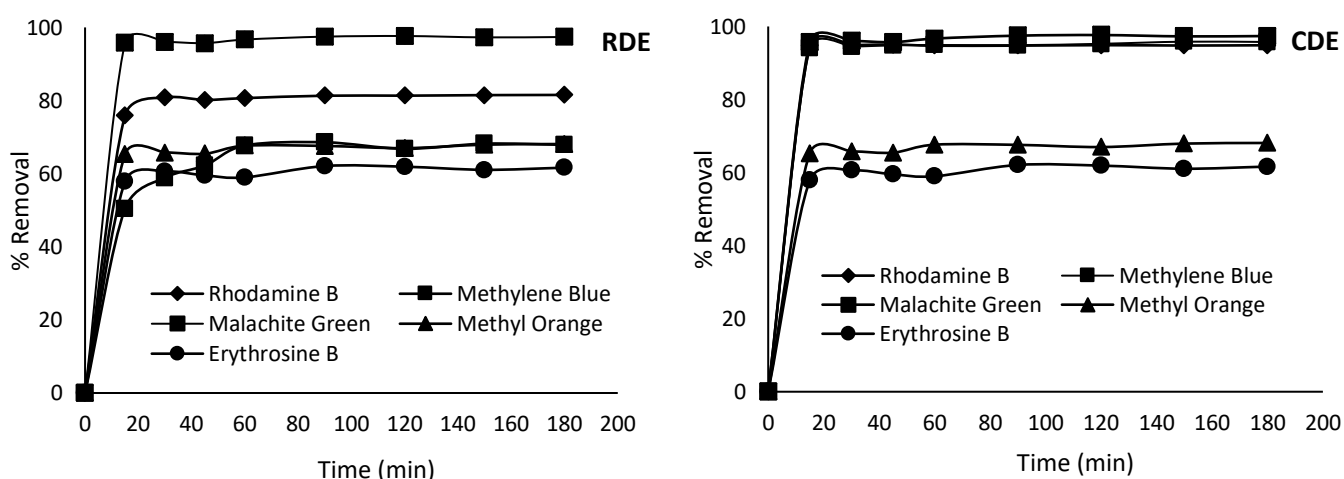


Figure 4.29: Removal efficiency of RDE and CDE on selective dyes

#### 4.5 Adsorption kinetics

The kinetics of adsorption of CR dye onto RL, CL and RDE, CDE biosorbents were investigated to determine the rate of adsorption process. Kinetic (effect of time) data obtained were fitted into pseudo first order, pseudo second order and Intra-particle diffusion kinetic models. The linearised plots of these models are presented in Figures 4.30, 4.31, 4.32 and 4.33. The results of kinetic model parameters are likewise presented in Tables 4.3 and 4.4. From the results obtained, adsorption of CR dye onto all biosorbents best fit model is pseudo second order kinetic model because its correlation coefficients ( $R^2$ ) values are the highest and well close to unity. In addition, the experimental (Exp) and calculated (Cal) values of pseudo second order equilibrium adsorption capacity ( $q_e$ ) are very close, this shows accuracy of the experiments conducted and further affirms that adsorption of CR dye onto RL, CL, RDE and CDE are pseudo second order fitted reactions. Similar outcome has been reported in literature on adsorption of CR or other anionic dyes on various biosorbents (Wanyonyi et al., 2014; Khan et al., 2015; Olakunle et al., 2017; Zhou et al., 2018; Zhang et al., 2019; Lafi et al., 2019; Felista et al., 2020; Wekoye et al., 2020).

In addition, Webber-Morris Intra-particle diffusion model was further used to test the adsorption data to have understanding about the mechanism and rate controlling steps affecting the adsorption kinetics. This fitting of this model consists of various parts that has to do with migration of CR dye from aqueous solution to the surface of the adsorbent. These parts are (i) diffusion of CR dye molecules from aqueous solution to the biosorbent's surface i.e., boundary layer diffusion, (ii) transport of CR dye molecules into the intra-particle active sites i.e. intra-particle diffusion and, (iii) adsorption of CR dye molecules to biosorbent's active sites, which is the equilibrium stage (Rapo et al., 2020). According to the results obtained from the plot of  $q_e$  against  $t^{0.5}$ , the linearity of the plots indicate that intra-particle diffusion is involved in the rate controlling step. However, the fact that the linear plot does not pass through the origin indicates that intra-particle diffusion is not the only rate-controlling step. This suggests that both surface adsorption and intra-particle diffusion are included in the adsorption process, therefore a complex adsorption mechanism (Singh et al., 2020).

**Table 4.3: Kinetic model parameters for RL and CL**

RL										
Mass (g)	Pseudo first order			Pseudo second order				Intra-particle diffusion		
	$q_e$ (mg/g)	$K_1$ ( $\text{min}^{-1}$ )	$R^2$	Exp $q_e$ (mg/g)	Cal $q_e$ (mg/g)	$K_2$ (mg/g $\text{min}^{-1}$ )	$R^2$	$K_p$ (mg/g $\text{min}^{0.5}$ )	C	$R^2$
0.05	3.664	0.0180	0.4575	17.168	17.889	0.0063	0.9981	0.4608	11.042	0.7806
0.10	2.073	0.0152	0.6497	12.744	12.84	0.0213	0.9995	0.1716	10.351	0.6814
0.15	1.062	0.0150	0.5691	9.339	9.515	0.0259	0.9996	0.1427	7.457	0.7348

CL										
Mass (g)	Pseudo first order			Pseudo second order				Intra-particle diffusion		
	$q_e$ (mg/g)	$K_1$ ( $\text{min}^{-1}$ )	$R^2$	Exp $q_e$ (mg/g)	Cal $q_e$ (mg/g)	$K_2$ (mg/g $\text{min}^{-1}$ )	$R^2$	$K_p$ (mg/g $\text{min}^{0.5}$ )	C	$R^2$
0.05	0.824	0.00069	0.0094	19.704	19.802	0.0364	0.9992	0.0127	19.918	0.0156
0.10	0.375	0.00046	0.0151	9.948	9.980	0.354	0.9996	0.0007	9.998	0.0004
0.15	6.445	0.00023	0.0189	6.667	6.658	0.388	0.9999	-0.0010	6.694	0.0050

**Table 4.4: Kinetic model parameters for RDE and CDE**

RDE										
Mass (g)	Pseudo first order			Pseudo second order				Intra-particle diffusion		
	$q_e$ (mg/g)	$K_1$ ( $\text{min}^{-1}$ )	$R^2$	Exp $q_e$ (mg/g)	Cal $q_e$ (mg/g)	$K_2$ (mg/g $\text{min}^{-1}$ )	$R^2$	$K_p$ (mg/g $\text{min}^{0.5}$ )	C	$R^2$
0.05	12.128	0.0249	0.9778	10.544	13.624	0.00204	0.9880	0.6432	2.8465	0.8585
0.10	8.0334	0.0334	0.8304	9.8	11.351	0.00307	0.9813	0.4958	3.2641	0.7968
0.15	2.402	0.0327	0.6835	7.08	7.413	0.015	0.9989	0.1929	4.5482	0.7783

CDE										
Mass (g)	Pseudo first order			Pseudo second order				Intra-particle diffusion		
	$q_e$ (mg/g)	$K_1$ ( $\text{min}^{-1}$ )	$R^2$	Exp $q_e$ (mg/g)	Cal $q_e$ (mg/g)	$K_2$ (mg/g $\text{min}^{-1}$ )	$R^2$	$K_p$ (mg/g $\text{min}^{0.5}$ )	C	$R^2$
0.05	7.449	0.021	0.7492	25.899	26.316	0.0062	0.9969	0.8152	16.18	0.6240
0.10	1.674	0.019	0.9237	11.256	11.173	0.0484	0.9993	0.1338	9.5415	0.6575
0.15	0.786	0.0028	0.3063	7.04	7.391	0.0335	0.9957	0.0577	6.4435	0.4426

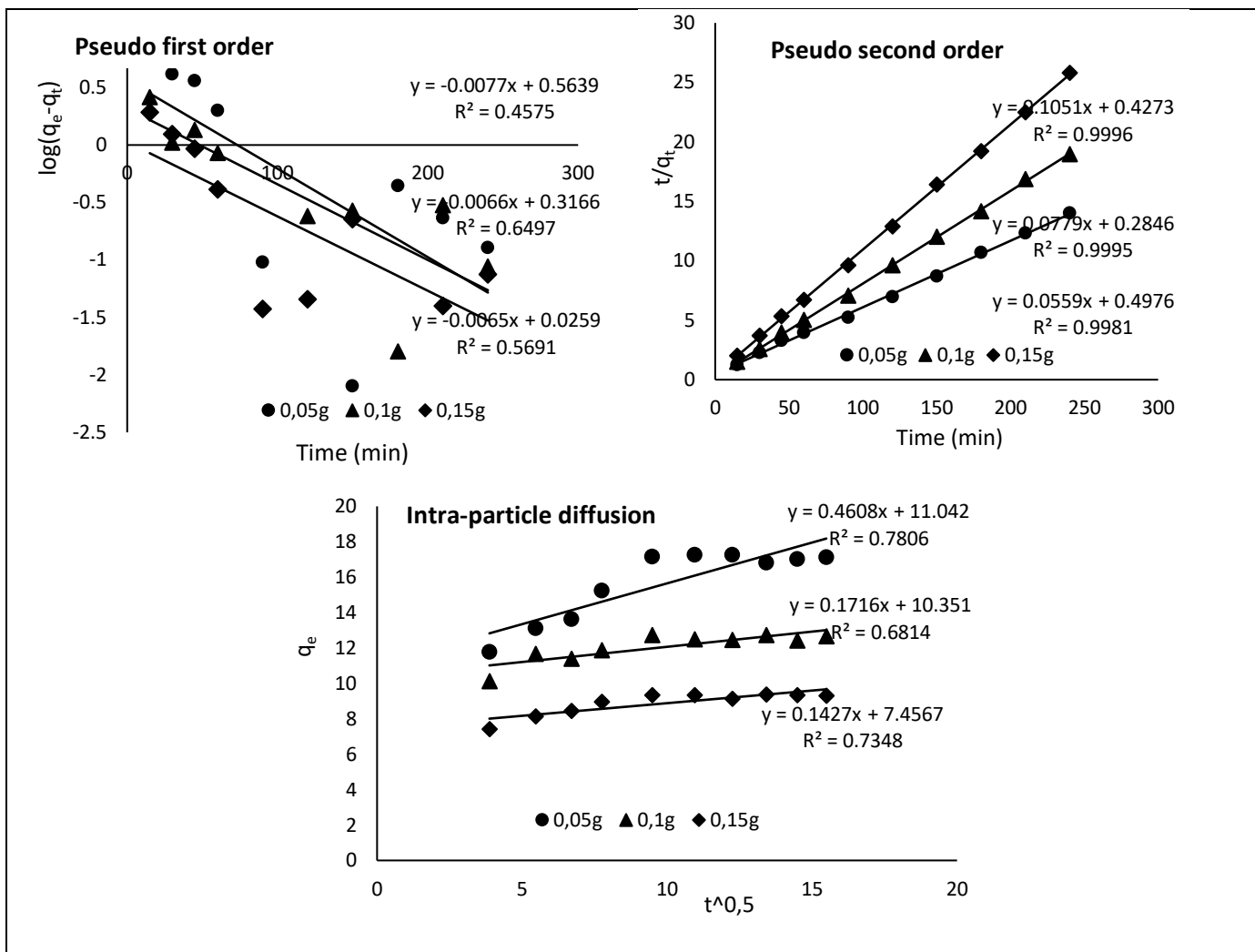


Figure 4.30: Kinetic model plots of RL



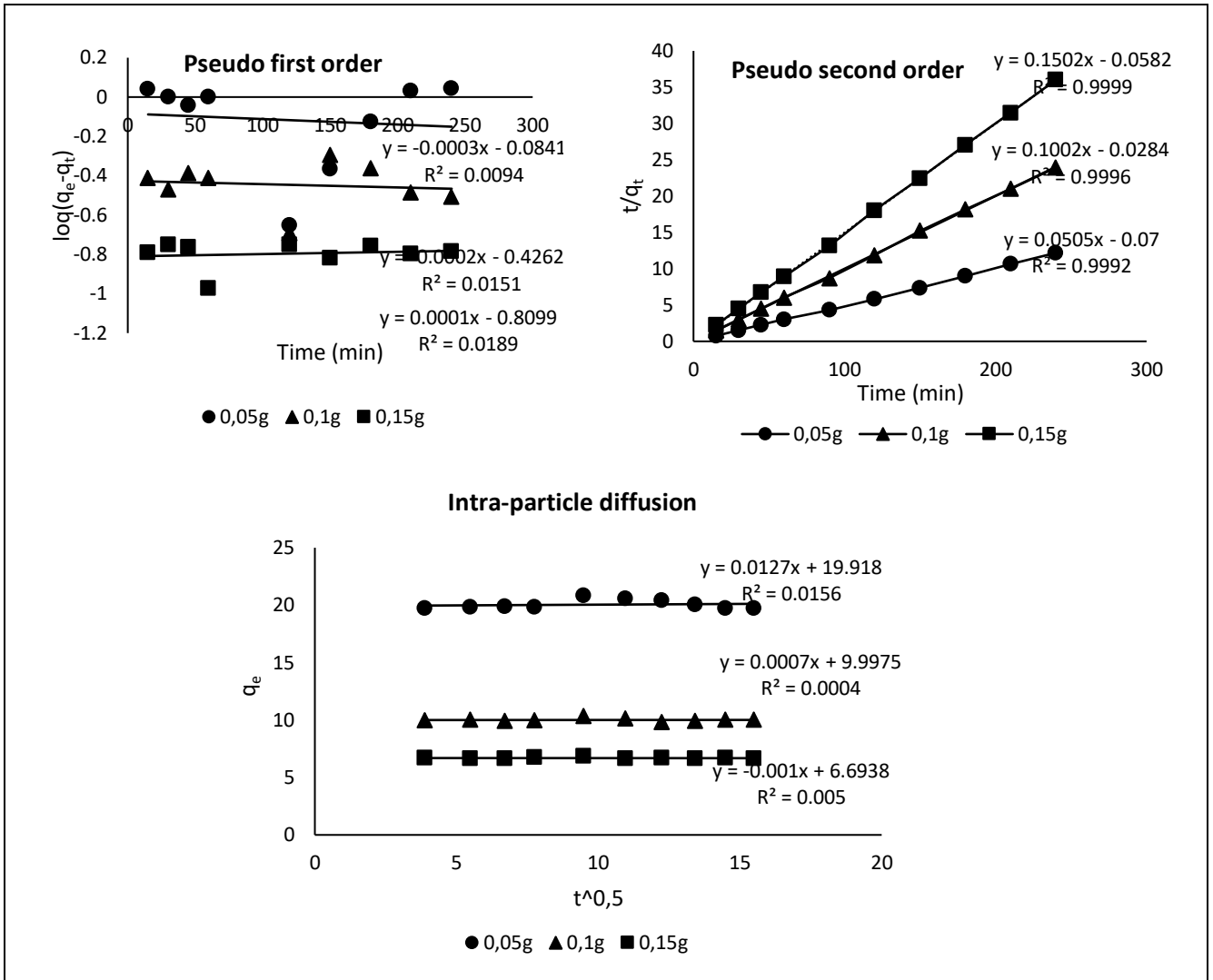


Figure 4.31: Kinetic model plots of CL

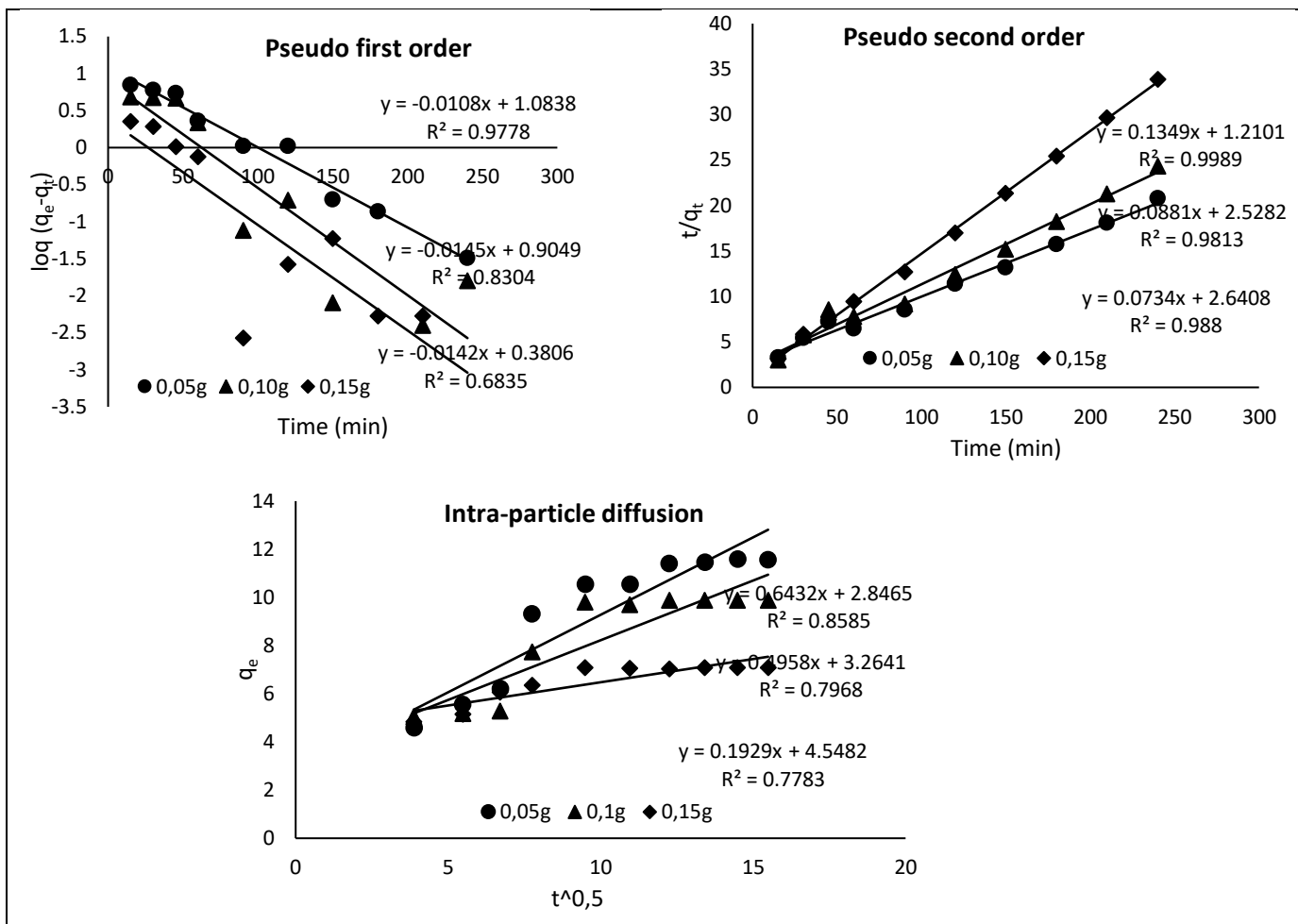


Figure 4.32: Kinetic model plots of RDE

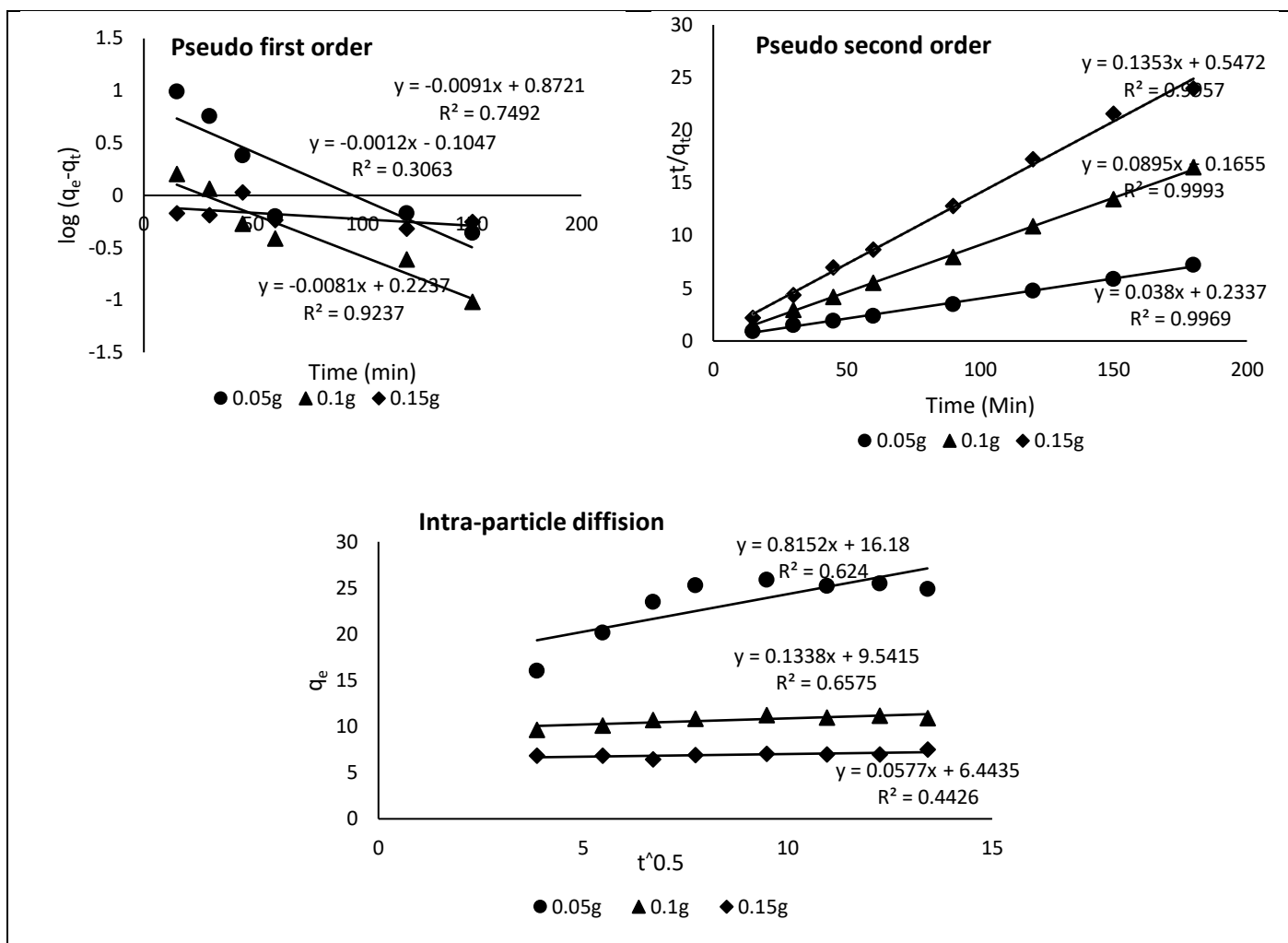


Figure 4.33: Kinetic model plots of CDE

#### 4.6 Adsorption isotherms

Langmuir, Freundlich and Temkin isotherm adsorption models were employed to analyse the equilibrium data at different concentrations and temperatures. These models help to adequately investigate the type of adsorption that took place on the surface of the adsorbents during adsorptive sequestration of CR dye from aqueous solution. Various linearised plots of these models for raw and modified biosorbents are graphically presented in Figures 4.34, 4.35, 4.36 and 4.37. Also, calculated isotherm model parameters determined from respective slopes and intercepts of these plots are presented in Table 4.5 (RL and CL) and Table 4.6 (RDE and CDE).

With reference to the results obtained, all the three models to an extent described the adsorption process because they all showed correlation coefficient ( $R^2$ ) values greater than 0.7. However, the adsorption data best fit is Langmuir isotherm model because it displayed the highest  $R^2$  values. This assumes monolayer adsorption occurred on a uniform and homogenous adsorbent's surface. The conformity of the adsorption process to Langmuir model was further affirmed by a separation factor also known as dimensionless constant (RL). Dimensionless constant-  $R_L$  values

obtained was between Zero and one, which implies that the adsorption process is favourable. In addition, Freundlich model's adsorption intensity ( $n$ ) displayed values greater than unity, which is also an indication of favourable adsorption process. Temkin isotherm model is of the assumption that the heat of adsorption of the adsorbate's molecule linearly decreases with adsorbent layer coverage due to adsorbate–adsorbent interactions (Temkin and Pyzhev, 1940). The plots of  $q_e$  against  $\ln C_e$  yielded linear graphs and from the results of the parameters obtained,  $K_T$  decreased with increase in temperature for raw biosorbents and increased with increase in temperature for modified biosorbents. However, Temkin model displayed lowest  $R^2$  value of the three models and does not provide best fit for adsorption data.

Comparable studies on adsorptive sequestration of CR dye from aqueous solution using various plant-based adsorbents also showed conformity to Langmuir isotherm model. Comparison of their maximum adsorption capacity to this study showed that the novel biosorbents achieved higher adsorption capacities as presented in Table 4.7. Maximum adsorption capacities ( $q_{max}$ ) values of 55.56 mg/g and 51.02mg/g were recorded for RL and RDE respectively at temperature of 303K while CL and CDE recorded higher  $q_{max}$  values of 58.48mg/g and 53.19mg/g respectively at temperature of 353K. It is noteworthy to emphasis that modified adsorbents achieved higher adsorption capacity than the raw adsorbents which could be attributed to significant effect of acid modification. Studies conducted by Yan et al. (2018) and Zhang et al. (2019) also recorded higher adsorption capacity for citric acid modified adsorbents over raw adsorbents.

Table 4.5: Isotherm model parameters for adsorption of CR dye onto RL and CL

RL										
Temp (K)	Langmuir model				Freundlich model			Temkin model		
	$q_{max}$ (mg/g)	$K_L$ (L/mg)	$R^2$	$R_L$	$K_F$ (L/mg)	$N$	$R^2$	$K_T$ (L/g)	$B$ (J/mol)	$R^2$
303	55.56	0.043	0.9856	0.205	2.149	1.049	0.9777	0.897	7.961	0.8321
323	35.21	0.051	0.9838	0.179	1.639	1.135	0.9552	0.704	6.884	0.7759
333	23.42	0.058	0.9770	0.161	1.626	1.454	0.9740	0.664	4.939	0.8957
353	19.92	0.062	0.9715	0.152	1.512	1.511	0.9607	0.623	4.524	0.8677
CL										
Temp (K)	Langmuir model				Freundlich model			Temkin model		
	$q_{max}$ (mg/g)	$K_L$ (L/mg)	$R^2$	$R_L$	$K_F$ (L/mg)	$N$	$R^2$	$K_T$ (L/g)	$B$ (J/mol)	$R^2$
303	15.67	0.127	0.9567	0.081	1.998	1.653	0.9529	0.886	4.312	0.8436
323	21.37	0.156	0.9595	0.067	2.845	1.454	0.9464	1.303	5.600	0.8032
333	52.08	0.159	0.9864	0.065	6.866	1.149	0.9835	2.897	8.167	0.9175
353	58.48	0.163	0.9903	0.064	7.921	1.189	0.9773	3.467	8.037	0.9372

Table 4.6: Isotherm models parameters for adsorption of CR dye onto RDE and CDE

RDE										
Temp (K)	Langmuir model				Freundlich model			Temkin model		
	$q_{max}$ (mg/g)	$K_L$ (L/mg)	$R_L$	$R^2$	$K_F$ (L/mg)	N	$R^2$	$K_T$ (L/g)	B (J/mol)	$R^2$
303	51.02	0.012	0.481	0.9990	0.714	1.143	0.9983	0.332	5.557	0.9389
323	40.16	0.015	0.426	0.9985	0.682	1.158	0.9981	0.320	5.340	0.9160
333	25.77	0.022	0.336	0.9951	0.644	1.205	0.9940	0.304	4.826	0.8888
353	22.83	0.023	0.326	0.9915	0.610	1.219	0.9908	0.292	4.609	0.8785

CDE										
Temp (K)	Langmuir model				Freundlich model			Temkin model		
	$q_{max}$ (mg/g)	$K_L$ (L/mg)	$R_L$	$R^2$	$K_F$ (L/mg)	N	$R^2$	$K_T$ (L/g)	B (J/mol)	$R^2$
303	16.48	0.086	0.114	0.9469	1.269	1.318	0.9450	0.541	5.258	0.7621
323	28.57	0.087	0.113	0.9543	2.707	1.453	0.9074	1.143	5.711	0.9327
333	48.54	0.098	0.102	0.9630	4.397	1.234	0.9555	1.815	7.503	0.9414
353	53.19	0.126	0.081	0.9735	6.058	1.426	0.9358	2.951	6.722	0.9635

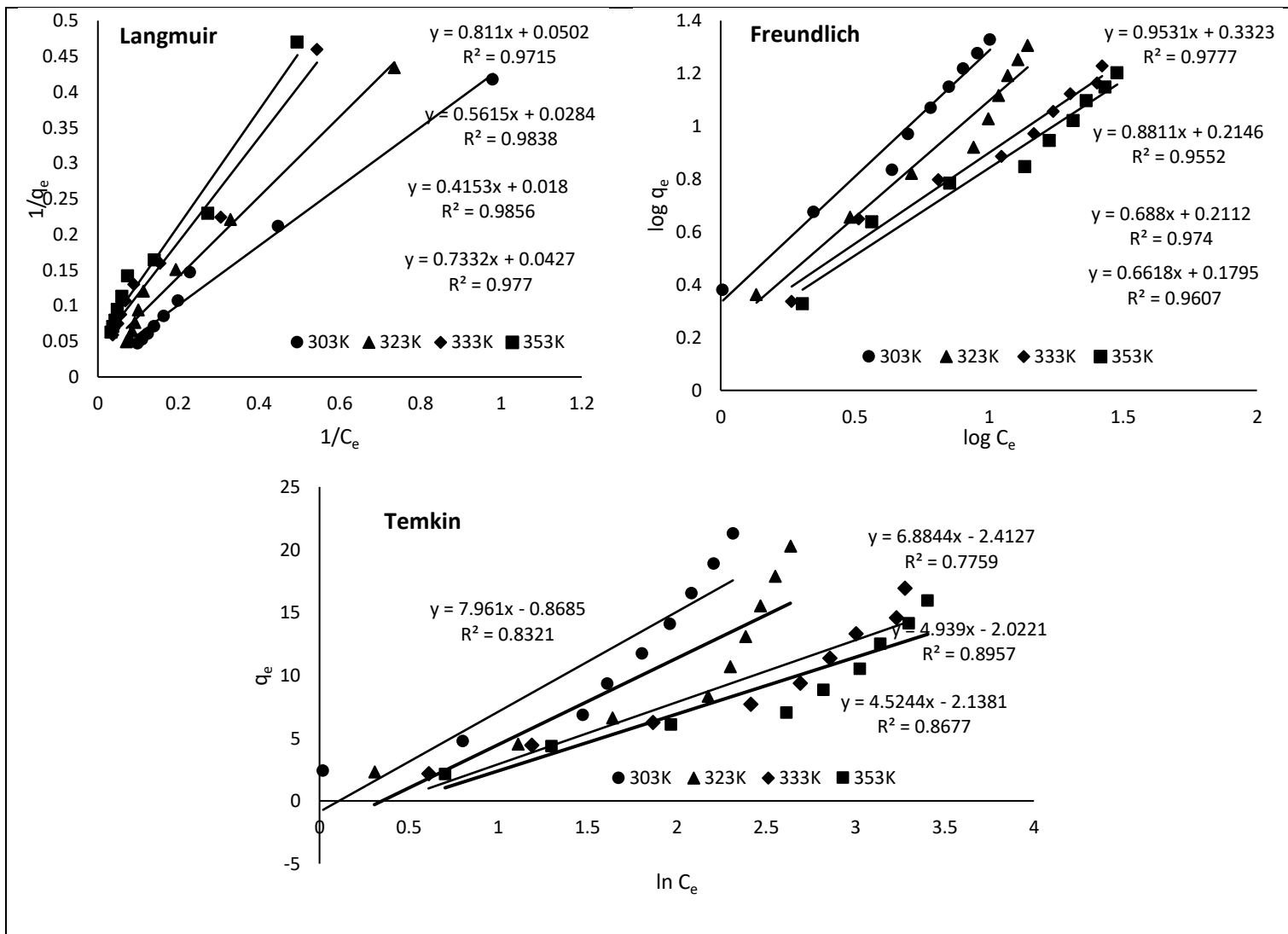


Figure 4.34: Isotherm model plots of RL

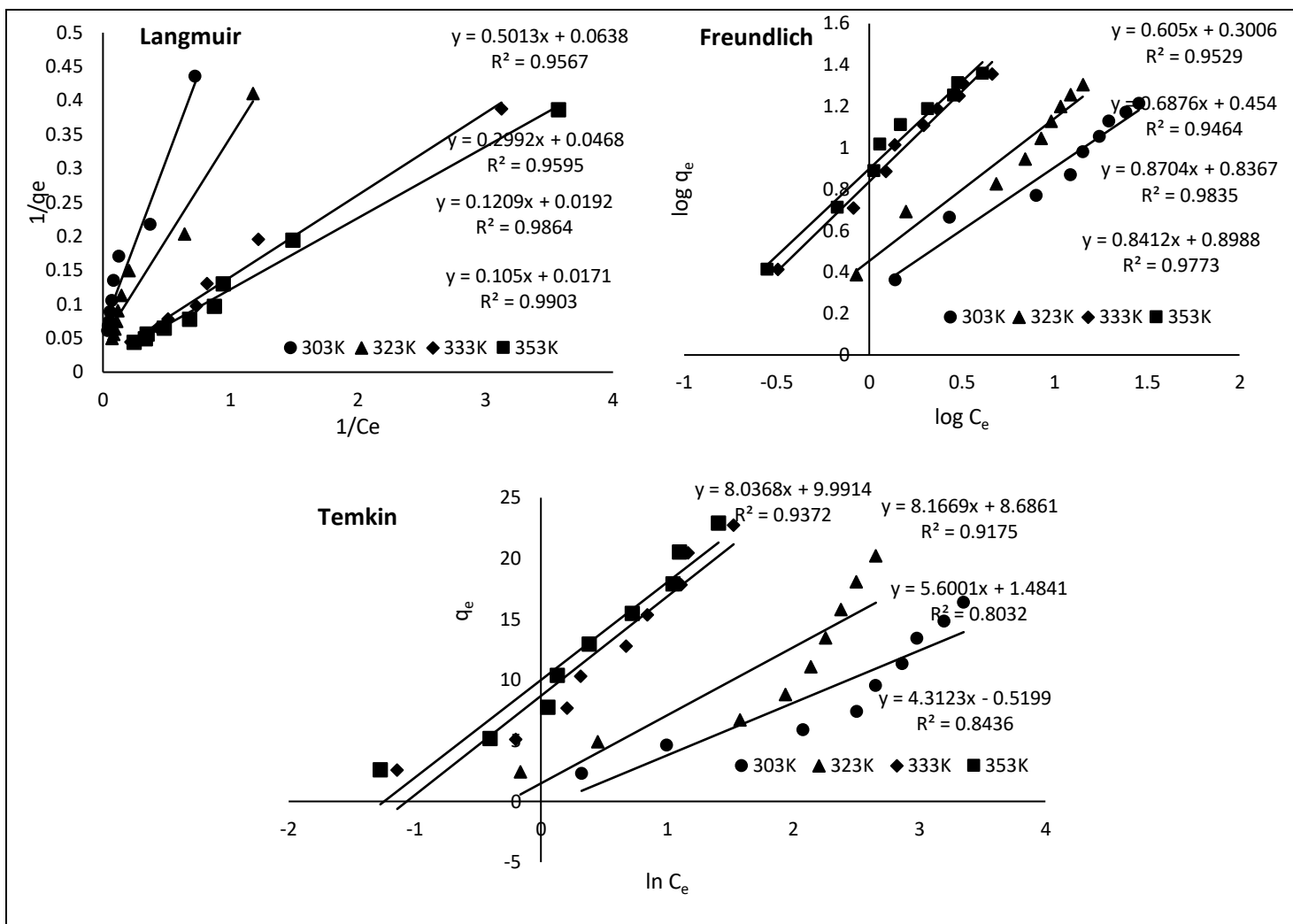


Figure 4.35: Isotherm model plots of CL

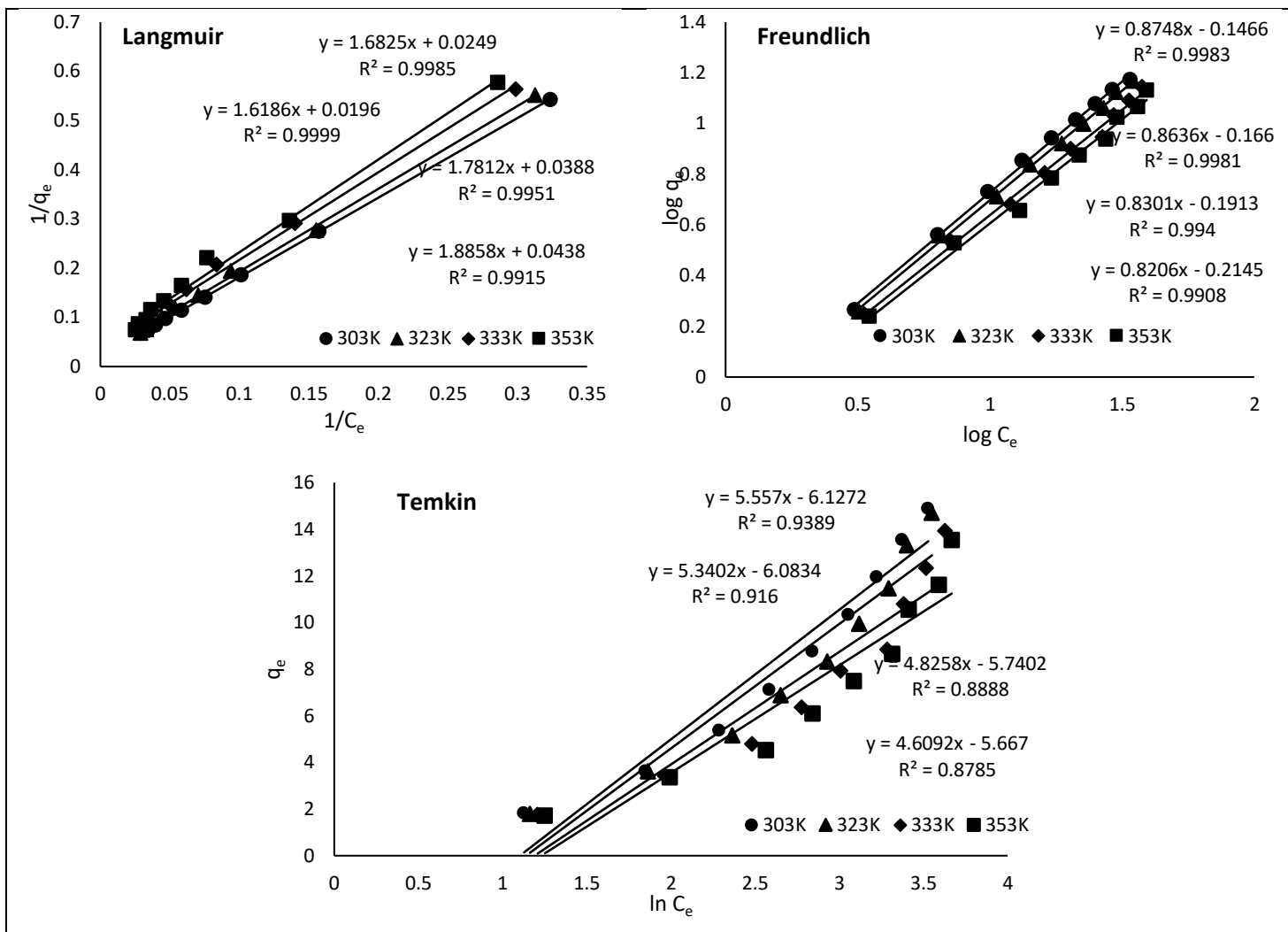


Figure 4.36: Isotherm model plots of RDE

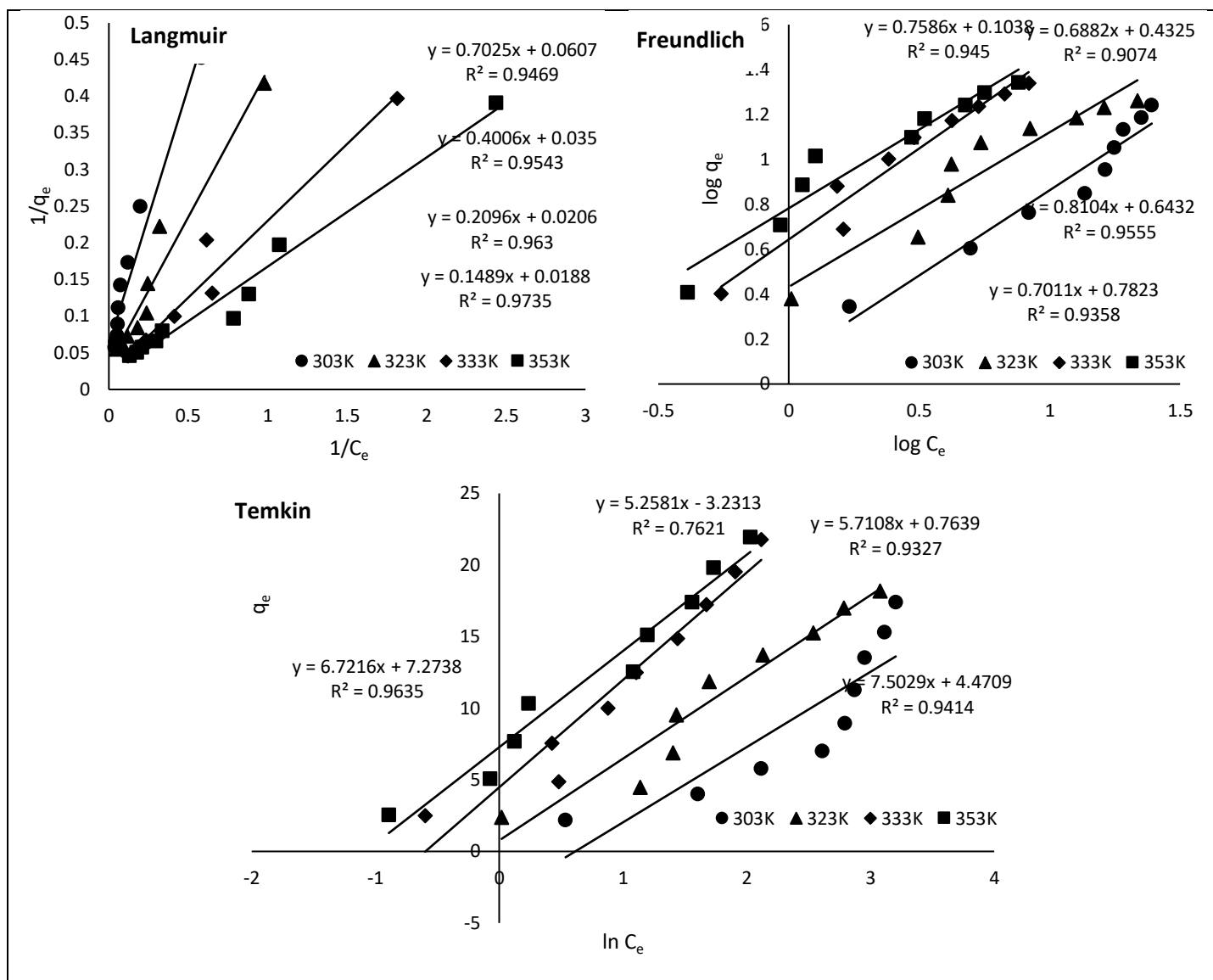


Figure 4.37: Isotherm model plots of CDE



Table 4.7: Maximum adsorption capacity of CR dye onto various biosorbents in literature

Adsorbents	Adsorption capacity $q_{\max}$ (mg/g)	References
Cashew nutshell	5.184	Kumar et al., 2010
E. crassipes roots	1.580	Wanyonyi et al., 2014
Cocoa pod husk (acid activated)	43.67	Olakunle et al., 2017
Modified Walnut shell	40	Ojo et al., 2017
Pine bark	3.92	Litefti et al., 2019
Cabbage waste powder	2.313	Wekoye et al., 2020
Modified coffee waste	34.36	Wong et al., 2020
Litchi seed powder	20.49	Edokpayi and Makete, 2021
Raw Litchi peel powder (RL)	55.56	This study
Modified Litchi peel powder (CL)	58.48	This study
Raw DE seed powder (RDE)	51.02	This study
Modified DE seed powder (CDE)	53.19	This study

#### 4.7 Adsorption thermodynamics

Thermodynamic parameters such as Gibb's free energy, enthalpy change and, entropy change was calculated from equations 3.12 and 3.13 as stated in the methodology section 3.10 of chapter 3. The Van't Hoff plot of  $\ln K_0$  against  $(1/T)$  gives linear graphs for all novel biosorbents as shown in Figures 4.38 and 4.39. The change in enthalpy ( $\Delta H^\circ$ ) and entropy ( $\Delta S^\circ$ ) were calculated from the slope and intercept of the graphs respectively. The values obtained for all the parameters are presented in Tables 4.8 and 4.9.

With regards to adsorption of CR dye from aqueous solution unto raw biosorbents- RL and RDE, negative  $\Delta G^\circ$  values were obtained at all working temperatures. This is an indication that the adsorption process was spontaneous and feasible. The negative  $\Delta H^\circ$  value confirmed that the adsorption process was exothermic. The positive value of  $\Delta S^\circ$  is an indication that there is increased randomness at the adsorbent–adsorbate interface during the adsorption of CR dye molecules on the active sites of the adsorbent surface. Also, the positive value of  $\Delta S^\circ$  infers good attraction of CR dye molecules towards the biosorbents. Comparable observations have been reported in literature for adsorbents of CR unto other bio-sorbents like coffee waste powder (Lafi et al., 2019) and pine bark powder (Litefti et al., 2019).

Furthermore, adsorption of CR dye unto modified biosorbents (CL and CDE) also showed negative values of  $\Delta G^\circ$  and positive value for  $\Delta S^\circ$ . However, the adsorption process was an endothermic one because of the positive  $\Delta H^\circ$  values obtained. Comparable observations have

also been reported in literature for adsorbents of CR onto other biosorbents like acid modified crab shell powder (Rao and Rao, 2016) and acid modified walnut shell powder (Ojo et al., 2017).

Table 4.8: Thermodynamic parameters for CR dye adsorption onto RL and CL

RL					
Temp (K)	$K_o$	$\ln K_o$	$\Delta G$ (kJ/mol)	$\Delta H$ (kJ/mol)	$\Delta S$ (J/mol/K)
303	72173.98	11.18683	-28.18	-16.51	39.65
313	72042.21	11.18501	-29.11		
323	63547.37	11.05954	-29.69		
333	47161.94	10.76134	-29.79		
343	37247.40	10.52534	-30.02		
353	30620.63	10.32943	-30.32		
CL					
Temp (K)	$K_o$	$\ln K_o$	$\Delta G$ (kJ/mol)	$\Delta H$ (kJ/mol)	$\Delta S$ (J/mol/K)
303	18349.802	9.817374	-24.73	41.86	218.19
313	23439.245	10.06217	-26.19		
323	33893.368	10.43097	-28.01		
333	73685.913	11.20757	-31.03		
343	93574.248	11.44651	-32.64		
353	187969.59	12.14404	-35.64		

Table 4.9: Thermodynamic parameters for CR dye adsorption onto RDE and CDE

RDE					
Temp (K)	$K_o$	$\ln K_o$	$\Delta G$ (kJ/mol)	$\Delta H$ (kJ/mol)	$\Delta S$ (J/mol/K)
303	20352.83	9.920975	-24.99	-5.44	64.64
313	19992.35	9.903105	-25.77		
323	17202.62	9.752817	-26.19		
333	17443.32	9.766712	-27.04		
343	15726.22	9.663085	-27.56		
353	15289.85	9.634944	-28.28		
CDE					
Temp (K)	$K_o$	$\ln K_o$	$\Delta G$ (kJ/mol)	$\Delta H$ (kJ/mol)	$\Delta S$ (J/mol/K)
303	19992.35	9.903105	-24.95	55.21	260.56
313	19970.10	9.901992	-25.77		
323	26316.67	10.17796	-27.33		
333	88119.68	11.38645	-31.52		
343	194874.90	12.18011	-34.73		
353	322288.40	12.68320	-37.22		

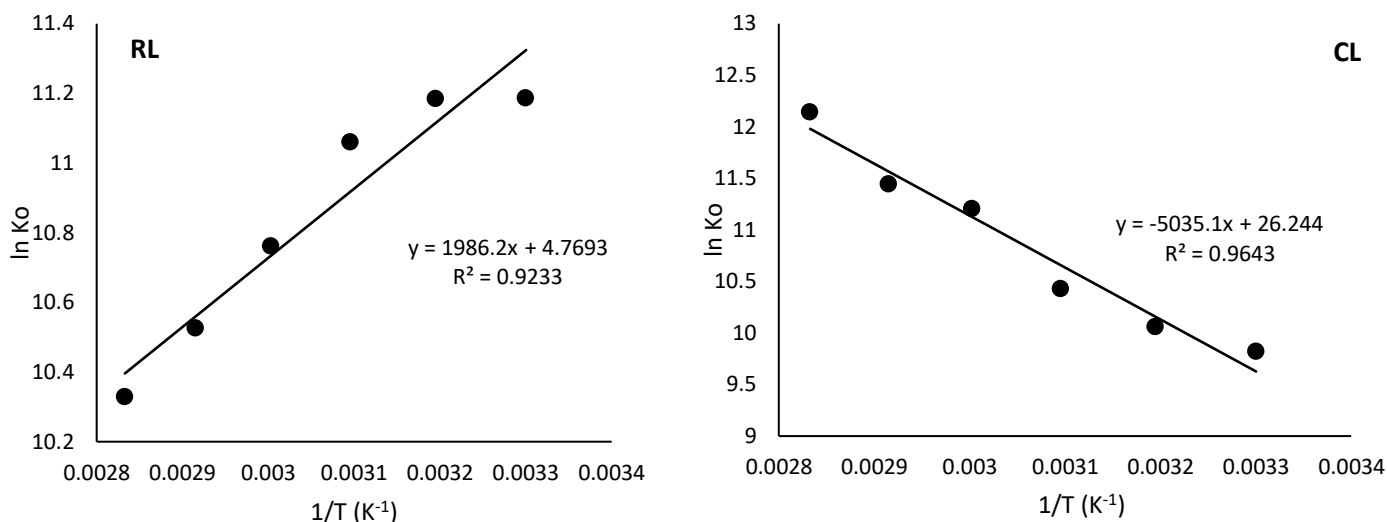


Figure 4.38: Van't Hoff plots of CR dye adsorption onto RL and CL

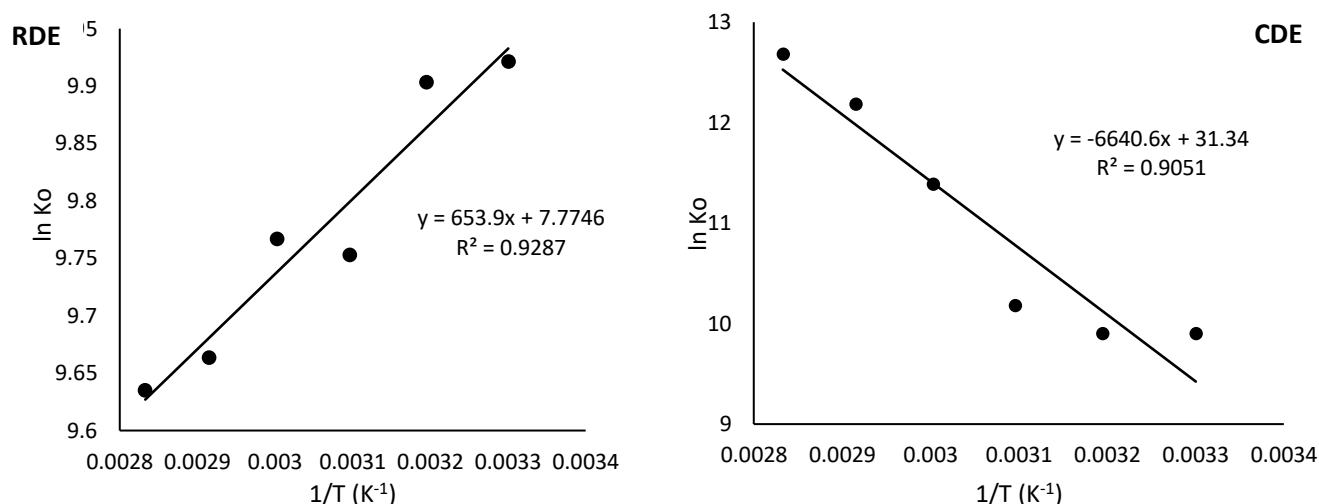


Figure 4.39: Van't Hoff plots of CR dye adsorption onto RDE and CDE

#### 4.8 Desorption study/Regeneration

The plots of the data obtained from desorption experiment of spent biosorbents, i.e. spent raw Litchi peel powder (SRL), spent citric acid modified Litchi peel powder (SCL), spent raw DE seeds powder (SRDE) and, spent citric acid modified DE seeds powder (SCDE) are presented in Figures 4.40 and 4.41. Desorption experiment was investigated with three desorbing agents which are 0.1 M HCl, 0.1 M NaOH and de-ionized water. Among the three studied solvents, 0.1 M NaOH solution is the most effective for regenerating the spent adsorbents as it recorded the highest desorption efficiency of 97,52% for SRL, 94.78% for SCL, 96.91% for SRDE and 94.04% for SCDE. The highest desorption efficiency by alkaline solution suggests that the adsorption process is dominated by electrostatic interaction and hydrogen bonding (Ahmad and Kumar, 2010; Lafi et al., 2019). The solvating strength and concentration of the desorbing agent together with other

parameters like agitation speed and time; all contributed to the migration of CR dye molecules from the solid to liquid phase (Momina et al., 2019).

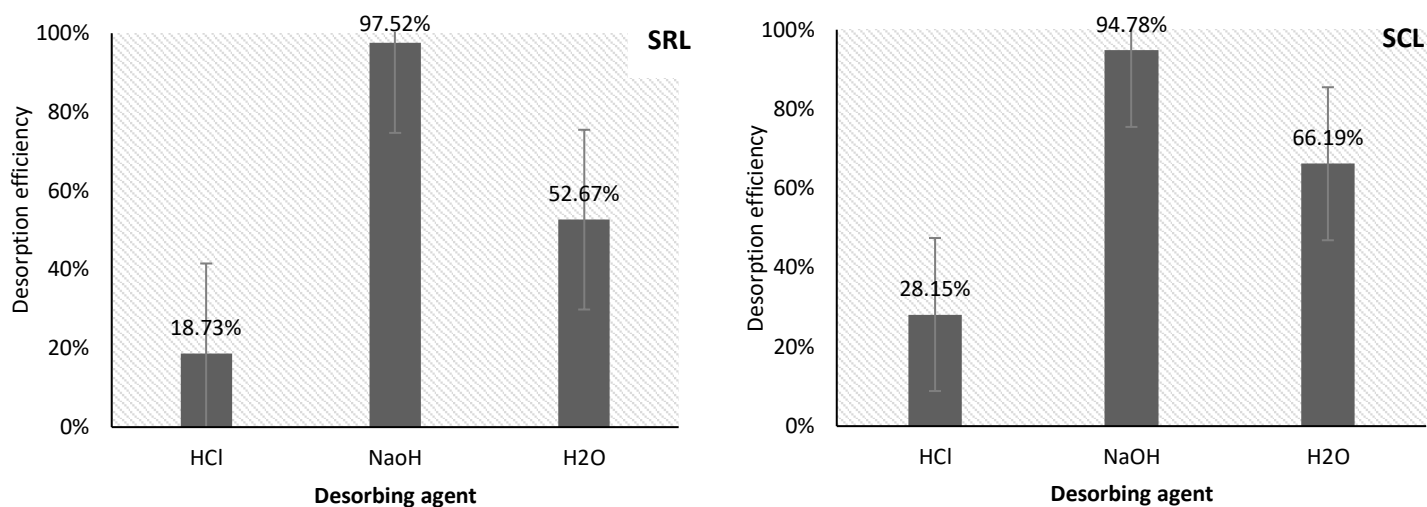


Figure 4.40: Desorption of SRL and SCL

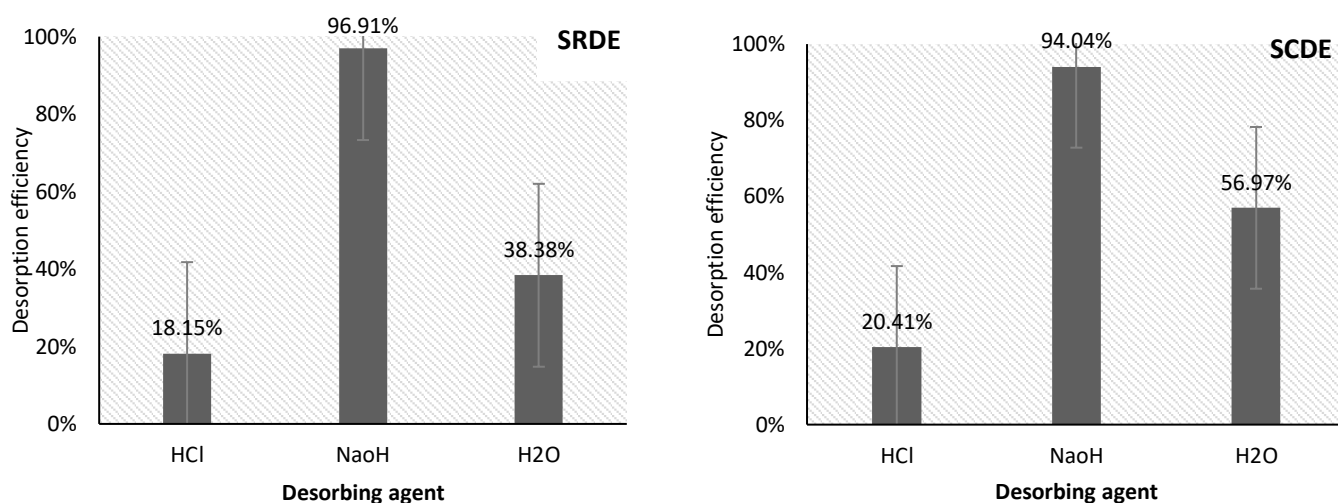
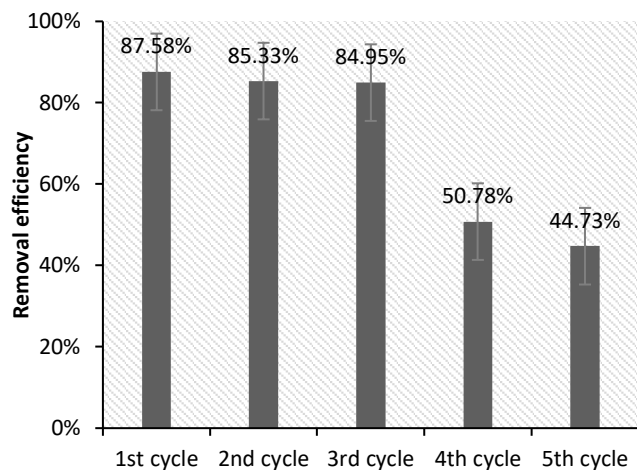


Figure 4.41: Desorption of SRDE and SCDE

Furthermore, regeneration and reuse experiment were thereafter performed by repeated washing of biosorbents with 0.1 M NaOH for five successive cycles. With reference to regeneration data obtained as presented graphically in Figures 4.42 and 4.43, the biosorbents were able to adsorb CR dye at an amount close to the virgin (1st cycle) samples of biosorbents at the 2nd and 3rd cycle. Drastic decline is noticeable in adsorption efficiencies of the 4th and 5th cycle. The decline in adsorption efficiency could be attributed to difficulty in recovering 100% mass of adsorbent in solution and, change in superficial structures of adsorbents by the alkaline solution (Liu et al., 2018). This may subsequently lead to loss and damage/blockage of adsorption sites. Similar use

of NaOH as effective desorbing solvent has been reported in literature by Lafi et al. (2019) and Lin et al. (2020). In summary, sodium hydroxide proved to be effective desorbing agent for CR dye. Also, novel biosorbents in this study can be regenerated and reused to safe cost or be discharged safely into the environment without fear of secondary dye contamination.

RL



CL

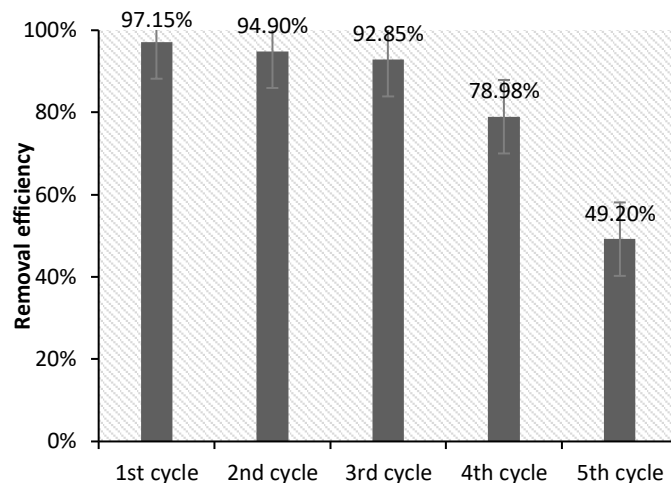
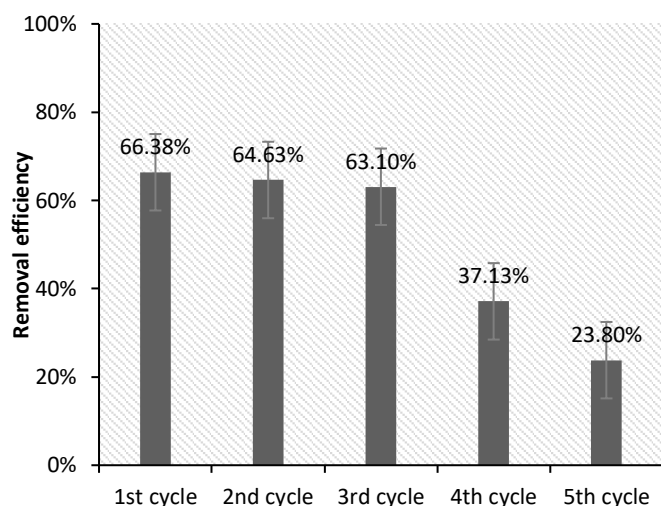


Figure 4.42: Regeneration and reuse cycles of RL and CL

RDE



CDE

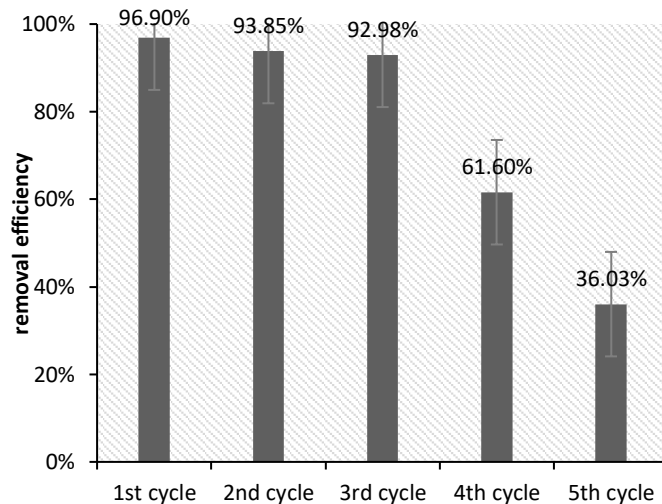


Figure 4.43: Regeneration and reuse cycles of RDE and CDE

## CHAPTER FIVE: CONCLUSION AND RECOMMENDATION

### 5.1 Preamble

This chapter is a summary of the outcome of this research principally aimed at investigating the adsorptive sequestration of hazardous dye (Congo red) from aqueous solution using raw and modified agricultural waste materials. Effects of parameters and their optimisation for effective removal of dye from aqueous solution, Kinetics, isotherms and thermodynamics of adsorption process, regeneration, and characterization of biosorbents are all presented. This study also incorporated the usage of its novel biosorbents on removal of dye in natural water (apart from simulated dye solution) and on other selective dyes from aqueous solution to authenticate its findings.

### 5.2 Conclusion

Raw and modified Litchi peel powder (RL and CL); raw and modified DE seed powder (RDE and CDE) were utilised for adsorptive sequestration of Congo red (CR) dye from aqueous solution through batch scale experiment. Characterisation of biosorbents revealed that the nature, active adsorbent sites, certain functional groups present and elemental composition of the biosorbents; all contributed to effective adsorptive sequestration of hazardous dyes from aqueous solution. Experimental parameters for optimum removal of CR dye using raw biosorbents (RL and RDE) were 0.15 g mass of adsorbent, 90 min equilibrium time, 200 rpm agitation speed, temperature at 30°C, pH of 2 and particle size of <125 µm. Also, experimental parameters for optimum removal of CR dye using modified biosorbents (CL and CDE) were 0.05 g mass of adsorbent, 15 min equilibrium time for CL, 90 min equilibrium time for CDE, 200 rpm agitation speed, temperature at 80°C, pH of 2 and particle size of <125 µm. Optimisation of all these parameters achieved adsorption efficiency close to 100 % for all biosorbents.

Kinetic and isotherm study on equilibrium data revealed that pseudo second order kinetic model and Langmuir isotherm model provided the best fit adsorption process. Maximum adsorption capacities for various biosorbents were found to be: RL- 55.56 mg/g, CL- 58.48 mg/g, RDE- 51.02 mg/g and CDE- 53.19 mg/g. Thermodynamic investigation revealed the adsorption mechanism between CR and raw biosorbents (RL and RDE) was feasible, spontaneous and exothermic process while that of modified biosorbents (CL and CDE) was feasible, spontaneous and endothermic process.

Adsorption process using these novel biosorbents looks practicable for sequestration of dyes as experiment conducted using natural water gave higher removal efficiency than that of deionised water. Likewise, the biosorbents were effective for sequestration of other selective dyes from

aqueous solution. Moreover, desorption study revealed 0.1 M NaOH as the most suitable desorbing agent for desorbing CR dye from spent biosorbents. Five cycled regeneration/adsorption experiment conducted thereafter suggested that regenerated adsorbents could adsorb CR dye at an amount close to their virgin samples for the first three cycles.

This study is unique in the sense that it utilises plant materials readily available in South Africa; especially DE that is indigenous to Venda area of South Africa. It converts these plant materials which are often regarded as wastes to useful products for wastewater treatment and mitigate their disposal problem. Both raw and modified biosorbents displayed good adsorption efficiency for sequestration of CR. However, the modified biosorbents utilised lesser mass of biosorbents, lesser equilibrium time (CL), and higher temperature for maximum removal with higher removal capacity. Therefore, this research establishes raw and modified *Litchi chinensis* peel powder, raw and modified *Dicerocaryum eriocarpum* seed powder as potential eco-friendly, available, abundant, and effective biosorbents for adsorptive sequestration of hazardous dye from wastewater.

### 5.3 Recommendation

Though agricultural plant materials- RL, CL, RDE, CDE are potential biosorbents for the adsorptive sequestration of hazardous dye from wastewater, most of the experiments for operating parameters and their effects were conducted through batch reactor system. Other reactor systems such as a column mode reactor or continuous stirred tank reactor (CSTR) should be thoroughly investigated in the future when considering large scale treatment of wastewater. Moreover, other kinetic models such as Elovich and Boyd kinetic models; together with isotherm models such as Dubinin-Radushkevich isotherm, Flory-Huggins isotherm, Redlich-Peterson isotherm, Sip isotherm, and Toth isotherm models should be further researched for comprehensive understanding of probable adsorption behaviour.

## REFERENCES

- Abbas, F.S. (2013). Dyes Removal from wastewater using Agricultural Waste. *Advances in Environmental Biology*, vol. 7, (6), pp. 1019-1026.
- Abdallah, R. and Taha, S. (2012). Biosorption of methylene blue from aqueous solution by nonviable *Aspergillus fumigates*. *Chemical Engineering Journal*, vol. 195, pp. 69-76.
- Abd El-Latif, M.M., Ibrahim, A.M. and El-Kady, M.F. (2010). Adsorption Equilibrium, kinetics and thermodynamics of methylene blue from aqueous solutions using biopolymer oak sawdust composite. *Journal of American Science*, vol. 6, (6), pp. 1-17.
- Abukhadra, M.F. and R, Mohamed, M and S. (2018). Removal of safranin dye from water using polypyrrole nanofiber/Zn-Fe layered double hydroxide nanocomposite (Ppy NF/Zn-Fe LDH) of enhanced adsorption and photocatalytic properties. *Science of The Total Environment*, pp. 640-641.
- Achmad, A., Kassim, J., Suan, T.K., Amat, R.C. and Seey, T.L. (2012). Equilibrium, kinetic and thermodynamic studies on the adsorption of a direct dye onto a novel green adsorbent developed from *uncaria gambir* extract. *Journal of Physical Science*, vol. 23, (1), pp.1-13.
- Akar, S.T., Özcan, A.S., Akar, T., Özcan, A. and Kaynak, Z. (2009). Biosorption of a reactive textile dye from aqueous solutions utilizing an agro-waste. *Desalination*, vol. 249, pp. 757-761.
- Alex S. (2015). Cutting out textile pollution. *Chemical and Engineering News*, vol 93, (41), pp. 18-19.
- Aljeboree, A.M., Alshirifi, A.N. and Ayad F. Alkaim, A.F. (2017). Kinetics and equilibrium study for the adsorption of textile dyes on coconut shell activated carbon. *Arabian Journal of Chemistry*, vol. 10, pp. S3381-S3393.
- Al-Kdasi, A., Idris, A., Saed, K. and Guan, C. (2004). Treatment of Textile Wastewater by Advanced Oxidation Processes-A Review. *Global Nest International Journal*, vol. 6, pp. 222-230.
- Anbia, M., Amirmahmoodi, S. (2016). Removal of Hg (II) and Mn (II) from aqueous solution using nanoporous carbon impregnated with surfactants. *Arabian Journal of Chemistry*, vol. 9, pp. S319-S325.
- Antoniadis, A., Takavakoglou, V., Zalidis, G., Darakas, E. and Poullos, I. (2010). Municipal wastewater treatment by sequential combination of photocatalytic oxidation with constructed wetlands. *Catalysis Today*, vol. 151, pp. 114-118.
- Arslan-Alaton, I., Gursoy, B.H., Jens-Ejbye Schmidt (2008). Advanced oxidation of acid and reactive dyes: Effect of Fenton treatment on aerobic, anoxic and anaerobic processes. *Dyes and Pigments*, vol. 78, pp. 117-130.



- Artioli, Y., Adsorption, in Encyclopedia of Ecology, J. Editors-in-Chief: Sven Erik and F. Brian, Editors. 2008, *Academic Press*: Oxford, pp. 60-65.
- Ahmad, R. and Kumar, R. (2010) Adsorptive removal of congo red dye from aqueous solution using bael shell carbon. *Applied Surface Science*, vol. 257, pp.1628-1633.
- Ashok, K.P., Ramesh, N.M., Bangaraiah, P., Prashanti, G. (2016). Color Removal from Dye Wastewater Using Adsorption. *International Journal of Pharmaceutical Sciences Review and Research*, vol. 39, (23), pp. 115-118.
- Balamurugan, B., Thirumarimurugan, M. and Kannadasan, T. (2011). Anaerobic degradation of textile dye bath effluent using *Halomonas* sp. *Bioresource Technology*, vol. 102, pp. 6365-6369.
- Balapure, K., Bhatt, N. and Madamwar, D. (2015) Mineralization of reactive azo dyes present in simulated textile wastewater using down flow microaerophilic fixed film bioreactor. *Bioresource Technology*, vol. 175, pp. 1-7.
- Bandosz, T.J. (2009). Surface Chemistry of Carbon Materials. In Carbon Materials for Catalysis. Serp, P., & Figueiredo, J.L. (Eds.), pp. 58-78.
- Barrett, E.P., Joyner, L.G. and Halenda, P.P. (1951). The determination of pore volume and area distributions in porous substances. I. Computations from nitrogen isotherms. *Journal of the American Chemical society*, vol. 73, pp. 373-380.
- Bello, O.S., and Ahmad, M.A. (2012). Adsorptive Removal of Synthetic Dye Using Cocoa Pod Husks. *Toxicological and Environmental Chemistry*, vol. 93, (7), pp. 1298-1308.
- Bello, O. S., Auta, M. and Ayodele, O.B. (2013). Ackee apple (*Blighia sapida*) seeds: A novel adsorbent for the removal of Congo red dye from aqueous solutions. *Chemistry and Ecology*, vol. 29, (1), pp. 58-71.
- Benkhaya, S., El Harfi, S. and El Harfi, A. (2017). Classifications, properties and applications of textile dyes: A review. *Applied Journal of Environmental Engineering and Science*, vol. 3, (3), pp. 311-320.
- Benkhaya, S., Rabet, S.M. and El Harfi, A. (2020). A review on classifications, recent synthesis and applications of textile dyes. *Inorganic Chemistry Communications*, vol. 115, (107891), pp. 1-35.
- Berradi, M. and El Harfi, A. (2017). Discoloration of charged models wastewater with reactive and dispersed dyes by the combined process of coagulation-ultrafiltration. *Journal of Materials and Environmental Science*, vol. 8, (5), pp. 1762-1769.
- Berradi, M., Hsissou, R., Khudhair, M., Assouag, M., Cherkaoui, O., El Bachiri, A. and El Harfi, A. (2019). Textile finishing dyes and their impact on aquatic environs. *Heliyon*, pp. 1-11.
- Biniak, S., Pakuła, M., Świątkowski, A., Bystrzejewski, M. and Błażewicz, S. (2010). Influence of high-temperature treatment of granular activated carbon on its structure and

- electrochemical behaviour in aqueous electrolyte solution. *Journal of Material Research*, vol. 25, (8), pp. 1617-1628.
- Booth, G. (2000). *Dyes, General Survey*. Wiley-VCH.
- Brunauer, S., Emmett, P.H. and Teller, E. (1938). Adsorption of Gases in Multimolecular Layers. *Journal of the American Chemical Society*, vol. 60, (2), pp. 309-319.
- Burkinshaw, S.M. and Salihu, G. (2017). The role of auxiliaries in the immersion dyeing of textile fibres: Part 8 practical aspects of the role of inorganic electrolytes in dyeing cellulosic fibres with commercial reactive dyes. *Dyes and Pigments*, vol. 161, pp. 614-627.
- Calvino-Casilda, V., López-Peinado, A.J., Durán-Valle, C.J. and Martín-Aranda, R.M. (2010). Last Decade of Research on Activated Carbons as Catalytic Support in Chemical Processes. *Catalysis Reviews: Science and Engineering*, vol. 52, (3), pp. 325-380.
- Cao, D.M., Xiao, X., Wu, Y.M., Ma, X.B., Wang, M.N. (2013). Role of electricity production in the anaerobic decolorization of dye mixture by exoelectrogenic bacterium *Shewanella oneidensis* MR-1. *Bioresource Technology*, vol. 136, pp. 176-181.
- Chanda, S., Shanmugam, S., Pottipadu, M.J. and Thiagarajan, Y.R. (2019). Adsorption of Aniline Blue from Aqueous Solution Using *Litchi chinensis* Peel: Kinetic and Equilibrium Studies. *Journal of Environmental Science and Technology*, vol. 12, (6), pp. 235-241.
- Chander, M. and Arora, D.S. (2007). Evaluation of some white-rot fungi for their potential to decolourise industrial dyes. *Dyes and Pigments*, vol. 72, pp. 192-198.
- Chaukura, N., Murimba, E.C. and Gwenzi, W. (2017). Synthesis, characterisation and methyl orange adsorption capacity of ferric oxide–biochar nano-composites derived from pulp and paper sludge. *Applied Water Science*, vol. 7, pp. 2175-2186.
- Chequer, F.M., Lizier, T.M., De Felício, R., Zanoni, M.V., Debonisi, H.M., Lopes, N.P. and De Oliveira, D.P. (2015). The azo dye Disperse Red 13 and its oxidation and reduction products showed mutagenic potential. *Toxicology in Vitro*, vol. 29, (7), pp.1906-1915.
- Chong, M.N., Jin, B., Chow, CWK, and Saint, C. (2010). Recent developments in photocatalytic water treatment technology: A review. *Water Research*, vol. 44, pp. 2997-3027.
- Cillie, G.G., Coombs, P. and Odendaal, P.E. (1979). Water pollution Research in South Africa. *Journal (Water Pollution Control Federation)*, vol. 51, (3), pp. 458-466.
- Clark, M. (2011). *Handbook of Textile and Industrial Dyeing: Principles, Processes and Types of Dyes*.
- Cloete, T.E., Gerber, A., and Maritz, L.V. (2010). A first order inventory of water use and effluent production by SA industrial, mining and electricity generation sectors. *Water Research Commission Report No. 1547/1/10*. ISBN 978-1-77005-958-0.
- Coates, J. (2000). Interpretation of infrared spectra, a practical approach. In: Meyers, R.A. (Ed.), *Encyclopedia of Analytical Chemistry*. John Wiley & Sons Ltd, Chichester, pp. 10815–10837.

- Corda, N.C. and Kini, M.S. (2018). Review on Adsorption of Cationic Dyes using Activated Carbon. *MATEC Web of Conferences*, vol. 144, (02022), pp. 1-16.
- Croce, R., Cina, F., Lombardo, A., Crispeyn, G., Cappelli, C.I., Vian, M., Maiorana, S., Benfenati, E. and Baderna, D. (2017). Aquatic toxicity of several textile dye formulations: acute and chronic assays with *Daphnia magna* and *Raphidocelis subcapitata*. *Ecotoxicology and Environmental Safety*, vol. 144, pp. 79-87.
- Cundari, L., Afrah, B.D., Utami, D.I. and Matondang, N.I. (2019). Adsorption model in removal of direct synthetic dyes in aqueous solution onto tea waste. *Journal of Physics: Conference Series*, vol. 1167, (1), pp. 12-46.
- Dave, S.R., Patel, T.L. and Tipre, D.R. (2015). Bacterial degradation of azo dye containing wastes. In: Springer International Publishing. *Microbial degradation of synthetic dyes in wastewaters*, pp. 57-83.
- Dawkar, V.V., Jadhav, U.U., Tamboli, D.P. and Govindwar, S.P. (2010). Efficient industrial dye decolorization by *Bacillus sp.* VUS with its enzyme system. *Ecotoxicology and Environmental Safety*, vol. 73, pp. 1696-1703.
- Dawood S. and Sen T.K., (2012). Removal of anionic dye Congo red from aqueous solution by raw pine and acid-treated pinecone powder as adsorbent: equilibrium, thermodynamic, kinetics, mechanism and process design. *Water Resources*, vol. 46, (6), pp.1933-1946.
- Das, D., Samal, D.P. and Meikap, B.C. (2015). Preparation of Activated Carbon from Green Coconut Shell and its Characterization. *Journal of Chemical Engineering & Process Technology*, vol. 6, (5), pp. 1-7.
- Deniz, F., and Karaman, S. (2011). Removal of Basic Red 46 dye from aqueous solution by pine tree leaves. *Chemical Engineering Journal*, vol. 170, pp. 67-74.
- Dicerocaryum eriocarpum* plant. [Internet]- <http://pza.sanbi.org/dicerocaryum-eriocarpum/> accessed (2019/06/12).
- Dos Santos, A.B., Cervantes, F.J., Van Lier, J.B. (2007). Review paper on current technologies for decolourisation of textile wastewaters: Perspectives for anaerobic biotechnology. *Bioresource Technology*, vol. 98, (12), pp. 2369-2385.
- Dubin, M.M., Zaverina, E.D. and Radushkevich, L.V. (1947). Sorption and structure of active carbons. I. Adsorption of organic vapors. *Zhurnal Fizicheskoi Khimii*, vol. 21, pp. 1351-1362.
- Duran-Valle, C.J. (2012). Techniques Employed in the Physicochemical Characterization of Activated Carbons, Lignocellulosic Precursors Used in the Synthesis of Activated Carbon - Characterization Techniques and Applications in the Wastewater Treatment. *Intech*, pp. 1-21.

- Edokpayi, J.N. and Makete, E. (2021). Removal of Congo red dye from aqueous media using Litchi seeds powder: Equilibrium, kinetics and thermodynamics. *Physics and Chemistry of the earth*, vol. 123, (7), pp. 1-9.
- Edokpayi, J.N., Alayande, S.O., Adetoro, A. and Odiyo, J.O. (2020). The Equilibrium, Kinetics, and Thermodynamics Studies of the Sorption of Methylene Blue from Aqueous Solution Using Pulverized Raw Macademia Nut shells. *Journal of Analytical Methods in Chemistry*, pp.1-10.
- Edokpayi, J.N., Enitan-Folami, A.M., Adeeyo, A.O., Durowoju, O.S., Jegede, A.O. and Odiyo, J.O. (2020). Recent trends and national policies for water provision and wastewater treatment in South Africa. In Singh, P., Milshina, Y., Tian, K., Gusain, D. and Bassin, J.P. *Water Conservation and Wastewater Treatment in BRICS Nations: Technologies, Challenges, Strategies and Policies* (Elsevier), pp. 187-211.
- Edokpayi, J.N., Ndlovu, S.S. and Odiyo, O.J. (2019). Characterization of pulverized Marula seed husk and its potential for the sequestration of methylene blue from aqueous solution. *BMC Chemistry*, vol. 13, (10), pp. 1-14.
- Edokpayi, J.N., Odiyo, J.O. and Durowoju, O.S. (2017). Impact of Wastewater on Surface Water Quality in Developing Countries: A Case Study of South Africa, Water Quality Hlanganani Tutu. *IntechOpen*, pp. 401-416.
- Edokpayi, J.N., Odiyo, J.O., Msagati, T.A.M. and Popoola, E.O. (2015). A Novel Approach for the Removal of Lead (II) Ion from Wastewater Using Mucilaginous Leaves of *Diceriocaryum eriocarpum* Plant. *Sustainability*, vol. 7, pp. 14026-14041.
- Elavarasan, A., Chitradevi, S., Nandhakumar, V., Sivajiganesan, S. and Kadhiravan, S. (2018). FT-IR Spectra, XRD and EDX Studies on the Adsorption of Methylene Blue Dye Present in Aqueous Solution onto Acid Activated Carbon Prepared from *Mimusops Elengi* Leaves. *Journal of applied chemistry*, vol. 11, (7), pp. 45-51.
- Elhadj, M., Samira, A., Mohamed, T., Djawad, F., Asma, A. and Djamel, N. (2020). Removal of Basic Red 46 dye from aqueous solution by adsorption and photocatalysis: equilibrium, isotherms, kinetics, and thermodynamic studies. *Separation Science and Technology*, vol. 55, (5), pp. 867-885.
- Eslami, H., Khavidak, S.S., Salehi, F., Khosravi, R., Fallahzadeh, R.A., Peirovi, R. and Sadeghi, S. (2017). Biodegradation of methylene blue from aqueous solution by bacteria isolated from contaminated soil. *Journal of Advances in Environmental Health Research*, vol. 5, pp.10-15.
- Farias, R.S., Buarque, H.L., Cruz, M.B., Cardoso, L.M.F., Gondim, T.A. and Paulo, V.R. (2018). Adsorption of congo red dye from aqueous solution onto amino-functionalized silica gel. *Engenharia sanitária e ambiental*, vol.23, (6), pp. 1053-1060.
- Farouk, R. and Gaffer, H.E. (2013). *Carbohydrate Polymers*, 97, pp. 138-142.

- Fathy, N.A., Ahmed, S.A.S. and El-enin, R.M.M.A. (2012). Effect of Activation Temperature on Textural and Adsorptive Properties for Activated Carbon Derived from Local Reed Biomass: Removal of p-Nitrophenol. *Environmental Research Engineering and Management*, vol. 59, (1), pp. 10-22.
- Felista, M.M., Wanyonyi, W.C. and Gilbert, O. (2020). Adsorption of Anionic Dye (Reactive Black 5) Using Macadamia Seed Husks: Kinetics and Equilibrium Studies. *Scientific African*, pp. 1-10.
- Feng, Y.F., Yang, F., Wang, Y.Q., Ma, L., Wu, Y.H., Kerr, P.G. and Yang, L.Z. (2011). Basic dye adsorption onto an agro-based waste material- Sesame hull (*Sesamum indicum L.*). *Bioresource Technology*, vol. 102, pp. 10280-10285.
- Foo, K.Y. and Hameed B.H. (2011). Microwave assisted preparation of activated carbon from pomelo skin for the removal of anionic and cationic dyes. *Chemical Engineering Journal*, vol. 173, pp. 385-390.
- Freundlich, H. (1907). Über die Adsorption in Lösungen. Z Für. *Physical Chemistry*, vol. 57U, pp. 385-470.
- Gao, M., Zeng, Z., Sun, B., Zou, H. and Chen, J. (2012). Ozonation of azo dye Acid Red 14 in a microporous tube-in-tube microchannel reactor: decolorization and mechanism. *Chemosphere*, vol. 89, pp. 190-197.
- Gao, Y. and Cranston, R. (2008). Recent advances in antimicrobial treatments of textiles. *Textile Research Journal*, vol. 78, pp. 60-72.
- Ge, L.Q., Zhou, Y.Z. and Fan, N. (2017). Congo red adsorption on shell powder and chitosan-coated shell powder biosorbents: Experiments and theoretical calculation. *Desalination and Water Treatment*, vol. 81, pp. 291-302.
- Girish, C.R. (2018). Various Impregnation Methods Used for the Surface Modification of the Adsorbent: A Review. *International Journal of Engineering & Technology*, vol. 7, (4.7), pp. 330-334.
- Goldberg, S. and Criscenti, L.J. (2008). Modelling of adsorption of metals and metalloids by soil components. In: Violante, P.M. Huang and G.M. Gadd (eds) biophysico-chemical processes of heavy metals and metalloids in soil environments. *John Wiley and Sons*, pp. 215-264.
- Gong, N., Liu, Y. P., and Huang, R. H. (2018). Simultaneous adsorption of Cu<sup>2+</sup> and Acid fuchsin (AF) from aqueous solutions by CMC/bentonite composite. *International Journal of Biological Macromolecule*, vol. 115, pp. 580-589.
- Guppy, L. and Anderson, K. (2017). Water Crisis Report. United Nations University Institute for Water, Environment and Health, Hamilton, Canada. Pp. 1-12.
- Gurten, I.I., Ozmak, M., Yagmur, E. and Aktas, Z. (2012). Preparation and characterisation of activated carbon from waste tea using K<sub>2</sub>CO<sub>3</sub>. *Biomass Bioenergy*, vol. 37, pp 73-81.

- Hai, F.I., Yamamoto, K., Fukushi, K. (2007). Hybrid treatment system for dye wastewater. *Critical Review in Environmental Science & Technology*, vol. 37, pp. 315-377.
- Hameed, B.H. (2009). Grass waste: A novel sorbent for the removal of basic dye from aqueous solution. *Journal of Hazardous Materials*, vol. 166, pp. 233-238.
- Hameed, B.H. and Lee, T.W. (2009). Degradation of malachite green in aqueous solution by Fenton process. *Journal of Hazardous Materials*, vol. 164, (2-3), pp.468-472.
- Hassaan, M.A. and El Nemr, A. (2017). Health and Environmental Impacts of Dyes: Mini Review. *American Journal of Environmental Science and Engineering* vol. 1, (3), pp. 64-67.
- Hassaan, M.A., El Nemr, A. and Madkour, F.F. (2017). Testing the advanced oxidation processes on the degradation of direct blue 86 dye in wastewater. *Egyptian Journal of Aquatic Research*, vol. 1, pp. 11-19.
- Ho, Y.S. and McKay, G. (1999). Pseudo-second order model for sorption processes. *Process Biochemistry*, vol. 344, pp. 51-65.
- Hoveka, L. (2017). *Diecerocaryum eriocarpum*. South African National Biodiversity Institute. *African journal of plant and biotechnology*, vol. 5, (11), pp. 1-7.
- Hubner, K. (2006). "History – 150 Years of mauveine". *Chemie in unserer Zeit.*, vol. 40, (4), pp. 274-275.
- Hunger, K. (2003). Chemistry, Properties, Application.
- Hussain, R., Qadeer, R., Ahmad, M., and Saleem, M. (2000). X-Ray Diffraction Study of Heat-Treated Graphitized and Ungraphitized Carbon. *Turkish Journal of Chemistry*, vol. 24, (2), pp. 177-183.
- Ibrahim, S.R. and Mohamed, G.A. (2015). *Litchi chinensis*: medicinal, phytochemistry and pharmacology. *Journal of Ethnopharmacology*, vol. 174, pp. 492-513.
- Ikenyiri, P.N. and Ukpaka, C.P. (2016). Overview on the Effect of Particle Size on the Performance of Wood Based Adsorbent. *Journal of Chemical Engineering and Process Technology*, vol. 7, (315), pp. 1-16.
- Inyinbor, A.A., Adekola, F.A. and Olatunji, G.A. (2015). Adsorption of Rhodamine B Dye from Aqueous Solution on *Irvingia gabonensis* Biomass: Kinetics and Thermodynamics Studies. *South African Journal of Chemistry*, vol. 68, pp. 115-125.
- Jain, R., Mathur, M., Sikarwar, S. and Mittal, A. (2007). Removal of hazardous dye Rhodamine B through photocatalytic and adsorption treatment. *Journal of Environmental Management*, vol. 85, (4), pp. 956-964.
- Jain, R., and Sikarwar, S. (2014). Adsorption and Desorption Studies of Congo Red Using Low-cost Adsorbent: Activated De-oiled Mustard. *Desalination and Water Treatment*, vol. 52, pp. 7400-7411.

- Jawad, A.H., Mamat, N.H., Abdullah, M.F. and Ismail, K. (2017). Adsorption of methylene blue onto acid-treated mango peels: kinetic, equilibrium and thermodynamic study. *Desalination and Water Treatment*, vol. 59, pp. 210-219.
- Jegede, A.O. and Shikwambane, P. (2021). Water 'Apartheid' and the Significance of Human Rights Principles of Affirmative Action in South Africa. *Water*, vol. 13, pp. 1-14.
- Kabra, K., Chaudhary, R. and Sawhney, R.L. (2004). Treatment of hazardous organic and inorganic compounds through aqueous phase photocatalysis: A review. *Industrial and Engineering Chemistry Research*, vol. 43, pp. 7683-7696.
- Kanagaraj, J., Senthilvelan, T. and Panda, R.C. (2015). Degradation of azo dyes by laccase: biological method to reduce pollution load in dye wastewater. *Clean Technologies and Environmental Policy*, vol. 17, (6), pp. 1443-1456.
- Kant, R. (2012). Textile dyeing industry; an environmental hazard. *Natural Science Journal*, vol. 4, (1), pp. 22-26.
- Kaur, S., Rani, S. and Mahajan, R.K. (2013). Adsorption Kinetics for the Removal of Hazardous Dye Congo Red by Biowaste Materials as Adsorbents. *Hindawi Journal of Chemistry*, pp. 1-12.
- Khan, M.I., Akhtar, S., Zafar, S., Shaheen, A., Khan, M.A, Luque, R. and Rehman, A. (2015). Removal of Congo Red from Aqueous Solution by Anion Exchange Membrane (EBTAC): Adsorption Kinetics and Thermodynamics. *Materials*, vol. 8, pp. 4147-4161.
- Khataee, A.R., Dehghan, G., Ebadi, A., Zarei, M. and Pourhassan, M. (2009). Biological treatment of a dye solution by macro algae *Chara* sp.: Effect of operational parameter intermediates, Identification and artificial neural network modelling. *Bioresource Technology*, vol. 101, (7), pp. 2252-2258.
- Khouni, I., Marrot, B. and Amar, R.B. (2012). Treatment of reconstituted textile wastewater containing a reactive dye in an aerobic sequencing batch reactor using a novel bacterial consortium. *Separation and Purification Technology*, vol. 87, pp. 110-119.
- Kooh, M.R.R., Dahri, M.K. and Lim L.B.L. (2016). The removal of Rhodamine B dye from aqueous solution using *Casuarina equisetifolia* needles as adsorbent. *Cogent Environmental Science*, vol. 2, (1), pp. 1-15.
- Kowanga, K.D., Gatebe, E., Mauti, G.O. and Mauti, E.M. (2016). Kinetic, sorption isotherms, pseudo-first-order model and pseudo-second-order model studies of Cu(II) and Pb(II) using defatted *Moringa oleifera* seed powder. *The Journal of Phytopharmacology*, vol. 5, (2), pp. 71-78.
- Kumar, P.S., Ramalingam, S., Senthamarai, C., Niranjanaa, M. and Vijayalakshmi, P., (2010). Adsorption of dye from aqueous solution by cashew nutshell: Studies on equilibrium isotherm, kinetics and thermodynamics of interactions. *Desalination*, vol. 261, pp. 52-60.

- Kumar, P.S., Abhinaya, R.V., Lashmi, K.G., Arthi, V., Pavithra, R., Sathyaselvabala, V., Kirupha, S.D., Sivanesan, S. (2011). Adsorption of methylene blue dye from aqueous solution by agricultural waste: Equilibrium, thermodynamics, kinetics, mechanism and process design. *Colloid Journal*, vol. 73, pp. 647-657.
- Mahmood, S., Azeem, K., Muhammad, A., Mahmood, T. and Crowley, D.E. (2016). Detoxification of azo dyes by bacterial oxidoreductase enzymes. *Critical Reviews in Biotechnology*, vol 36, (4), pp. 639-651.
- Mansour, H.B., Ayed-Ajmi, Y., Mosrati, R., Corroler, D., Ghedira, K., Barillier, D. and Chekir-Ghedira, L. (2010). Acid violet 7 and its biodegradation products induce chromosome aberrations, lipid peroxidation, and cholinesterase inhibition in mouse bone marrow. *Environmental Science and Pollution Research*, vol 17, (7), pp. 1371-1378.
- Moreki, J C., Tshireletso, K. and Okoli, I.C. (2012). Potential use of ethnoveterinary medicine for retained placenta in cattle in Mogonono, Botswana. *Journal Animal Production Advance*, vol. 2, (6), pp. 303-309.
- Munagapati, V. S. and Kim, D. S. (2016). Adsorption of Anionic Azo Dye Congo Red from Aqueous Solution by Cationic Modified Orange Peel Powder. *Journal of Molecular Liquids*, vol. 220, pp. 540-548.
- Lafi, R., Montasser, I. and Hafiane, A. (2019). Adsorption of congo red dye from aqueous solutions by prepared activated carbon with oxygen-containing functional groups and its regeneration. *Adsorption Science & Technology*, vol. 37, (1-2), pp. 160-181.
- Lagergren, S.K. (1898). About the theory of so-called adsorption of soluble substances. *Kung Svenska Veenskapsakad Handlingari*, vol. 24, pp.1-39.
- Langmuir, I. (1916). The constitution and fundamental properties of solids and liquids. *Journal of American Chemical Society*, vol. 38, (11), pp. 2221-2295.
- Li, W.Y., Chen, F.F. and Wang, S.L. (2010) Binding of reactive brilliant red to human serum albumin: insights into the molecular toxicity of sulfonic azo dyes. *Protein and peptide letters*, vol. 17, (5), pp. 621-629.
- Liang, J., Ning, X., Kong, M., Liu, D., Wang, G., Cai, H., Sun, J., Zhang, Y., Lu, X. and Yuan, Y. (2017). Elimination and ecotoxicity evaluation of phthalic acid esters from textile-dyeing wastewater. *Environmental Pollution*, vol. 231, pp. 115-122.
- Lin, D., Wu, F., Hu, Y., Zhang, T., Liu, C., Hu, Q., Hu, Y., Xue, Z., Han, H., and Ko, T. (2020). Adsorption of Dye by Waste Black Tea Powder: Parameters, Kinetic, Equilibrium, and Thermodynamic Studies. *Hindawi Journal of Chemistry*, pp. 1-13.
- Lin, L., (2013). Dye adsorption of mesoporous activated carbons produced from NaOH pre-treated rice husks. *Bioresource Technology*, vol. 136, pp. 437-443.



- Litefti, K., Freire, M.S., Stitou, M. and González-Álvarez, J. (2019). Adsorption of an anionic dye (Congo red) from aqueous solutions by pine bark. *Nature Scientific Report*, vol. 9, pp. 1-13.
- Litchi chinensis* fruit tree. [Internet]- <https://en.wikipedia.org/wiki/Lychee/> (accessed 2019/06/12).
- Liu, L., Fan, S., and Y. Li, Y. (2018). Removal behavior of methylene blue from aqueous solution by tea waste: kinetics, isotherms and mechanism. *International Journal of Environmental Research and Public Health*, vol. 15, (7), pp. 1321-1337.
- Liu, Y., Ma, X., Yi, X., and Zhu, Y. (2012). Controllable synthesis and photocatalytic performance of bismuth phosphate nanorods. *Acta Physico-Chimica Sinica*, vol. 28, pp. 654-660.
- Lippens, B. and De Boer, J. (1965). Studies on pore systems in catalysts: V. The t method. *Journal of Catalysis*, vol. 4, pp. 319-323.
- Luseba, D., Elgorashi, E.E., Ntloedibe, D.T. and Van Staden, J. (2007). Antibacterial, anti-inflammatory and mutagenic effects of some medicinal plants used in South Africa for the treatment of wounds and retained placenta in livestock. *South African Journal of Botany*, vol. 73, (3), pp. 378-383.
- Magdalena, R., Hassanein, M.M.M., Abdel-Razek, A.G., Kmiecik, D., Siger, A., and Ratusz, K. (2018). Influence of composition on degradation during repeated deep-fat frying of binary and ternary blends of palm, sunflower and soybean oils with health-optimised saturated-to-unsaturated fatty acid ratios. *International Journal of Food Science Technology*, vol. 53, pp. 1021-1029.
- Makeswari, M., Santhi, T. and Ezhilarasi, M.R. (2016). Adsorption of methylene blue dye by citric acid modified leaves of *Ricinus communis* from aqueous solutions. *Journal of Chemical and Pharmaceutical Research*, vol. 8, (7), pp. 452-462.
- Malik, R., Romteke, D.S. and Wate, S.R. (2007). Adsorption of malachite green on ground nut shell waste based powdered activated carbon. *Waste Management*, vol. 27, pp.1129-1138.
- Malik, D. S., Jain C. K., Anuj K. Y., Richa K. and Vinayak V. P. (2016). Removal of methylene blue dye in aqueous solution by agricultural waste. *International Research Journal of Engineering and Technology*, vol. 3, (7), pp. 864-880.
- Mani, S. and Bharagava, R.N. (2016). Exposure to crystal violet is toxic genotoxic and carcinogenic effects on environment and its degradation and detoxification for environmental safety. *Reviews of Environmental Contamination and Toxicology*, vol. 237, pp. 71-104.
- Mann, S. and Mandal, A. (2014). Removal of fluoride from drinking water using sawdust. *International Journal of Engineering Research and Applications*, vol. 4, (7), pp. 116-123.
- Mathur, N., and Bhatnagar, P. (2007). Mutagenicity assessment of textile dyes from Sangner (Rajasthan). *Journal of Environmental Biology*, vol. 28, pp 123-126.

- Maurya, N.S., Mittal, A.K., and Cornel, P. (2008). Evaluation of adsorption potential of absorbents: A case of uptake of cationic dyes. *Journal of Environmental Biology*, vol. 29, (1), pp. 31-36.
- Mittal, A., Mittal, J., Malviya, A. and Gupta, V.K. (2009). Adsorptive removal of hazardous anionic dye "Congo red" from wastewater using waste materials and recovery by desorption. *Journal of Colloid and Interface Science*, vol. 340, pp. 16-26.
- Momina, Rafatullah, M., Ismail, S. and Ahmad, A. (2019). Optimization Study for the Desorption of Methylene Blue Dye from Clay Based Adsorbent Coating. *Water*, vol. 11, (1304), pp.1-13.
- Moreno-Castilla, C. (2004). Adsorption of organic molecules from aqueous solutions on carbon materials. *Carbon*, vol. 42, (1), pp. 83-94.
- Mwangi, I.W., Ngila, J.C. and Okonkwo, J.O. (2012). A comparative study of modified and unmodified maize tassels for the removal of selected trace metals in contaminated water. *Toxicology and Environmental Chemistry*, vol. 94, pp. 20-39.
- Nagia, F.A. and El Mohamedy, R.S.A. (2007). Dyeing of wool with natural anthraquinone dyes from *Fusarium oxysporum*. *Dyes and Pigments*, vol. 75, (3), pp. 550-555.
- Nandi, B., Goswami, A. and Purkait, M. (2009). Removal of cationic dyes from aqueous solution by kaolin: kinetic and equilibrium studies. *Applied Clay Science*, vol. 42 (3-4), pp. 583-590.
- Ngoh, Y. Y., Leong, Y.-H. and Gan, C. Y., (2015). Optimization study for synthetic dye removal using an agricultural waste of *Parkia speciosa* pod: A sustainable approach for wastewater treatment. *International Food Research Journal*, vol. 22, (6), pp. 2351-2357.
- Nguyen, V.S. and Dang, K.C. (2016). Removal of Rhodamine B from aqueous solution via adsorption onto microwave-activated rice husk ash. *Journal of dispersion science and technology*, vol. 38, pp. 216-222.
- Odiyo, J.O., Basey, O.J., Chieng, A.O. and Chimuka, L. (2017). Coagulation efficiency of *Dicerocaryum eriocarpum* (DE) plant. *Water SA*, vol. 43, (1), pp. 1-6.
- Ojo, T.A., Ojedokun, A.T. and Bello, O.S. (2017). Functionalization of powdered walnut shell with orthophosphoric acid for Congo red dye removal. *Particulate Science and Technology*, pp. 1-13.
- Olakunle, M.O., Inyinbor, A.A., Dada, A.O and Bello, O.S. (2017). Combating dye pollution using cocoa pod husks: a sustainable approach, *International Journal of Sustainable Engineering*, pp. 1-13.
- Ologundudu, T.O., Odiyo, J.O. and Ekosse, G.E. (2016). Fluoride Sorption Efficiency of Vermiculite Functionalised with Cationic Surfactant: Isotherm and Kinetics. *Applied Sciences*, vol. 6, (277), pp. 1-15.

- Olorundare, O.F., Msagati, T.A.M., Krause, R.W.M., Okonkwo, J.O. and Mamba, B.B. (2014). Steam activation, characterization and adsorption studies of activated carbon from maize tassels. *Chem Ecol.*, vol. 30, pp. 473-490.
- Owamah, H.I., Chukwujindu, I.S., and Asiagwo, A.K. (2013). Biosorptive capacity of yam peels waste for the removal of dye from aqueous solutions. *Civil and Environmental Research*, vol. 3, pp. 36-48.
- Oyekanmi, A.A., Ahmad, A., Hossain, K. and Rafatullah, M. (2019). Adsorption of Rhodamine B dye from aqueous solution onto acid treated banana peel: Response surface methodology, kinetics and isotherm studies. *PLoS ONE*, vol. 14, (5), pp. 1-20.
- Pang, Y.L. and Abdullah, A.Z. (2013). Current Status of Textile Industry Wastewater Management and Research Progress in Malaysia: A Review. *Clean (Weinh)*, vol. 41, pp. 751-764.
- Pastor-Villegas, J., Gómez-Serrano, V., Durán-Valle, C.J. and Higes-Rolando, F.J. (1999). Chemical study of extracted rockrose and of chars and activated carbons prepared at different temperatures. *Journal of Analytical and Applied Pyrolysis*, vol. 50, (1), pp. 1-16.
- Pooja, T. and Bhupendra, K. (2016). Phytochemistry and Pharmacology properties of Lyche (*Litchi chinensis* sonn). *Journal of chemical and pharmaceutical research*, vol. 8, (10), pp. 35-48.
- Pradhan, B.K. and Sandle, N.K. (1999). Effect of different oxidizing agent treatments on the surface properties of activated carbons. *Carbon*, vol. 37, (8), pp. 1323-1332.
- Purkait, M.K., Maiti, A. and DasGupta, S., De, S. (2007). Removal of congo red using activated carbon and its regeneration. *Journal of Hazardous Materials*, vol. 145, pp. 287-295.
- Qiu, H., Lv, L., Pan, B., Zhang, Q., Zhang, W. and Zhang, Q. (2009). Critical review in adsorption kinetic models. *Journal of Zhejiang University Science A*, vol. 10, (5), pp. 716-724.
- Qu, Y., Cao, X., Ma, Q., Shi, S. and Tan, L. (2012). Aerobic decolorization and degradation of Acid Red B by a newly isolated *Pichia* sp. TCL. *Journal of Hazardous Materials*, pp. 31-38.
- Ramathai, S., Nandhakumar, V., Thiruchelvi, M., Arivoli, S. and Vijayakumaran, V. (2009). Rhodamine 6 dye adsorption -Kinetic mechanistic and thermodynamic studies. *European Journal of Chemistry*, vol. 6, pp. 51-65.
- Ramesh, B.B., Parande, A.K., Raghu, S. and Kumar, T.P. (2007). Textile technology. Cotton Textile Processing: Waste Generation and Effluent Treatment. *The Journal of Cotton Science*, vol. 11, pp.141-153.
- Rashed, M.N., Eltaher, M.A. and Abdou, A.N.A. (2017). Adsorption and photocatalysis for methyl orange and Cd removal from wastewater using TiO<sub>2</sub>/sewage sludge-based activated carbon nanocomposites. *Royal Society of open science*, vol. 4, pp. 1-14.
- Rao, T.M. and Rao, V.V.B. (2016). Biosorption of Congo Red from aqueous solution by crab shell residue: a comprehensive study. *SpringerPlus*, vol. 5, (537), pp. 1-14.

- Reddy, D.H.K., Sessaiah, K., Reddy, A.V.R., Rao, M.M. and Wang, M.C. (2010). Biosorption of Pb<sup>2+</sup> from aqueous solutions by *Moringa oleifera* bark: Equilibrium and kinetic studies. *Journal of Hazardous Materials*, vol.174, (1-3), pp. 831-838.
- Rehman, A., Usman, M., Bokhari, T.H., Haq, A., Saeed, M., Rahman, H.M., Siddiq, M., Rasheed, A. and Nisa, M.U. (2020). The application of cationic-nonionic mixed micellar media for enhanced solubilization of Direct Brown 2 dye. *Journal of Molecular Liquid*, vol. 301, (112408), pp. 1-10.
- Ren, Y., Cui, C. and Wang, P. (2018). Pomelo Peel Modified with Citrate as a Sustainable Adsorbent for Removal of Methylene Blue from Aqueous Solution. *Molecule*, vol. 23, pp. 1-13.
- River of Blood: China's Jian River turns red after chemical dump [Internet]. Available online: [https://www.huffpost.com/entry/jian-river-blood-china\\_n\\_1158679?slideshow=true#gallery/5bb105f4b09bbe9a593be5/0/](https://www.huffpost.com/entry/jian-river-blood-china_n_1158679?slideshow=true#gallery/5bb105f4b09bbe9a593be5/0/) (accessed 2019/11/15).
- Robinson, T., McMullan, G., Marchant, R. and Nigam, P. (2001). Remediation of dyes in textile effluent: a critical review on current treatment technologies with a proposed alternative. *Bioresource Technology*, vol. 77, pp. 247-255.
- Roes-Hill, M., Muanda, C., Rohland, J. and Durrell, K. (2017). Water and wastewater Management in The Textile Industry (Edition 2). *Water Research Commission*, Report No. TT 724/17.
- Rosa, A. D., Elvis, C., Guilherme, L. D., Hedda, S., and Liliana, A. F. (2018). Biosorption of rhodamine B dye from dyeing stones effluents using the green microalgae *Chlorella pyrenoidosa*. *Journal of Cleaner Production*, vol. 198, pp. 1302-1310.
- Saini, R.D. (2017). Textile Organic Dyes: Polluting effects and Elimination Methods from Textile Wastewater. *International Journal of Chemical Engineering Research*, vol 9, (1), pp. 121-136.
- Salleh, M.A.M., Mahmoud, P.K., Karim, A.W.A., and Idris, A. (2011). Cationic and Anionic Adsorption by Agricultural Solid Wastes: A comprehensive review. *Desalination*, vol. 280, pp. 1-13.
- Sarkar, S., Banerjee, A., Halder, U., Biswas, R. and Bandopadhyay, R. (2017). Degradation of Synthetic Azo Dyes of Textile Industry: A Sustainable Approach Using Microbial Enzymes. *Water Conservation Science Engineering*, vol. 2, pp.121-131.
- Sarvajith, M., Reddy, G.K.K. and Nancharaiah, Y.V. (2018). Textile dye biodecolourization and ammonium removal over nitrite in aerobic granular sludge sequencing batch reactors, *Journal of Hazardous Materials*, vol. 342, pp. 536-543.

- Saving Water SA. Over half of wastewater treatment plants are well below standard. [Internet]. 2011. Available online: <http://www.savingwater.co.za/tag/wastewater-treatment-plants/> (Accessed 2018/10/14).
- Schorr, D., Blanchet, P., and Essoua, G. G. E. (2018). Glycerol and citric acid treatment of lodgepole pine. *Journal of Wood Chemistry and Technology*, vol. 2, pp. 123-136.
- Sen T.K., Afroze, S and Ang, H.M., (2011). Equilibrium, kinetics and mechanism of removal of methylene blue from aqueous solution by adsorption onto pinecone biomass of *Pinus radiata*. *Water, Air, and Soil Pollution*, vol. 218, pp. 499-515.
- Sen, S.K., Raut, S. and Bandyopadhyay, P. (2016). Fungal decolouration and degradation of azo dyes: a review. *Fungal Biology Reviews*, vol. 30, (3), pp. 112-133.
- Shaban, M., Abukhadra, M.R., Khan, A.A.P. and Jibali, B.M. (2017). Removal of congo red, methylene blue and Cr (VI) ions from water using natural serpentine. *Journal of the Taiwan Institute of Chemical Engineering*, vol. 82, pp. 102-116.
- Sharma, Y.C., Uma, S.N. Upadhyay. (2011). An economically viable removal of methylene blue by adsorption on activated carbon prepared from rice husk. *Canadian Journal of Chemical Engineering*, vol. 189, pp. 377-383.
- Sharma, P., Kaur, H, Sharma, M. and Sahore, V. (2011). A review on applicability of naturally available adsorbents for the removal of hazardous dyes from aqueous waste. *Environmental Monitoring Assessment*, vol. 183, pp. 151-195.
- Sharma, S., Buddhdev, J., Patel, M. and Ruparelia, J.P., (2013). Studies on Degradation of Reactive Red 135 Dye in Wastewater using Ozone. *Procedia Engineering*, vol. 51, pp. 451-455.
- Sharma, S. and Kaur, A. (2016). Various Methods for Removal of Dyes from Industrial Effluents - A Review. *Indian Journal of Science and Technology*, vol. 11, (12), pp. 1-21.
- Sharma, S. and Tiwari, D.P. (2016). Model-fitting approach for methylene blue dye adsorption on Camelina and Sapindus seeds-derived adsorbents. *Adsorption Science & Technology*, vol. 34, (9-10), pp. 565-580.
- Shen, W., Li, Z., and Liu, Y. (2008). Surface Chemical Functional Groups Modification of Porous Carbon. *Recent Patents on Chemical Engineering*, vol. 1, (1), pp. 27-40.
- Singh, R., Singh, T.S., Odiyo, J.O., Smith, J. A. and Edokpayi, J.N. (2020). Evaluation of Methylene Blue Sorption onto Low-Cost Biosorbents: Equilibrium, Kinetics, and Thermodynamics. *Journal of Chemistry*, pp. 1-12.
- Smaranda, C., Gavrilescu, M. and Bulgariu, D. (2011). Studies on sorption of Congo Red from aqueous solution onto soil. *International Journal of Environmental Resources*, vol. 5, (1), pp. 177-188.
- Srinivasan, A. and Viraraghavan, T. (2010). Decolorization of dye wastewaters by biosorbents: a review. *Journal of Environmental Management*, vol. 91, pp.1915-1929.

- Srivastava, S., Sinha, R. and Roy, D. (2004). Toxicological effects of malachite green. *Aquatic Toxicology*, vol. 66, pp. 319-329.
- Su, C. and Wang, Y. (2011). Influence factors and kinetics on Crystal Violet Degradation by Fenton and optimization parameters using response surface methodology. *International conference on Environmental and agricultural engineering*, vol. 15, pp. 76-80.
- Sugumaran, P., Susann V.P., Ravichandran, P. and Seshadri, S. (2012). Production and characterization of activated carbon from banana empty fruit bunch and *Delonix regia* fruit pod. *Journal of Sustainable Energy and Environment*, vol. 3, pp. 125-132.
- Suteu, D., Doina, B. and Dan, F. (2007). Synthesis and characterization of polyamide powders for sorption of reactive dyes from aqueous solution, *Journal of Applied Polymer Science*, vol. 105, (4), pp. 1833-1843.
- Swan, N.G. and Zaini, M.A.A. (2019). Adsorption of Malachite Green and Congo Red Dyes from Water: Recent Progress and Future Outlook. *Ecological Chemistry and Engineering Science*, vol. 26, (1), pp. 119-132.
- Tan, L., Ning, S., Zhang, X. and Shi, S. (2013). Aerobic decolorization and degradation of azo dyes by growing cells of a newly isolated yeast *Candida tropicalis* TL-F1. *Bioresource Technology*, vol. 138, pp. 307-313.
- Tarmizi, T., Risfidian, M., Rohendi, D., and Lesbani, A. (2017). Kinetic and thermodynamic adsorption studies of congo red on bentonite. AIP Conference Proceedings, *Yogyakarta: AIP Publishing*, vol. 1823, pp. 020028-1–020028-8.
- Tay, T., Ucar, S. and Karagöz, S. (2009). Preparation and characterization of activated carbon from waste biomass. *Journal of Hazardous Materials*, vol. 165, pp. 481-485.
- Teles de Vasconcelos, L.A. and Gonzalez, C.G. (1993). Adsorption equilibrium between pine bark and several ions in aqueous solution Cd (II), Cr (III) and Hg (II). *European Water Pollution Control*, vol. 3, (6), pp. 29-39.
- Temkin, M. and Pyzhev, V. (1940). Kinetics of ammonia synthesis on promoted iron catalysts. *Acta Physicochimica. URSS*, vol. 12, (3), pp. 217-222.
- Thao, N.T. and Nguyen, H.D.K. (2017). Advanced oxidation of Rhodamine-B with hydrogen peroxide over Zn-Cr layered double hydroxide catalysts. *Journal of Science: Advanced Materials and Devices*, vol. 2, (3), pp. 317-325.
- The Constitution of the Federal Republic of South Africa, 1996; Section 24.
- Toor, M.K. (2010). Enhancing adsorption capacity of Bentonite for dye removal: Physiochemical modification and characterization in Department of Chemical Engineering. *University of Adelaide*, p. 209.
- Toor, M., Jin, B., Dai, S., and Vimonses, V. (2015). Activating natural bentonite as a cost-effective adsorbent for removal of Congo Red in wastewater. *Journal of Industrial and Engineering Chemistry*, vol. 21, pp. 653-661.

- Topac, F.O., Dindar, E., Ucaroglu, S. and Baskhaya, H.S. (2009). Effect of a sulfonated azo dye and sulfanilic acid on nitrogen transformation processes in soil. *Journal of Hazardous Materials*, vol. 170, (2), pp.1006-1013.
- Turhan, K., Durukan, I., Ozturkcan, S.A. and Turgut, Z. (2012). Decolorization of textile basic dye in aqueous solution by ozone. *Dyes and Pigments*, vol. 92, pp. 897-901.
- Tushar K. S. and Dawood, S. (2014). Review on Dye Removal from Its Aqueous Solution into Alternative Cost Effective and Non-Conventional Adsorbents. *Journal of Chemical and Process Engineering*, vol. 1, (104), pp. 1-7.
- Uddin, M.K. and Nasar, A. (2020). Walnut shell powder as a lowcost adsorbent for methylene blue dye: isotherm, kinetics, thermodynamic, desorption and response surface methodology examinations. *Scientific report*, vol. 10, pp. 1-13.
- Van't Hoff, J.H. (1884). Studies in dynamic chemistry. <https://www.nobelprize.org/prizes/chemistry/1901/hoff/biographical/>.
- Vijayageeta, V.A., Pandia R.A., Arockiaraj, S. P., Annamalai, V., Janakarajan, V.N., Saravana Balaji M.D. and Dheenadhayalan M.S. (2014). Treatment Study of Dyeing Industry Effluents using Reverse Osmosis Technology. *Research Journal of Recent Sciences*, vol. 3, pp. 58-61.
- Vimonses, V., Lei, S.M., Jin, B. (2009). Kinetic study and equilibrium isotherm analysis of Congo Red adsorption by clay materials. *Chemical Engineering Journal*, vol. 148, (2-3), pp. 354-364.
- Vital R.K., Saibaba K.V.N. and Shaik K.B. (2016). Dye Removal by Adsorption: A Review. *Journal of Bioremediation and Biodegradation*, vol. 7, pp. 1-4.
- Wang, C., Yediler, A., Linert, D., Wang, Z. and Kettrup, A. (2002). Toxicity evaluation of reactive dye stuff, auxiliaries and selected effluents in textile finishing industry to luminescent bacteria *vibrio fischeri*. *Chemosphere*, vol. 46, pp. 339-344.
- Wang, L, Li, J., Wang, Y. and Zhao, L. (2011). Preparation of nanocrystalline Fe<sub>3</sub>-xLaxO<sub>4</sub> ferrite and their adsorption capability for Congo red. *Journal of Hazardous Materials*, vol. 196, pp. 342-349.
- Wang, P., Ma, Q., Hu, D. and Wang, L. (2015). Adsorption of methylene blue by a low-cost biosorbent: citric acid modified peanut shell. *Desalination and water treatment*, vol 57, (22), pp. 10261-10269.
- Wang, J., Rafatullah, M., Norhashimah, M., Kaizar, H and Teng, T.T. (2016). Extraction of Toxic Rhodamine B Dye by Using Organic Solvent: A Statistical Analysis. *Research Journal of Environmental Toxicology*, vol. 10, pp. 152-158.
- Wang, Y. Y., Shi, H. Z., Zhang, H. B., Yu, S. M., Chen, N. H., and Tong, Z. F. (2017). Research on Cr (VI) adsorption with magnetic citric acid bentonite. *Journal of Chemical Engineering of Chinese Universities*, vol 3, pp. 726-732.

- Wanyonyi, W.C., Onyari, J.M. and Shiundu, P.M. (2014). Adsorption of Congo Red Dye from Aqueous Solutions Using Roots of *Eichhornia Crassipes*: Kinetic and Equilibrium Studies. *Energy Procedia*, vol. 50, pp. 862-869.
- Weber, W. J., and Morris, J.C. (1963). Kinetics of Adsorption on Carbon from Solution. *Journal of Sanitary Engineering Division ASCE*, vol. 89, pp. 31-60.
- Wekoye, J.N., Wanyonyi, W.C., Wangila, P.T. and Tonui, M.K. (2020). Kinetic and equilibrium studies of Congo red dye adsorption on cabbage waste powder. *Environmental Chemistry and Ecotoxicology*, vol. 2, pp. 24-31.
- Wong, S., Abd Ghafar, N., Ngadi, N., Razmi, F.A., Inuwa, I.M., Mat, R. and Amin, N.A.S. (2020). Effective removal of anionic textile dyes using adsorbent synthesized from coffee waste. *Scientific reports*, pp. 1-10.
- Yagub, M.T., Sen, T.K., Afroze S. and Ang, H.M. (2014). Dye and its removal from aqueous solution by adsorption: a review. *Advances in Colloid and Interface Science*, vol. 209, pp. 172-184.
- Yan, J., Lan, G., Qiu, H., Chen, C., Liu, Y., and Du, G. (2018). Adsorption of heavy metals and methylene blue from aqueous solution with citric acid modified peach stone. *Separation Science and Technology*, vol. 11, pp. 1678-1688.
- Yaneva, Z.L. and Georgieva, N.V., (2012). Insights into Congo Red adsorption on agro-industrial materials - spectral, equilibrium, kinetic, thermodynamic, dynamic and desorption studies. A review. *International Review of Chemical Engineering*, vol. 4, pp. 127-146.
- Zaharia, C. and Suteu, D. (2009). Optimization study of Orange 16 dye sorption onto sawdust wastes. *Bul. Inst. Politechnic, Iasi, series: Chemistry and Chemical engineering*, tom LV (LIX), f. vol. 4, pp. 103-113.
- Zaharia, C., Şuteu, D., Muresan, A., Muresan, R. and Popescu, A. (2009). Textile wastewater treatment by homogenous oxidation with hydrogen peroxide. *Environmental Engineering and Management Journal*, vol. 8, (6), pp. 1359-1369.
- Zhang, H., Zhou, J., Muhammad, Y., Tang, R., Liu, K., Zhu, Y. and Tong, Z. (2019). Citric Acid Modified Bentonite for Congo Red Adsorption. *Frontiers in Materials*, vol. 6, (5), pp. 1-11.
- Zhao, J. B., Zou, Z. D., Ren, R., Sui, X. F., Mao, Z. P. and Xu, H. (2018). Chitosan adsorbent reinforced with citric acid modified  $\beta$ -cyclodextrin for highly efficient removal of dyes from reactive dyeing effluents. *European Polymer Journal*, vol. 108, pp. 212-218.
- Zhou, X. and Zhou, X. (2014). The Unit Problem in the Thermodynamic Calculation of adsorption using Langmuir Equation. *Chemical Engineering Communications*, vol. 201, (11), pp. 1459-1467.
- Zhou, Y., Ge, L. and Fan, N. (2018). Adsorption of Congo red from aqueous solution onto shrimp shell powder. *Adsorption Science & Technology*, vol. 36, (5-6), pp. 1310-1330.



- Zielinski, J.M. and Kettle, L. (2013). Physical characterization: surface area and porosity. *Intertek chemicals and pharmaceuticals*, pp. 1-7.
- Zolinger, H. (1987). Colour chemistry- Synthesis, Properties of organic dyes and pigments. *VCH publishers, New York*, p. 92.
- Zolinger, H., Color Chemistry: Syntheses, Properties, and Applications of Organic Dyes and Pigments, *John Wiley & Sons*, 2003.
- Zou, L., Huang, B., Huang, Y., Huang, Q., and Wang, C. (2003). An investigation of heterogeneity of the degree of graphitization in carbon-carbon composites. *Materials Chemistry and Physics*, vol. 82, (3), pp. 654-662.

## APPENDIX

### Appendix I(a-h): EDS elemental composition of biosorbents

#### Appendix Ia: Elemental composition of RL

<i>Element Line</i>	<i>Weight %</i>	<i>Weight % Error</i>	<i>Atom %</i>	<i>Atom % Error</i>
<b>C K</b>	8.74	± 0.51	14.40	± 0.85
<b>O K</b>	45.19	± 0.20	55.91	± 0.25
<b>Na K</b>	1.31	± 0.05	1.13	± 0.04
<b>Mg K</b>	11.14	± 0.09	9.08	± 0.07
<b>Al K</b>	4.49	± 0.09	3.30	± 0.06
<b>Si K</b>	14.76	± 0.08	10.40	± 0.06
<b>Si L</b>	---	---	---	---
<b>Cl K</b>	0.79	± 0.02	0.44	± 0.01
<b>Cl L</b>	---	---	---	---
<b>K K</b>	2.88	± 0.03	1.46	± 0.02
<b>K L</b>	---	---	---	---
<b>Ca K</b>	0.47	± 0.05	0.23	± 0.03
<b>Ca L</b>	---	---	---	---
<b>Mn K</b>	5.93	± 0.14	2.14	± 0.05
<b>Mn L</b>	---	---	---	---
<b>Fe K</b>	4.29	± 0.16	1.52	± 0.06
<b>Fe L</b>	---	---	---	---
<b>Total</b>	100.00		100.00	

**Appendix Ib Elemental composition of CL**

<i>Element Line</i>	<i>Weight %</i>	<i>Weight % Error</i>	<i>Atom %</i>	<i>Atom % Error</i>
<b>C K</b>	16.31	± 0.29	24.25	± 0.43
<b>O K</b>	48.45	± 0.16	54.07	± 0.18
<b>Na K</b>	1.28	± 0.04	0.99	± 0.03
<b>Mg K</b>	10.13	± 0.05	7.45	± 0.04
<b>Al K</b>	3.74	± 0.04	2.47	± 0.03
<b>Si K</b>	12.25	± 0.04	7.79	± 0.03
<b>Si L</b>	---	---	---	---
<b>Cl K</b>	0.60	± 0.01	0.30	± 0.01
<b>Cl L</b>	---	---	---	---
<b>K K</b>	2.53	± 0.02	1.16	± 0.01
<b>K L</b>	---	---	---	---
<b>Mn K</b>	1.85	± 0.06	0.60	± 0.02
<b>Mn L</b>	---	---	---	---
<b>Fe K</b>	2.86	± 0.07	0.91	± 0.02
<b>Fe L</b>	---	---	---	---
<b>Total</b>	100.00		100.00	

**Appendix Ic Elemental composition of SRL**

<i>Element Line</i>	<i>Weight %</i>	<i>Weight % Error</i>	<i>Atom %</i>	<i>Atom % Error</i>
<b>C K</b>	77.06	± 0.21	83.06	± 0.22
<b>O K</b>	19.18	± 0.20	15.52	± 0.16
<b>Na K</b>	0.12	± 0.03	0.07	± 0.02
<b>Mg K</b>	0.33	± 0.02	0.18	± 0.01
<b>Al K</b>	0.56	± 0.01	0.27	± 0.01
<b>Si K</b>	0.68	± 0.01	0.31	± 0.00
<b>Si L</b>	---	---	---	---
<b>P K</b>	0.20	± 0.02	0.08	± 0.01
<b>P L</b>	---	---	---	---
<b>K K</b>	1.03	± 0.01	0.34	± 0.00
<b>K L</b>	---	---	---	---
<b>Ca K</b>	0.28	± 0.01	0.09	± 0.00
<b>Ca L</b>	---	---	---	---
<b>Fe K</b>	0.22	± 0.03	0.05	± 0.01
<b>Fe L</b>	---	---	---	---
<b>Ti L</b>	---	---	---	---
<b>Ti M</b>	0.34	± 0.02	0.02	± 0.00
<b>Total</b>	100.00		100.00	

**Appendix Id Elemental composition of SCL**

<i>Element Line</i>	<i>Weight %</i>	<i>Weight % Error</i>	<i>Atom %</i>	<i>Atom % Error</i>
<b>C K</b>	36.79	± 0.53	59.62	± 0.85
<b>O K</b>	15.24	± 1.11	18.55	± 1.35
<b>Mg K</b>	3.00	± 0.10	2.40	± 0.08
<b>Al K</b>	5.20	± 0.06	3.75	± 0.05
<b>Si K</b>	4.15	± 0.05	2.88	± 0.03
<b>Si L</b>	---	---	---	---
<b>K K</b>	2.26	± 0.05	1.12	± 0.03
<b>K L</b>	---	---	---	---
<b>Ti K</b>	1.19	± 0.09	0.48	± 0.04
<b>Ti L</b>	---	---	---	---
<b>Cr K</b>	0.67	± 0.11	0.25	± 0.04
<b>Cr L</b>	---	---	---	---
<b>Fe K</b>	30.80	± 0.68	10.73	± 0.24
<b>Fe L</b>	---	---	---	---
<b>Cu K</b>	0.69	± 0.47	0.21	± 0.14
<b>Cu L</b>	---	---	---	---
<b>Total</b>	100.00		100.00	

**Appendix Ie Elemental composition of RDE**

<i>Element Line</i>	<i>Weight %</i>	<i>Weight % Error</i>	<i>Atom %</i>	<i>Atom % Error</i>
<b>C K</b>	52.09	± 0.55	64.64	± 0.69
<b>O K</b>	30.53	± 0.68	28.44	± 0.63
<b>Mg K</b>	0.21	± 0.05	0.13	± 0.03
<b>Al K</b>	3.98	± 0.11	2.20	± 0.06
<b>Si K</b>	0.98	± 0.10	0.52	± 0.05
<b>Si L</b>	---	---	---	---
<b>Ca K</b>	8.67	± 0.39	3.23	± 0.15
<b>Ca L</b>	---	---	---	---
<b>Mn K</b>	0.36	± 0.43	0.10	± 0.12
<b>Mn L</b>	---	---	---	---
<b>Cu K</b>	3.16	± 0.96	0.74	± 0.23
<b>Cu L</b>	---	---	---	---
<b>Total</b>	100.00		100.00	

**Appendix If Elemental composition of CDE**

<b>Element Line</b>	<b>Weight %</b>	<b>Weight % Error</b>	<b>Atom %</b>	<b>Atom % Error</b>
<b>C K</b>	69.23	± 0.28	76.21	± 0.30
<b>N K</b>	5.67	± 1.59	5.35	± 1.51
<b>O K</b>	20.76	± 0.40	17.16	± 0.33
<b>Mg K</b>	0.42	± 0.03	0.23	± 0.02
<b>Al K</b>	0.42	± 0.02	0.21	± 0.01
<b>Si K</b>	0.09	± 0.02	0.04	± 0.01
<b>Si L</b>	---	---	---	---
<b>P K</b>	0.36	± 0.05	0.15	± 0.02
<b>P L</b>	---	---	---	---
<b>Ca K</b>	1.69	± 0.04	0.56	± 0.01
<b>Ca L</b>	---	---	---	---
<b>Ti L</b>	---	---	---	---
<b>Ti M</b>	1.35	± 0.11	0.09	± 0.01
<b>Total</b>	100.00		100.00	

**Appendix Ig Elemental composition of SRDE**

<b>Element Line</b>	<b>Weight %</b>	<b>Weight % Error</b>	<b>Atom %</b>	<b>Atom % Error</b>
<b>C K</b>	60.34	± 0.43	67.93	± 0.48
<b>O K</b>	36.49	± 0.29	30.84	± 0.25
<b>Mg K</b>	0.52	± 0.03	0.29	± 0.01
<b>Si K</b>	0.12	± 0.01	0.06	± 0.01
<b>Si L</b>	---	---	---	---
<b>P K</b>	0.16	± 0.01	0.07	± 0.01
<b>P L</b>	---	---	---	---
<b>Cl K</b>	0.15	± 0.03	0.06	± 0.01
<b>Cl L</b>	---	---	---	---
<b>K K</b>	0.54	± 0.04	0.19	± 0.01
<b>K L</b>	---	---	---	---
<b>Ca K</b>	1.67	± 0.03	0.56	± 0.01
<b>Ca L</b>	---	---	---	---
<b>Total</b>	100.00		100.00	

**Appendix 1h Elemental composition of SCDE**

<b>Element Line</b>	<b>Weight %</b>	<b>Weight % Error</b>	<b>Atom %</b>	<b>Atom % Error</b>
<b>C K</b>	60.65	± 0.17	69.74	± 0.20
<b>O K</b>	31.43	± 0.18	27.13	± 0.15
<b>Mg K</b>	1.78	± 0.02	1.01	± 0.01
<b>Al K</b>	0.17	± 0.02	0.09	± 0.01
<b>P K</b>	0.11	± 0.01	0.05	± 0.00
<b>P L</b>	---	---	---	---
<b>K K</b>	2.95	± 0.02	1.04	± 0.01
<b>K L</b>	---	---	---	---
<b>Ca K</b>	2.68	± 0.04	0.92	± 0.01
<b>Ca L</b>	---	---	---	---
<b>Ti L</b>	---	---	---	---
<b>Ti M</b>	0.23	± 0.02	0.02	± 0.00
<b>Total</b>	100.00		100.00	